Ipsen

FINAL REPORT

Investigation of Foamed Metals for Launch and Space Vehicle Applications

GPO PRICE $ _____

CFSTI PRICE(S) $ _____

Hard copy (HC) 4.00

Microfiche (MF) 1.00

ff 653 July 65

GEORGE C. MARSHALL SPACE FLIGHT CENTER
NATIONAL AERONAUTICS AND SPACE ADMINISTRATIO
HUNTSVILLE, ALABAMA

May 1966

IPSEN INDUSTRIES, INC.
715 SOUTH MAIN STREET
ROCKFORD, ILLINOIS 61105

Investigation of Foamed Metals for Launch and Space Vehicle Applications

By

Edward R. Byrnes, Jr. and Charles J. Twine

Final Report

Contract No. NAS8-11048
Control No. TP3-85486 (1F)
CPB 02-1250-63

May, 1966

Ipsen Industries, Inc.
715 South Main Street
Rockford, Illinois 61105

FOREWORD

This report was prepared by Ipsen Industries, Incorporated under Contract No. NAS8-11048 entitled "Investigation of Foamed Metals for Launch and Space Vehicle Applications" for the National Aeronautics and Space Administration. The work was accomplished under the program management of Messrs. H. H. Kranzlein and W. B. McPherson, Materials Division, Propulsion and Vehicles Engineering Laboratory, George C. Marshall Space Flight Center.

This final technical report covers all work performed under the contract from June 29, 1963 to November 30, 1965. The manuscript was released by the authors for publication on April 21, 1966.

Dr. Einar P. Flint, Project Manager, and Mr. Edward R. Byrnes, Jr., Project Metallurgist, of the Research and Development Division of Ipsen Industries were in charge of the development and evaluation work. Technical assistance was given by Dr. Karl H. Seelandt, Chief Scientist; Don W. Bissell, Ceramic Engineer; James Cloud, Ceramic Engineer; Crawford Hallett, Senior Ceramic Engineer; Dr. M. A. H. Howes, Senior Metallurgist; Landis K. Lindell, Vacuum Engineer; and Dr. Helmut Vedder, Physicist.

A sub-contract was awarded to Melpar, Inc., Falls Church, Virginia for physical property testing.

ABSTRACT

Investigations of methods for manufacturing porous metals are reported. Effects of variables in processing and fabrication on the ultimate strength and integrity of foam metals are discussed. The foamed metals studied were aluminum, titanium, nickel, 316 stainless steel, H-11 tool steel, and molybdenum. No unusual difficulties were encountered in preparing foam metals of molybdenum, H-11 tool steel, 316 stainless steel and nickel; however, at densities less than 15% of theoretical, the foam metals exhibited brittle fracture characteristics.

Since no practical mechanical or chemical method was discovered to prevent or remove the formation of oxide film around the aluminum metal particles, a useable foamed aluminum was not produced. Titanium could be foamed and sintered, but oxide contamination between the grain boundaries resulted in a product with marginal ductility for structural applications.

Variable density beams were manufactured wherein the core material was of graduated density through the depth of the beam. The results of mechanical, physical, and thermal property tests are presented. Data concerning the machinability and fabrication techniques of foam metals are contained in the report.

TABLE OF CONTENTS

TABLE OF CONTENTS
(Continued)

BLANK PAGE

ILLUSTRATIONS

ILLUSTRATIONS
(Continued)

ILLUSTRATIONS
(Continued)

ILLUSTRATIONS
(Continued)

TABLES

I. INTRODUCTION

High quality, lightweight structural materials are a requisite for manned space flight. Porous metal in critical locations of spacecraft can significantly reduce weight penalties that arise, due to non-availability of low density material forms and configurations with large thicknesses and low mass concentrations. Thus, typical uses of lightweight porous metals could be impact protection barriers, vibration damping devices, noise suppressor systems and lightweight structures.

The objectives of this program were: to produce ductile porous metals of controlled densities and predictable properties by a foaming and sintering technique; to determine the relationships of density, pore size, and mechanical properties of the foamed metals; and to investigate fabrication, machining and forming techniques for these metals. Potential areas of application were to be shown by producing and evaluating (1) sandwich structures with low density foam metal cores and (2) variable density beams of foam metal for bending load applications.

The metals selected for study and evaluation were aluminum, titanium, stainless steel, tool steel, nickel, and molybdenum. Each metal was to be foamed, sintered, and evaluated in two or more densities with two pore sizes for each density.

The program reported herein has explored the production of foamed metals in a variety of densities and the prediction of the densities, pore sizes, and mechanical properties that would result when experimental foaming and sintering conditions were standardized. Each foamed metal produced was evaluated in a variety of densities by determining selected physical and mechanical properties, which included the following:

1. Tensile, compressive, flexural, and shear strength.
2. Vibration damping capacity.
3. Thermal expansions and conductivities.
4. Elevated temperature stability.

II. POROUS METAL PROCESSES

Various methods have been developed for manufacturing porous metals. Several have been based on foaming a melt, but these give products of heterogeneous pore size. Another method consists of infiltrating molten metal into a porous bed of a suitable pore former.

The bed is then leached out with a suitable solvent. A similar method consists of mixing a metal powder slurry with a pore forming material, which is subsequently burned or volatilized during sintering. The process treated here consists of entraining air in a metal powder slurry, which is subsequently dried and sintered to produce a homogeneous porous metal.

A. Foaming Metal Powders

The slurry contains metal powder, binder, and cementing and foaming agents. Air is entrained under conditions such that bubbles of uniform size are distributed evenly in a foam with metal particles suspended on the walls of the air bubbles. The suspension is then cast in a mold and dried. The cementing agents set and provide a cast form with adequate rigidity. This green metal billet is removed from the mold and presintered under vacuum or reducing conditions. The cementing and foaming agents are volatilized and driven off while the metal particles are partially sintered together at their points of contact. Final sintering is in a clean furnace with a vacuum of from 1 to 20 microns. Clean and well-bonded foamed metals of the desired density are thus produced.

The metals selected for investigation were aluminum, titanium, nickel, 316 stainless steel, molybdenum and H-11 tool steel. These were obtained in powder form from commercial sources. Each powder was procured in either or both grain sizes of -100 and -325 mesh. The sources, the chemical composition, the method of manufacture, the powder morphology and a sieve analysis of each of the powders received are listed in Appendix A-1.

Sieve analysis showed a wide variation in grain size for all powders of nominally -100 mesh grade. Those of -325 mesh, however, were almost entirely of that size. The variations in size of the coarser grain turned out to be an advantage. Experience showed that foams constituted of varying sizes in definite proportions gave optimum results. Since commercially available powders of nominally -100 mesh will yield the range of sizes required, it is not necessary to procure grain of several uniform sizes to prepare the aggregates needed. This, undoubtedly, represents a significant monetary saving in raw material costs.

1. Foaming

All of the powdered metals selected could be foamed. The presence of oxides, however, in the aluminum and titanium powders caused serious mechanical property deficiencies in the end product. Low ductility and low mechanical strengths were the most serious deficiencies. For this reason attention was directed to producing foams of molybdenum, nickel, tool steel and stainless steel. With minor variations, the process used for all six metals was as follows:

a. Weighing powder.
b. Mixing powders and cements.
c. Mixing powders and cements with foam.
d. Casting foamed powder into molds.
e. Binder and cement setting of the cast form in the molds.
f. Mold removal.
g. Air drying the cast metal form or billet.
h. Final drying at 180°F in an oven.

To manufacture foamed metals of a specific pore size and density, the above process must be completely predictable and reproducable. It may be assumed that these conditions would be met by laws of solid geometry and gravity and the surface tension of the foam working to control the bubble size. This, in turn, controls the density of a foamed metal sample when fixed quantities of uniform grain size powder are used. Experience shows, however, that there are certain variables present that must be controlled. The theoretical considerations and empirical observations which support this are presented in Appendix A-2. Suffice it to say, that pore size, density, and physical properties are achieved by careful control of:

a. Uniformity of grain size.
b. Foaming procedures.
c. Methods used to dry, presinter and sinter foamed metal material.

2. Sintering of Foamed Metal Powders

The dried green foams of metal powder were sintered in cold wall type, vacuum furnaces with foamed refractory insulation and graphite, molybdenum, or tungsten heating elements. Dried green foam contains an organic binder, foaming, and cementing agents. These must volatilize and be removed by presintering, or "dewaxing", prior to final sintering. Otherwise, these agents will retard the development of good sintered joints, between the metal particles.

Any oxide on the metal particles is an impurity and inhibits metal-to-metal sintering. Unfortunately, in producing green metal foam the metal powder is inevitably partially oxidized by water, which is an essential processing element. Some metals, such as nickel and molybdenum, have oxides which are easily reduced or dissociated by vacuum at sintering temperature. Iron oxide is dissociated partially by the obtainable vacuums at the stainless steel sintering temperature. This oxide is dissociated by the vacuum obtained at the higher sintering temperatures employed for H-11 tool steel. In the case of chromium in stainless steel, aluminum, and titanium, vacuum alone will not dissociate or reduce the oxides of these metals at sintering temperatures. Sintering is prevented by the oxide,

unless some chemical, mechanical, or thermal reducing means are provided. The chromium and iron oxides, formed during the foaming process, were reduced and the stainless steel foam sintered when a dry hydrogen atmosphere was provided during part of the sintering cycle. Foamed aluminum and titanium were not producible since no practical mechanical, thermal, or chemical means was found to eliminate the sinter retarding oxide film on the metal particles.

Dewaxing is difficult when the metal particles are cemented in a cellular network of thin bubble walls as in a foamed metal. Such foams are fragile once the binder and cements have been removed. There is a tendency for the foamed shape to revert to particulate powder unless partial sintering has been accomplished at the point of contact of the metal grains.

The fragility and sintering shrinkage of foam metal presented fixture problems during sintering. When foam materials were placed directly on the furnace hearth or on rigid fixtures, movement was restricted and the fragile foam cracked easily as illustrated in Figure 1. Small samples up to 1 x 2 x 3 inches could be fixtured on grooved plates of foamed zirconia insulation with no cracking during sintering. A good fixture consisted of imbedding foam metal samples in zirconia bubble grain within a metal retort. The bubble grain used in this method provided uniform heating and support as the samples shrank. Care was taken to ensure that the bubble grain did not collapse the samples, yet provided enough bubble grain to flow and fill the voids caused by sample shrinkage.

The early work consisted of doing the presintering and sintering in one furnace since it appeared advantageous to avoid moving the fragile parts after presintering. Cold wall vacuum furnaces were used for this.

When the binder and cements are volatilized under vacuum, part of the vapor condenses on the walls of the furnace. These condensations must be removed to maintain the vacuum. The remaining volatilized material is drawn into the oil diffusion and mechanical pumps, ultimately preventing their operation.

An expedient (Appendix A-3) was tried to seal off the vapors from the furnace itself, but a minor part of the vapors were still deposited on the cold walls and within the insulation of the furnace. The amount increased with the number of times the dewaxing process was carried out, and the furnace shell and insulation had to be periodically cleaned.

Dewaxing and sintering in one furnace was not satisfactory because of the excessive cleaning required, and it was difficult to maintain good

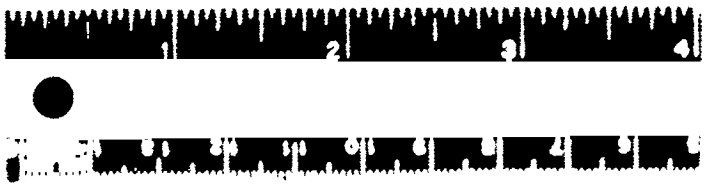

Figure 1. Foamed H-11 Tool Steel Samples Fixtured Improperly and Properly during Sintering

vacuums less than 10 microns (Hg). A two-step procedure was, therefore, adopted. This involved using a "dirty" vacuum furnace or a muffle furnace for expelling volatiles and initial sintering. A "clean" vacuum furnace was then used for final sintering.

The maximum operating temperature of the vacuum presinter furnace was 2300°F, and the attainable vacuum was 30-100 microns, since a mechanical pump was used without a diffusion pump. The organic volatiles appeared to decompose and form lower molecular weight products. These were caught partly in a cold trap between the furnace and the pump, partly in the oil of the pump, and the remainder were discharged to the atmosphere. Replacement of the pump oil and cleaning the furnace was required periodically.

A muffle furnace with a reducing atmosphere of dry hydrogen was used also for presintering. The externally heated muffle had a maximum temperature of 2060°F. The hydrogen atmosphere reduced the iron, chromium, nickel and molybdenum oxides and carried off the volatilized organics as it passed through the furnace.

For final sintering of small specimens, a laboratory-type vacuum furnace with a work space of 5 x 6 x 12 inches was used. For larger specimens, vacuum furnaces with a working space of 8 x 21 x 21 inches or 12 x 24 x 72 inches were used. Since the volatiles had been expelled during presintering, these furnaces could be kept uncontaminated. Usually absolute pressures of 0.1-10 microns (Hg) were maintained during the final sinter.

a. Presintering: Foamed metals of molybdenum, H-11 tool steel, 316 stainless steel and nickel were presintered at approximately 2300°F for 1-3 hours in vacuums of 50-250 microns. Stainless steel foams were oxidized severely after long presinter cycles at vacuums above 200 microns. To preclude this oxidation the vacuum should be kept below 100 microns with long presinter cycles or the presinter cycle less than two hours at vacuums above 100 microns. Oxidation was a minor problem with H-11 tool steel and even less so with molybdenum and nickel foams. These materials were successfully presintered at vacuums of 300-400 microns, or less, and in cycle times below 3 hours. The cycle time could be increased as the vacuum decreased below 300 microns.

Molybdenum with foam densities of 1000 gm/qt or greater was presintered at 2060°F in the hydrogen muffle furnace. The cycle consisted of holding at 2060°F for 5-10 hours. For an unexplainable reason, foamed molybdenum of 500 gm/qt casting density, foamed stainless, and tool steel were not presintered successfully in the muffle furnace using that presinter cycle. Possibly a longer soak at 2060°F to promote more

metal grain-to-grain sintering would result in success with these materials in the hydrogen muffle.

b. Sintering: Foamed molybdenum was sintered at 3800°F for 3-10 hours at vacuums of 10 microns or less. A three hour hold at 3800°F was sufficient in the small laboratory vacuum furnace, but longer soaks, up to 10 hours, were necessary in the larger furnaces to achieve strong, well-sintered samples. Figure 2 illustrates several samples of well-sintered foamed molybdenum. Figure 3 illustrates the pore structure.

The sinter cycle for H-11 tool steel foam consisted of soaking the presintered material at 2650°F for 2-4 hours at vacuums of 200 microns or less. Again the shorter time at 2650°F was used in the smaller furnaces. When the material had been oxidized during presintering, vacuums of 10 microns or less were necessary to produce clean, well-sintered samples. H-11 tool steel was also produced using a one cycle sinter without a presinter. The dried material was heated to 2650°F in a clean uncontaminated furnace. The vacuum maintained was usually about 200 microns, though there were periods of higher absolute pressures ("outgassing"). A sample of sintered H-11 tool steel is shown in Figure 4. Pore structures of H-11 tool steel are illustrated in Figure 5.

Stainless steel foam materials were more difficult to sinter because of the affinity of chromium for oxygen. The initial sintering treatment involved alternating atmospheres of vacuum and hydrogen, the final process consisted of vacuum only. It was found that bright, foamed products could thus be obtained by a sufficiently long vacuum heat treatment. The sinter cycle consisted of heating to 2500°F and holding at this temperature for 40 hours at vacuums of 10 microns or less.

Figure 6 shows the increase in density and hardness for the foamed stainless steel as the sintering time is increased. An approximate plateau in both properties is indicated at a sintering time of 40 hours. To avoid oxidation, it was necessary to maintain good vacuum during the presinter and sinter cycles. Hence, relatively clean, uncontaminated vacuum furnaces must be used.

Several stainless steel foam samples were sintered in another manner. These samples oxidized during presintering because of a vacuum exceeding 200 microns. Sintering for 5 hours at 2500°F and vacuum of less than 10 microns reduced very little oxide. Figure 7 illustrates several of the oxidized samples. These samples were subsequently heated to 2060°F in the muffle furnace for periods of 55-75 hours in a pure, dry hydrogen atmosphere. The oxide was removed by

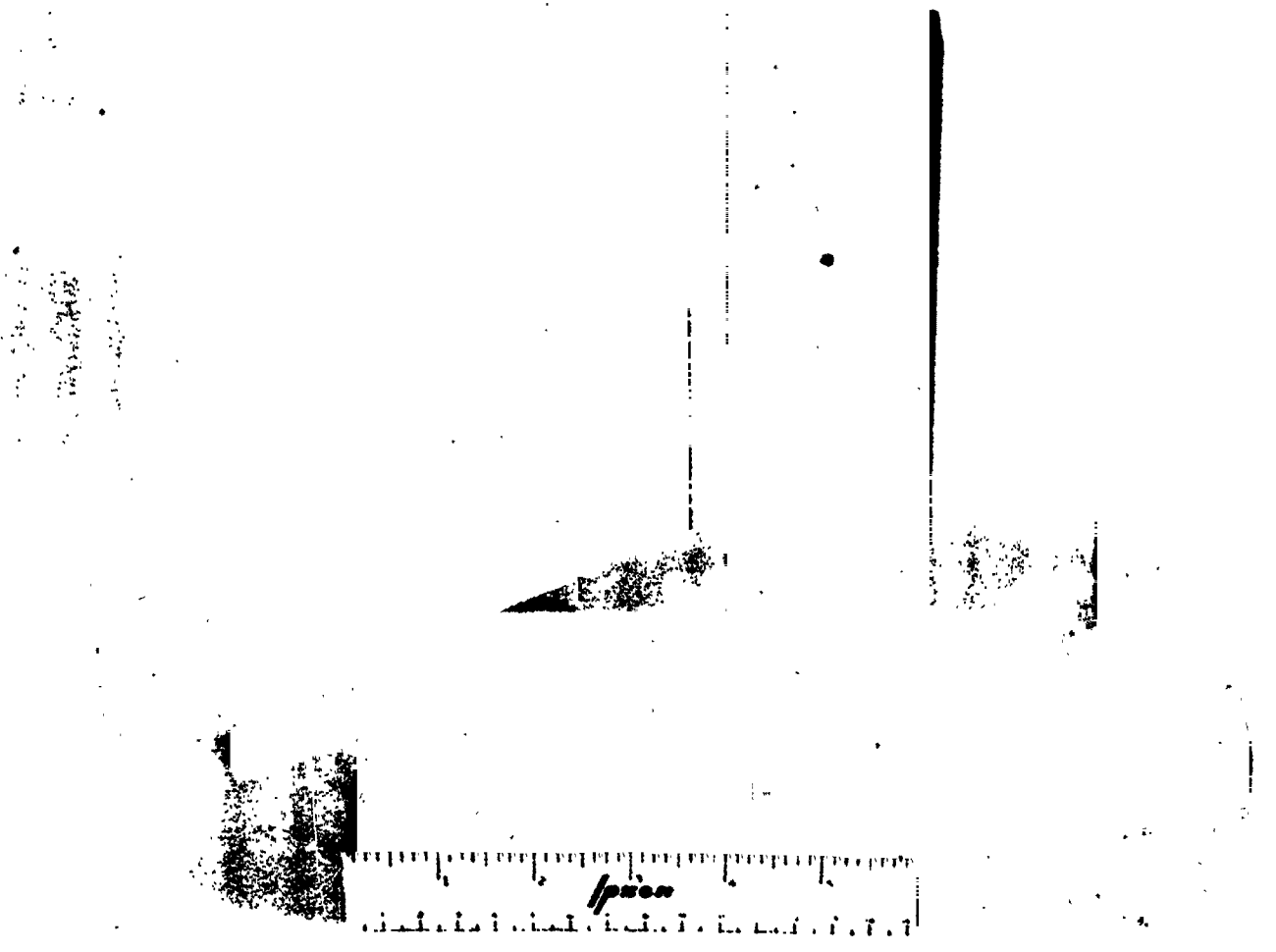

Figure 2. Sintered Samples of Foamed Molybdenum

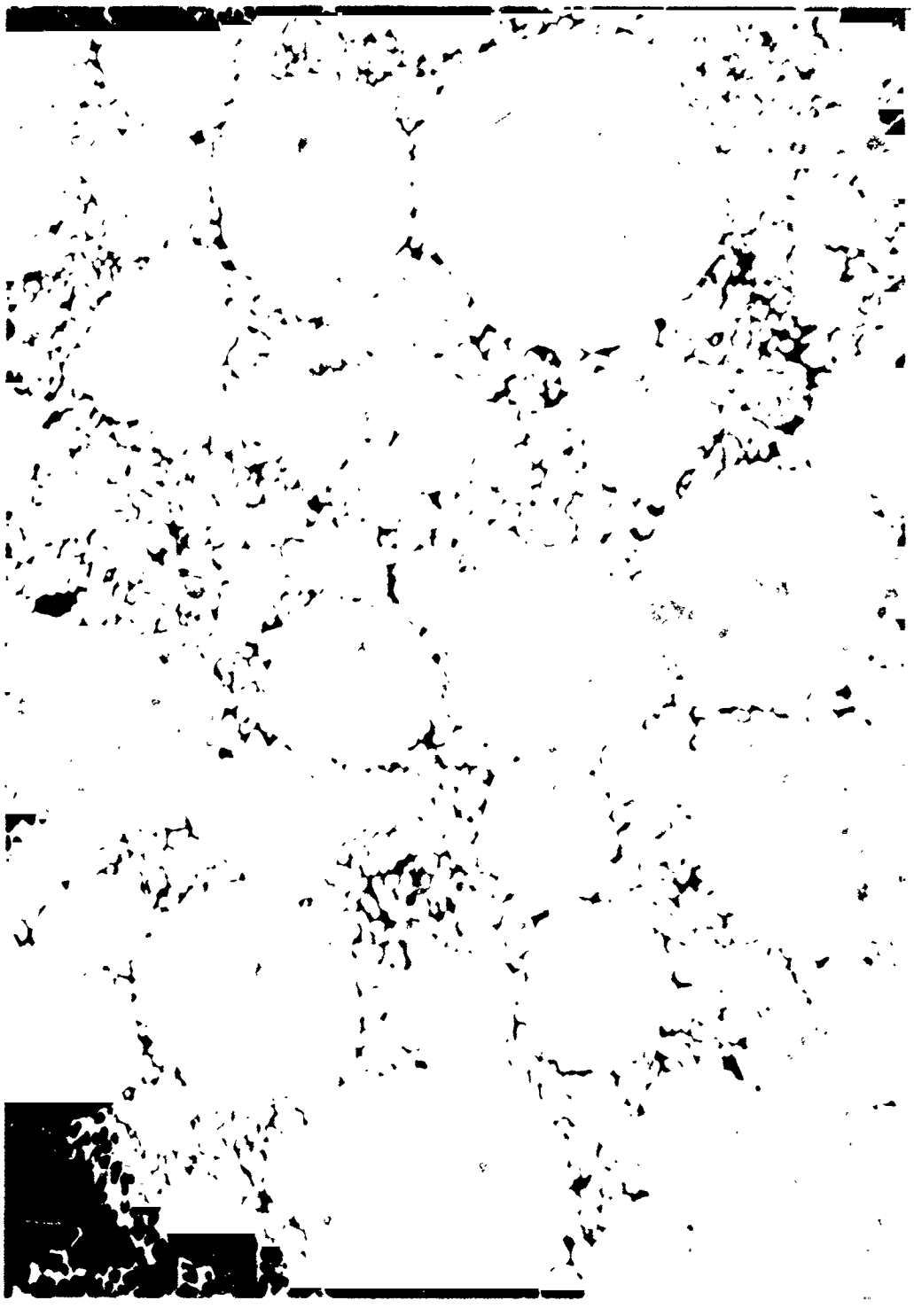

Figure 3. Pore Structure of Sintered Foamed Molybdenum, 155X

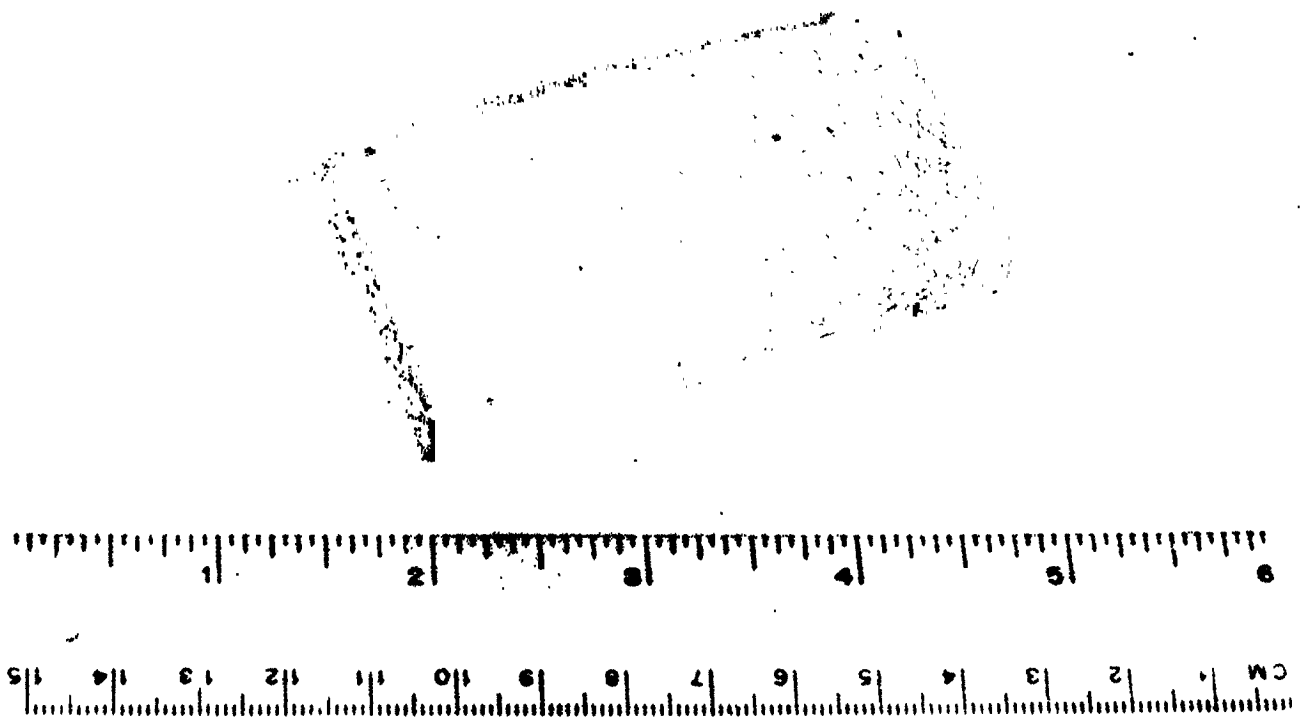

Figure 4. Sintered Sample of Foamed H-11 Tool Steel

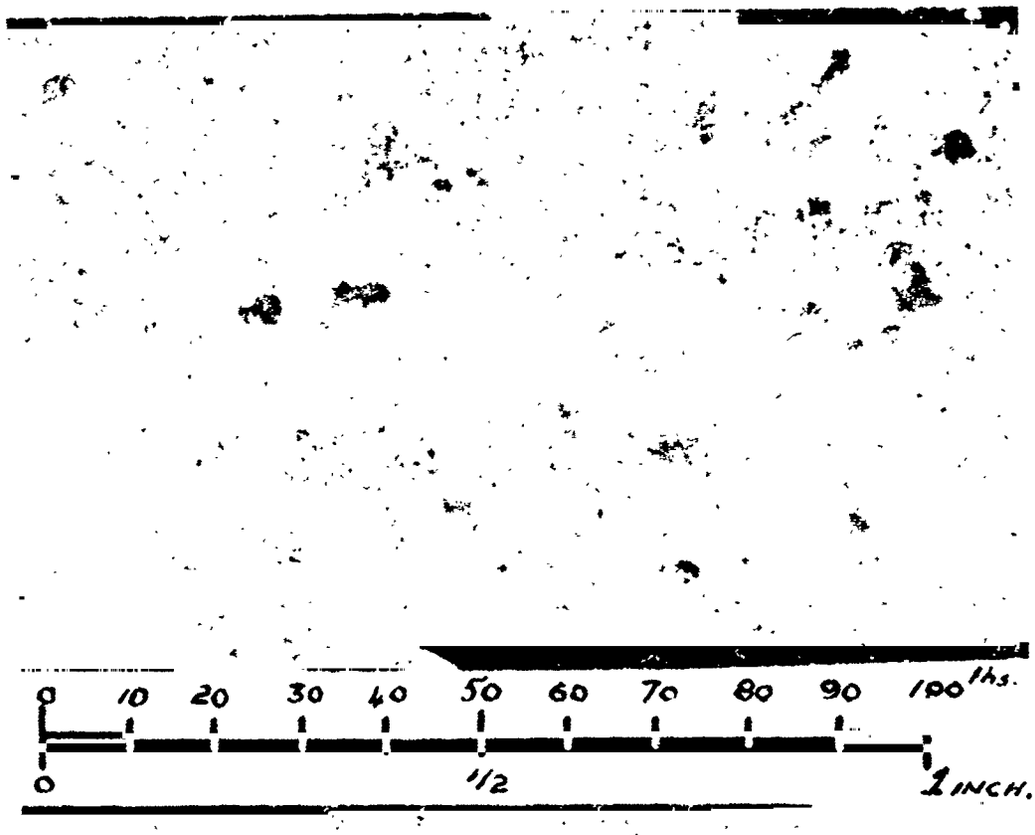

Figure 5. Foamed H-11 Tool Steel of Two Different Pore Sizes

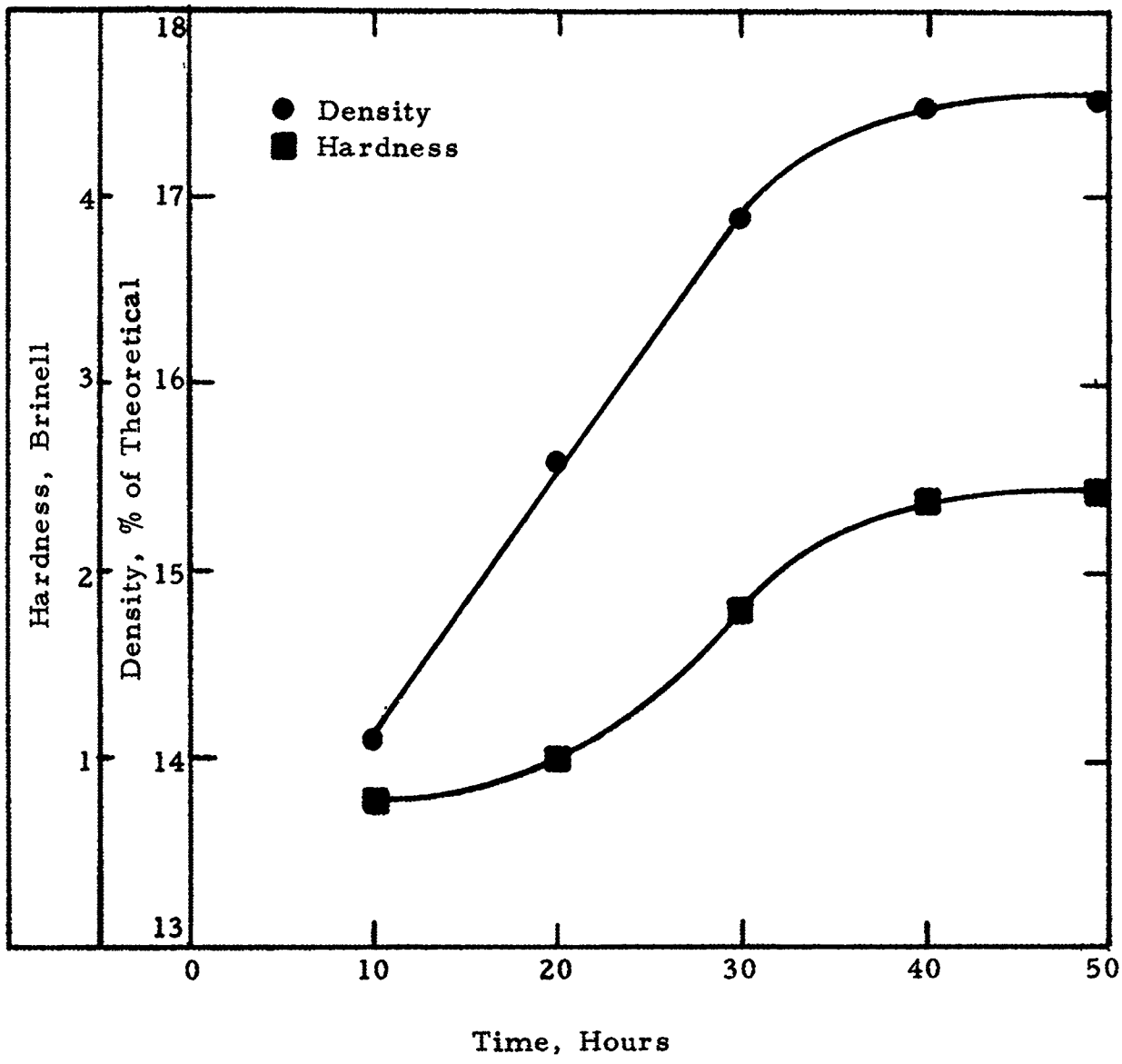

Figure 6. Sintering Time Effect on Foamed 316 Stainless Steel

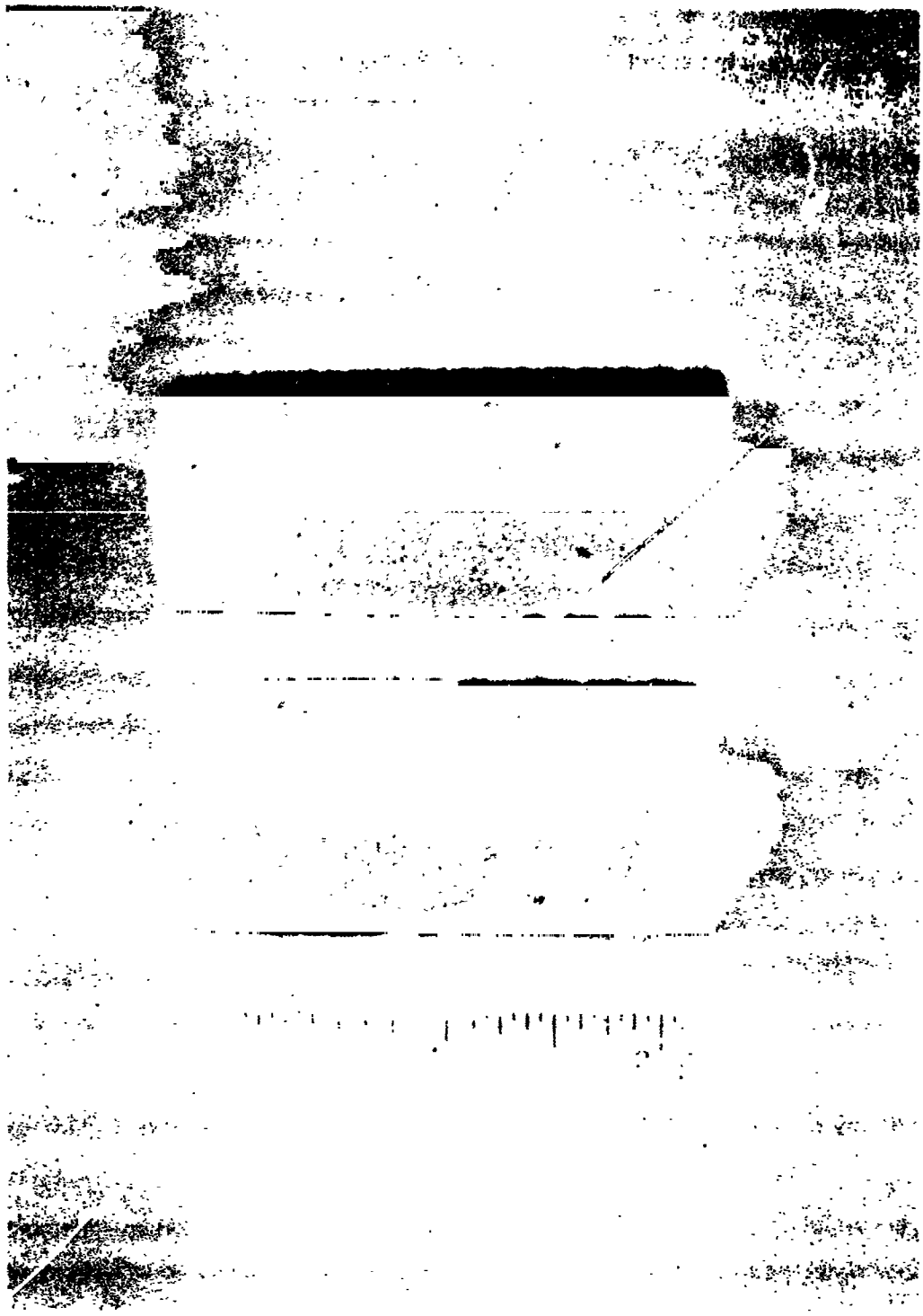

Figure 7. Oxidized Samples of Sintered 316 Stainless Steel Foam

this treatment. Sintering was then completed in a vacuum furnace at 2500°F for 10 hours with a vacuum of 5 microns or less.

Nickel foam materials, illustrated in Figure 8, were sintered easily because of the ready dissociation of the oxide in vacuum at the sintering temperature. Foam nickel was sintered at 2550°F in vacuums below 50 microns for 20 hours following presintering at 2300°F in vacuum for 3 hours. Strong, well-sintered, and ductile foam nickel was produced in two densities. The density varied from 18.0 to 19.3% of theoretical for 12 samples and 27.0 to 27.8% for 10 samples.

3. Results

The considerations and work discussed in the preceding sections provided data for a "best mix" to produce ductile foamed metals within given ranges of density and pore size. These results are set forth in Table 1 and may be considered to be tentative capabilities of the foaming and sintering process.

4. Aluminum and Titanium

Foamed aluminum and titanium are of special interest as porous, low density, ductile metals for numerous applications on space vehicles. However, they are the most difficult to obtain as satisfactory foams because of the ready formation of a stable oxide film on the metal particles. This is particularly true with aluminum, which must be sintered at temperatures below the 1220°F melting point yet has an oxide stable at temperatures above 3000°F. Nevertheless, a sintered foam from a powder slurry is preferred to methods that proceed from a melt, because a more uniform pore structure can be obtained. Uniformity of pore size is difficult to accomplish when a melt is foamed.

Pure aluminum and aluminum alloy powders, made by atomization of the melt in an inert atmosphere, were foamed and dried. The appearance of a dried, green foam aluminum is shown in Figure 9. This material could not be vacuum sintered at 1220°F because of the oxide film on the particles. Hydrochloric acid, aluminum chloride, and fluoride compounds as listed below, were added to the casting mixture to break down the oxide film and permit metal-to-metal sintering.

a. Ammonium hexafluorophosphate, NH_4PF_6
b. Ammonium fluoraborate, NH_4BF_4
c. Ammonium fluoride, NH_4HF_2
d. Di-n-butyl ammonium fluoraborate, $(C_4H_9)_2NH_2BF_4$
e. Tetramethylammonium fluoraborate, $(CH_3)_4NBF_4$
f. Hydrazinium difluoride, $NH_2H_4 \cdot 2HF$

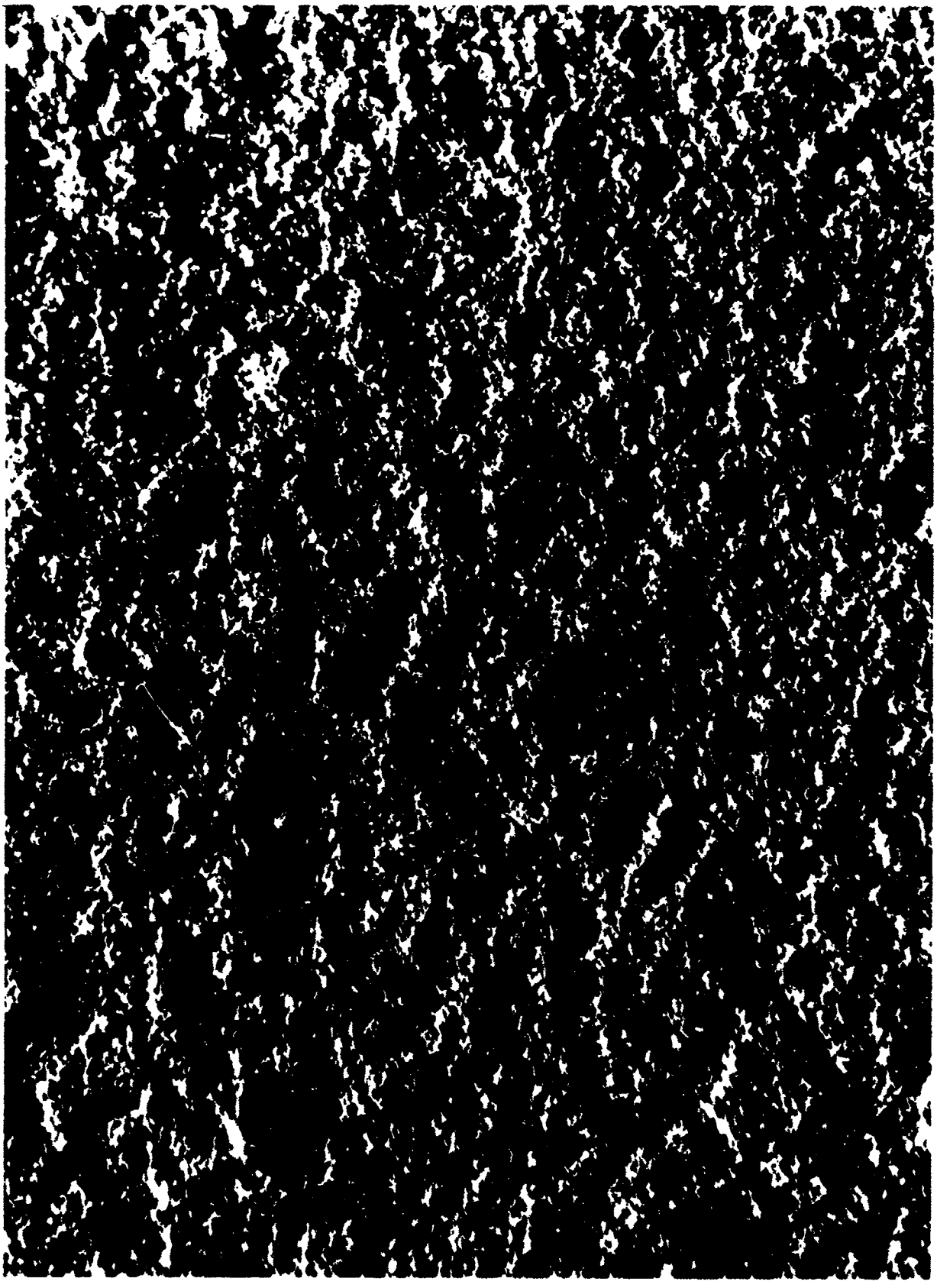

Figure 8. Sintered Foamed Nickel, 10X

TABLE 1: "Best Mix" of Metal Powder, Foam, Time, and Temperature To Produce Foam Metals of Pore Sizes and Percents of Theoretical Densities Shown

Material	Density % Theo.	Pore Size 10^{-3} inches	Formulation		Pre-sintering		Sintering	
			Metal to foam ratio gm/qt	Metal Powder particle sizes	Temp. °F	Time hr.	Temp. °F	Time hr.
Molybdenum	17 - 20	6	600	100% - 325	2300	3	3800	6
	24 - 26	4 - 5	1000	100% - 325	2300	3	3800	6
	28 - 30	5 - 16	1600	100% - 325	2300	3	3800	6
	12 - 13	10	500	50% coarse 50% - 325	2050	5 - 6	3800	10
	14 - 18	9 - 10	1000	50% coarse 50% - 325	2050	5 - 6	3800	10
	20 - 22	7 - 8	1500	50% coarse 50% - 325	2050	5 - 6	3800	10
H-11 Tool Steel	14 - 20	9 - 14	700	35% - 100 65% - 325	2300	3	2650	4
	20 - 22	8 - 11	1300	35% - 100 65% - 325	2300	3	2650	4
	16 - 20	9 - 13	700	100% - 100	----	---	2650	4
	25 - 28	8 - 10	1300	100% - 100	----	---	2650	4
Nickel	16 - 18	----	750	40% - 100 60% - 325	2300	3	2550	20
	26 - 28	----	1900	40% - 100 60% - 325	2300	3	2550	20
Stainless Steel Type 316	17 - 18	----	650	35% - 100 65% - 325	2300	3	2500	40
	26 - 28	----	1500	35% - 100 65% - 325	2300	3	2500	40
	10 - 11	10 - 12	700	35% - 100 65% - 325	----	---	2500[2]	10
	13 - 15	9 - 11	900	35% - 100 65% - 325	----	---	2500[2]	10
	15 - 17	8 - 10	1100	35% - 100 65% - 325	----	---	2500[2]	10
	17 - 19	8 - 10	1300	35% - 100 65% - 325	----	---	2500[2]	10
	17	4	700[1]	30% - 100 70% - 325	2000	5	2500[3]	15
	21 - 23	4	1100[1]	30% - 100 70% - 325	2000	5	2500[3]	15
	25 - 27	4	1300[1]	30% - 100 70% - 325	2000	5	2500[3]	15

NOTE: 1 - Samples prepared with excess cementing agent
2 - Oxidized Sintered Samples cleaned in dry (-90°F dewpoint) hydrogen for 55 hours
3 - Oxidized Sintered Samples cleaned in dry (-90°F dewpoint) hydrogen for 30 hours

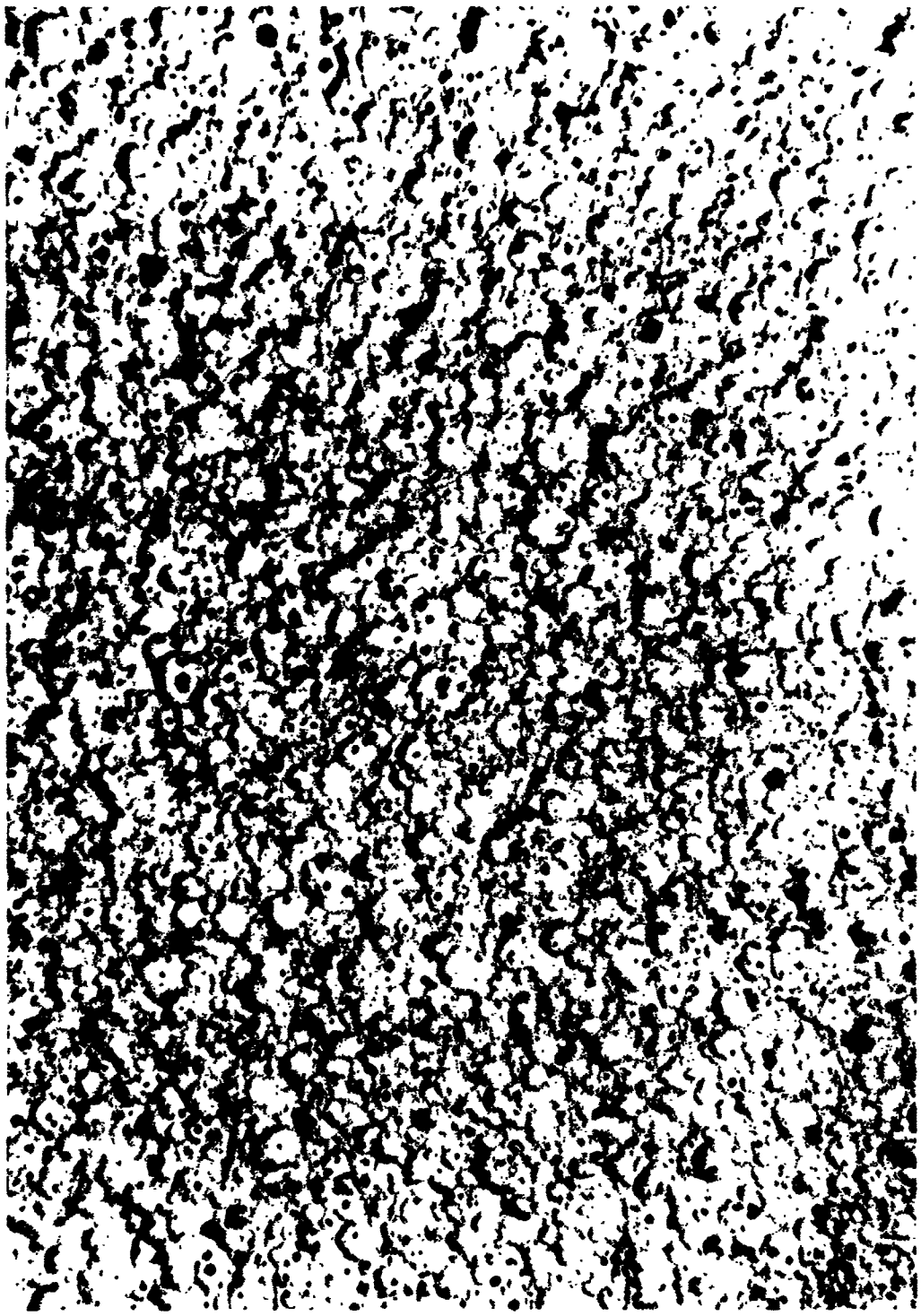

Figure 9. Foamed 1100 Series Aluminum in Green State, 30X

g. Hydrazinium fluoraborate, $N_2H_5 \cdot BF_4$.

However, these cast foams were weak and collapsed before they dried completely.

Samples of 7178 aluminum alloy were foamed, dried, and sintered in vacuum at temperatures up to 1150°F. This alloy was considered more suitable than pure aluminum for obtaining a foamed sintered structure because: (1) The aluminum oxide layer might be less adherent to the metal grains in the presence of alloying metals and (2) The relatively high concentration of zinc in the alloy could cause breakdown of the oxide film through volatilization of the zinc, since its vapor pressure is greater than 400 microns at 1100°F. Several partially sintered samples were obtained with densities from 17 to 20% of theoretical. However, they were brittle, powdery, and of insufficient strength.

Strengthening these porous aluminum samples was attempted by impregnating them with various aluminum brazing fluxes and corrosive materials. The samples were then dried and resintered at 1150°F. Hopefully, these additions would break down and remove the oxide film or convert it to compounds soluble in water. None of these additions gave a stronger, ductile sintered product.

The same methods were used to prepare foamed titanium. Titanium hydride was also added during foaming to provide a reducing atmosphere which would minimize oxide formation. The green samples were presintered at 2300°F for 2 to 3 hours and final sintered at 2600°F to 3000°F for 2 to 3 hours. However, the sintered titanium foams also were brittle, powdery and of insufficient strength.

Photomicrographs of 32% density foamed titanium are shown in Figures 10 and 11. It can be seen that interstitial material is in the grain boundaries. This was thought to be titanium oxide which caused the brittleness in the structure. It was hoped that titanium hydride in the mixture would prevent the formation of contaminants, such as titanium oxides, but apparently this reducing condition during sintering was not sufficient.

The preparation of a sintered titanium foam is theoretically much simpler than in the case of aluminum because of the higher melting point of titanium and the lower stability of titanium oxide compared to aluminum oxide. With this in mind, work proceeded to alter a small laboratory type vacuum furnace capable of 4000°F to provide reducing conditions with pure and dry hydrogen during the presintering and sintering. Regretfully, this work was never completed because of furnace alteration difficulties, and no strong and ductile foamed titanium could be produced by the foam process.

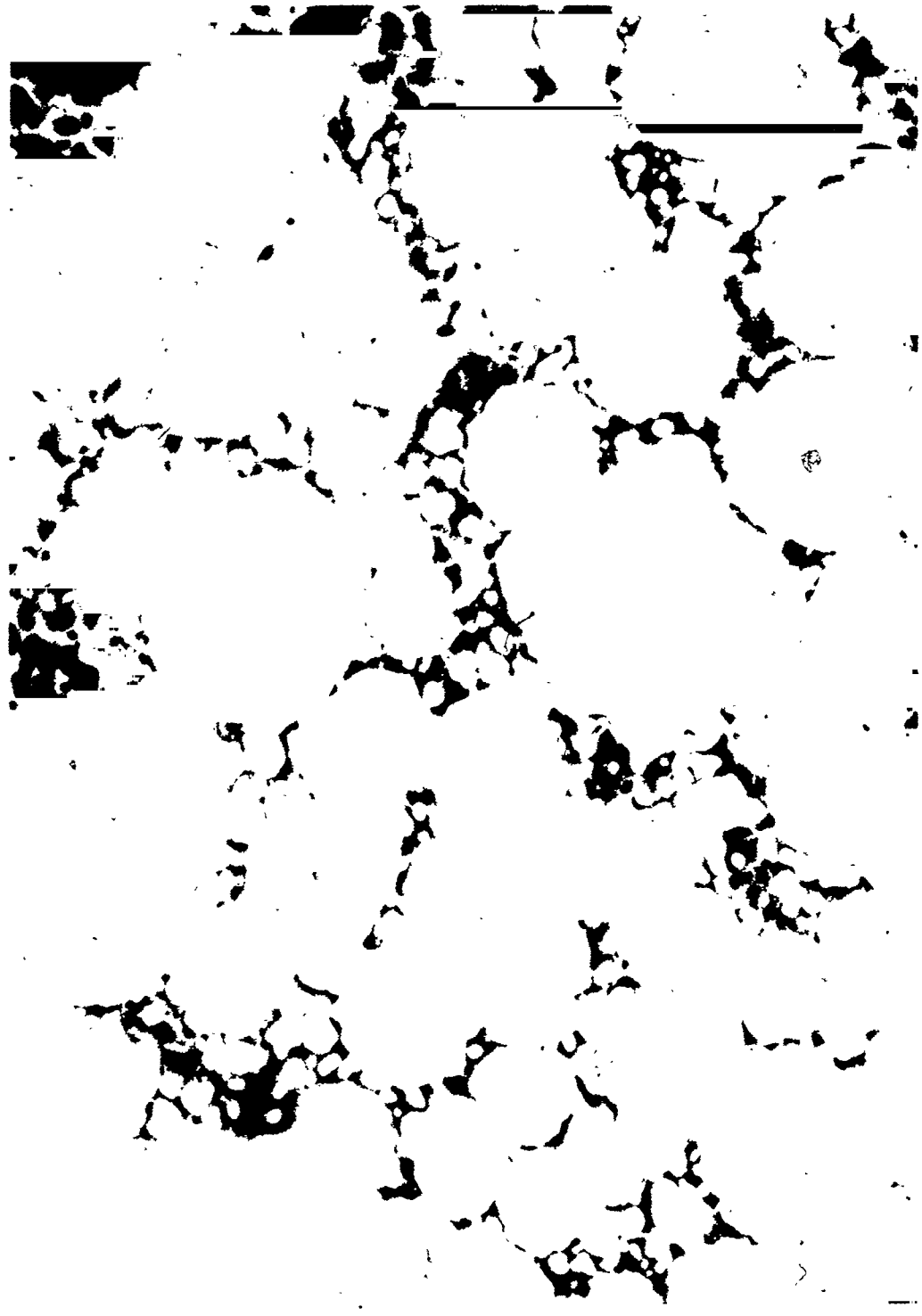

Figure 10. Presintered Foamed Titanium, 110X

Figure 11. Foamed and Sintered Titanium: Highly reflective metal contains some unidentified softer, lower reflective, interstitial phase (arrow). Dark areas are pores in sample. Reflected light, 563X, Enlarged 2X

The difficulties caused by oxide films on particles of aluminum and titanium led to consideration of other means of producing them as porous metals. These methods are summarized in the following sections.

B. Compacting Metal Powders with Pore Formers

A method of producing porous metals consists of compacting aluminum or titanium powders with a pore-forming material. This is done at pressures calculated to cause mechanical breakage of the oxide-film on the metal particles. Metal-to-metal contact is thereby obtained. The mixtures consisted of various percentages by weight of aluminum and titanium powder and an inert material which would volatilize during heating in vacuum.

Finely divided sodium chloride was used first as the volatile pore-forming material. The aluminum samples were pressed at 20,000 psi and sintered for one hour at temperatures from 1150 to 1200°F and an absolute pressure of 0.1 micron. The volatilization of the sodium chloride was incomplete in this vacuum and temperature range.

Mixtures of aluminum powder and naphthalene, as the low temperature volatile pore-forming medium, were next prepared and pressed at 20,000 and 40,000 psi. These were sintered in vacuum at temperatures up to 1200°F. Samples with a porous structure were obtained. However, the pore system was very irregular, and the samples were weak and powdery. The existence of unbroken oxide films was assumed to have inhibited sintering.

Titanium and titanium hydride powders were blended with ground sodium chloride granules, pressed 20,000 and 40,000 psi, and vacuum sintered by heating to 2300 or 2500°F and holding for one hour in vacuum. The titanium hydride, which dissociates above 500°F to titanium and hydrogen, was selected to act as a reducing agent during sintering. The cross-sections of the sintered titanium samples had a uniform pore structure. There was no evidence of sodium chloride residue. Though the densities of the sintered materials were excessive (between 48% and 51% of theoretical), the samples sintered at 2500°F were strong and somewhat ductile. Materials of lesser density, below 35% of theoretical, and samples sintered at 2250-2300°F exhibited a slight degree of sintering but were weak, brittle and powdery.

C. Melt Impregnation of Bed of Pore Formers[1]

A concept developed by Frankfort Arsenal involved pouring molten aluminum into a bed of salt granules, cooling, and subsequently leaching out the salt. This process has a serious weakness in that the pores are

not spherical. This is due to the angular shape of the salt granules which produces many irregular cracks throughout the material. Samples of this material are illustrated in Figure 12.

It was decided to follow the above method but to use salts with hollow spherical grains, and control pore size by controlling grain diameter. Density and pore size would be governed by the proportion of salts in relation to volume. A search for suitable salts yielded the materials listed in Table C-22.

A heated mold 3" diameter x 24" long was designed and built for pouring and infiltrating a bed of salts with aluminum melts. Figure 13 illustrates this equipment. Details are given in Appendix B.

Hollow spherical potassium chloride was selected for the first experiment. However, this material was not available in the desired form in adequate quantities. The same was true of potassium bromide. Sodium bromide of coarse, solid, and somewhat spherical form was finally selected. The temperature of the salt bed within the casting furnace was raised to 1300°F to gain control experience in establishing equilibrium at that temperature level.

The operation proceeded satisfactorily and a control procedure was established. During these trials, however, vapor was observed emanating from the salt bed at temperatures below 1300°F. Investigation disclosed some breakdown of the salt grains and considerable filling of the interstitial spaces with fused salt in the upper part of the bed. If molten metal had been poured into the bed, it is highly improbable that satisfactory penetration of the salt would have occurred. The salt used appeared to be $NaBr \cdot 2H_2O$ instead of the desired NaBr. Hydrated sodium bromide is unlikely to advance the proposed technology.

The difficulties encountered in obtaining salts of suitable composition, size and shape made it doubtful that tests could be successfully completed within the contractual time. This part of the investigation was, therefore, discontinued. It is not intended, however, to minimize the possibility of ultimate success with the Frankfort Arsenal concept, given time and the availability of suitable materials.

D. Hydrochloric Acid Foaming of Metal Powders

This method of making porous aluminum and titanium involved mixing or suspending the metal powder in isopropyl alcohol and adding hydrochloric acid. Due to the subsequent evolution of hydrogen and heat, this slurry expanded and, upon cooling, set up in a strong "as-cast" green state.

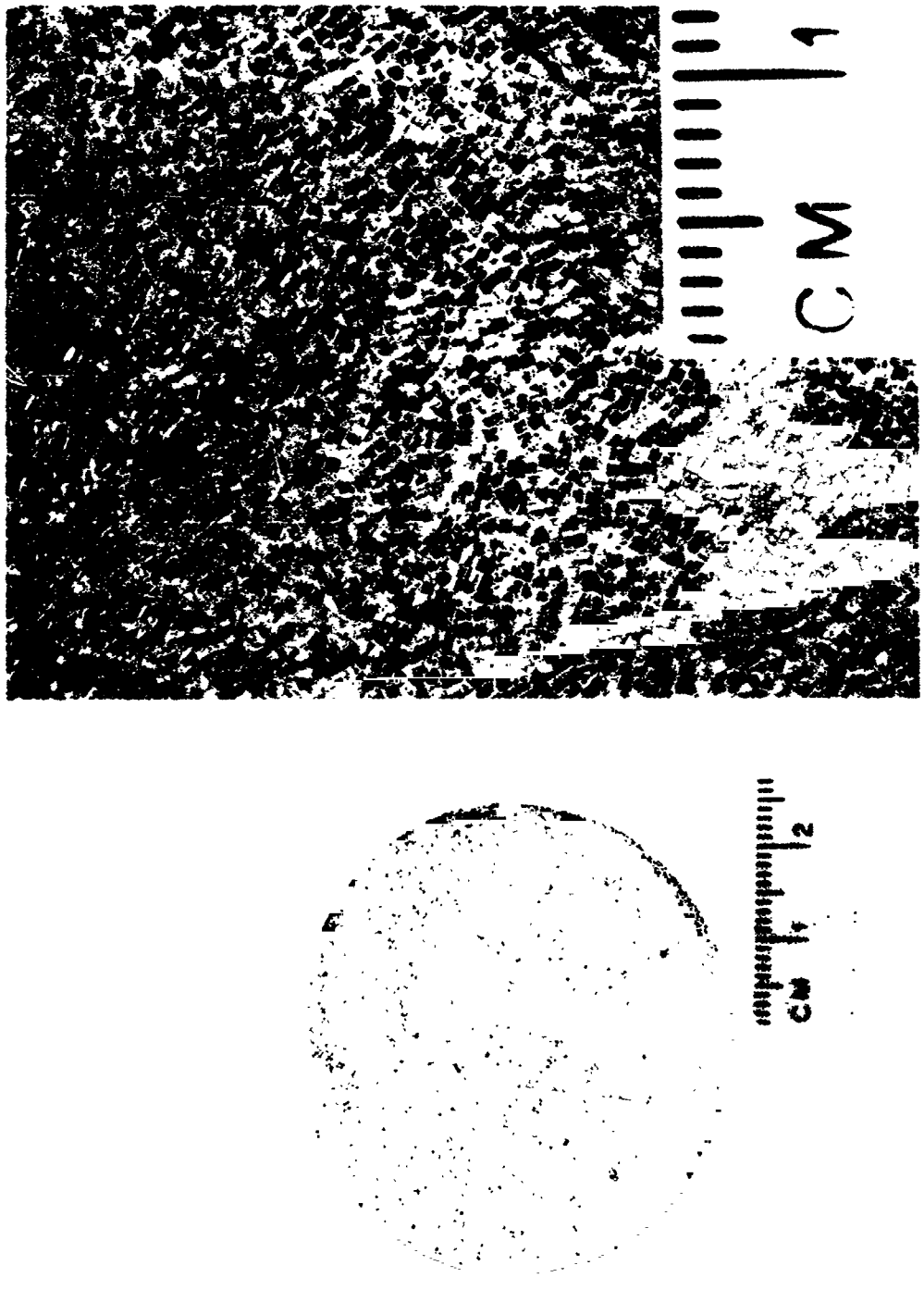

Figure 12. Porous Aluminum with Cubical Pores made by Frankfort Arsenal Process

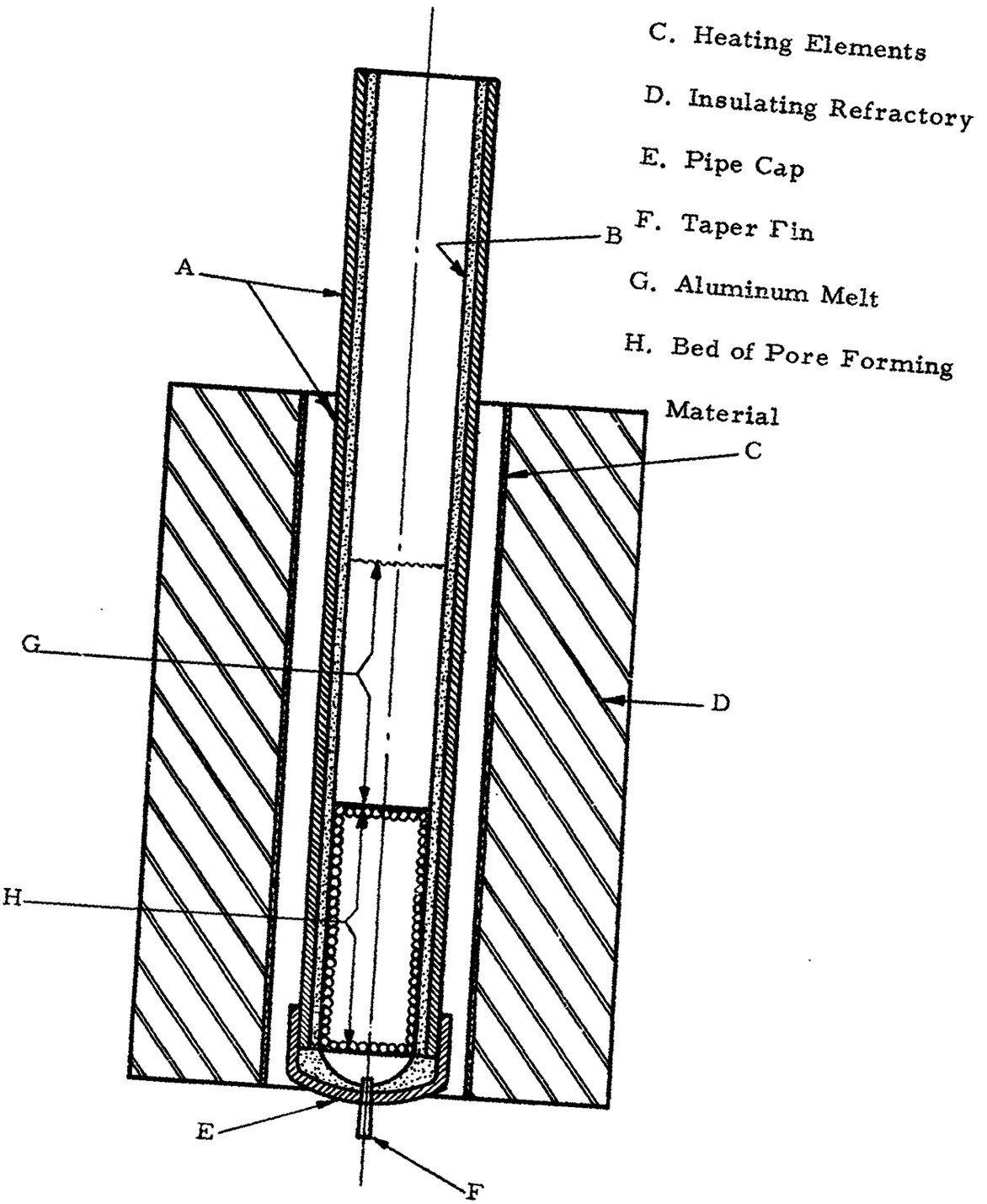

Figure 13. Mold Design and Furnace Setup for Pouring Molten Aluminum

Aluminum samples were presintered by heating to 400°F and holding one hour in vacuum and then heating to 600°F and holding for 6 hours in vacuum to drive off all volatiles prior to final sintering. The samples were final sintered at 1190°F for 6 hours at vacuums less than 0.1 microns (Hg). Good control of the pore size was not achieved as it ranged from a few thousandths to 1/4 inch diameter. Some sintering was observed, but the bonding was weak, friable and non-continuous between particles.

The titanium samples were soaked similarily at low temperatures and final sintered in a vacuum at 2550°F for 3 hours. The resulting material appeared fairly strong and smeared slightly during cutting, but fractured easily, however, when stressed. Coloration on the surfaces indicated that the samples were oxidized. In some cases, large surface pores allowed the oxidation to penetrate well into the material. Uniform pores were not obtained as they ranged from a few thousandths to 1/4 inch diameter.

E. Foaming Molten Metal[2&3]

Some producers make foamed aluminum by dispersing selected hydrides in molten aluminum or aluminum alloys. The hydride acts as a foaming agent by the delayed evolution of hydrogen. Aside from controlling the melt temperature and ratio of diameter to height of the sample melt, another factor produces a large scattering of pore sizes. This factor is the amount of dross at the liquid-metal and container interface. Samples of this material obtained had coarse, irregular pores much as in the powder, ispropyl alcohol, and hydrochloric acid method.

III. MACHINABILITY OF FOAMED METALS

Due to the severe shrinkages which occur during the manufacturing cycle, it is virtually impossible to produce a final sintered foam metal configuration within acceptable tolerance limits. To produce useable shapes of foamed metals and to fabricate test specimens, forming and machining experiments were conducted. Porous stainless steel and nickel can be shaped, but the operation distorts the pore structure and results in a surface area unlike the interior mass of material. Experiments involving several machining methods showed that foamed metals are relatively easy to machine and can be processed by normal machine shop practices. Special tools and fixtures may be required in some instances to expedite the machining operation.

All of the foamed metals produced had large, non-uniform dimen-

sional changes during manufacture. From the "as-cast" to the sintered shape, the range of shrinkages was as follows:

Volume	40 to 80%
Length	10 to 25%
Width	15 to 35%
Height	20 to 50%

The causes of shrinkage are described in Appendix A-2. Shrinkage can be controlled to produce foamed pieces of a particular shape, but the number of factors to be controlled and the time required make this expensive and impractical. Porous metals can be cast, however, in rough approximation of the desired shape. Machining is then used to produce final forms to reasonable tolerances. Production scrap will thereby be minimized with corresponding savings in raw material costs of foamed metal articles. It is concluded that machining will provide the most satisfactory and economical method of producing any desired configurations.

To obtain suitable pieces for mechanical property testing, sintered samples were machined. Irregularly shaped blocks of sintered metal were cut to approximate size on a band saw. The rough pieces obtained were lathe turned to produce cylinders for compression and tensile testing. Square bars required for flexural testing were shaped on a grinding machine or end mill. Cutting threads in foamed metals by lathe turning, drilling and tapping were explored.

A. Band Saw Cutting

Foamed metals were rough shaped without difficulty on a band saw. A DoAll model 1612-3 Contourmatic Band Saw and Filing Machine equipped with a servo-feed control and a powered table was used. The work was clamped on the table in such a way as to prevent closing of the cut and pinching of the material on the blade after the blade passed through. If the material pinched the blade, the cell walls were smeared.

Work speeds and pressures were varied with the sample's density. High density samples required high feed pressures and slower work speeds. A saw speed of 95 ft. per minute and a 5 lb pressure was satisfactory for most foamed metals. Cuts were made satisfactorily, both dry and with coolant, but it was thought that in most cases any coolant would be undesirable because of the hazard of contamination. The band saw operating conditions for foamed metals are listed in Table 2.

Table 2: Band Saw Operations for Foamed Metals

Material	Saw Blade	Saw Speed feet/min.	Work Feed Pressure (lb)
Molybdenum	10 Pitch Raker	95-150	5 and higher
H-11 Tool Steel	10 Pitch Raker	95-150	5 - 10
316 Stainless	8 Pitch Raker	95	5
Nickel	8 Pitch Raker	95	5

B. Lathe Turning

Foamed metals turned reasonably well. Some smearing of the surface was experienced, but this was corrected by slower cutting speeds and sharp tools. A minor difficulty was supporting and holding the work in the lathe due to the metal's ductility and compressibility. Tensile test specimens could not be supported at the tail-stock end by normal centering devices. Tightening the center compressed and crushed the material with the result that the work loosened and did not revolve on a true center. Chuck mounted collets also had to be continually tightened for the same reasons. To correct this, pieces of material were supported in long collets with only half its length protruding for turning. This increased the surface holding area and allowed higher total holding pressures. The lathe operating conditions are listed in Table 3.

Table 3: Lathe Turning Operations for Foamed Metals

Material	Tool Material	Tool Angle Degrees	Tool Speed in/min.	Depth of Cut		Work Spee RPM
				Rough in.	Finish in.	
Molybdenum	High Speed Tool Steel	10	.0046	.250	.010	540 - 900
H-11 Tool Steel	Carbide	10	.003	.050	.005	540
316 Stainless	Carbide	10	.002 - .003	.030	.005	540

C. Milling

Foamed molybdenum was readily milled, giving a good surface

without smearing. A wide range of tool and work speeds and depth of cut could be used. Several samples were milled as fast as the machine would permit. A maximum of 3/4" of material was removed at one cut. Though the surface was true, it was rough. Low density materials were more difficult to mill, due to larger pores and unsupported walls. Large pieces of material were pulled away rather than sheared off at the tool tip. Low feed rates and high tool speeds were found best for low density material. Finish cuts were generally best made at high tool speeds and feed rates.

Tool steel and 316 stainless steel did not mill as well as molybdenum because of their ductility. The observations made for molybdenum, however, generally hold for these materials. Carbide tipped tools were best, but surface finishes were rather rough throughout the range of tool rpm, feed rates and depths of cut. Mill operating conditions are listed in Table 4.

Table 4: Mill Operations for Foamed Metals

Material Being Machined	Tool				Depth of Cut inches		Feed Speed in/min.	
	Material	Type	Dia. in.	Speed rpm	Rough	Finish	Rough	Fini
Molybdenum	High Speed Tool Steel	4 flute end mill	.75	750	no limit	0.010	2.5-9.5	4.7
Molybdenum	High Speed Tool Steel	Sheel end Mill	2.5	1115	no limit	0.010	2.5-9.5	4.7
H-11 Tool Stl	Carbide	3 flute	2.5	2720	no limit	0.010	2.5-9.5	9.5
316 Stainless	Carbide	3 flute	1.5	660-1120	no limit	0.015	4.4-9.5	9.5

D. Grinding, Drilling, and Tapping

All the grinding was accomplished as follows:

Wheel Size	5 in. dia., 1/2 inch face
Wheel Speed	2850 RPM
Lubrication	None

Grinding molybdenum presented no real difficulties. There was no limit to the depth of cut. There seems to be no reason why normal grinding operations cannot be considered practical for this material.

Smearing was considerable with H-11 tool steel. To minimize smearing, a maximum surface cut of 0.010 inches and slow feed speeds were found necessary. The same criteria would apply to 316 stainless steel.

No problems were encountered in drilling foamed metals when specifications for milling were followed. The considerations in both cases are very similar. Tapping drilled holes with standard coarse threads was not successfully performed. Because of the friability of molybdenum, the tap does not obtain a "start" in a drilled hole. Special tooling with suitable thread configurations might facilitate tapping.

E. Summary

Experiments showed that foamed metals have a machinability rating of "very easy". Figure 14 illustrates several shapes machined from foamed metals. The principal problem in all operations was to prevent smearing the ductile cell walls. Foamed metal has a mat appearance with open pores when machined properly, but rapid or careless machining gives a shiny surface and almost completely closed pores. Tools for machining ductile foamed metals must be sharp, preferably carbide. The operation must be carried out at low feed and tool speeds creating minimal heat. When a coolant is used, the machining can be performed at faster cutting rates. A suitable coolant used was DoAll's H.D. 660. However, using a coolant is not recommended because of the contamination of the interior pores.

Molybdenum was the easiest foamed metal to machine because of its brittle nature at room temperature. This property caused the material to shear readily and chip off at the tool tip rather than bend and smear. With fast machining speeds, however, the material was heated above the brittle to ductile transition temperature and would bend and smear.

IV. THERMAL PROPERTY TESTING

Thermal property testing was subcontracted to Melpar, Inc., Falls Church, Virginia. The tests were confined to thermal expansion, conductivity, and stability for nickel and 316 stainless steel.

A. Thermal Stability

Prior to conducting mechanical tests at various temperatures on foamed nickel and stainless steel, the maximum temperature at which these would support their own weight was determined. Initially, a foamed metal bar 1/2 x 1/2 x 5 inches was placed on 2 supports with a 4 inch span.

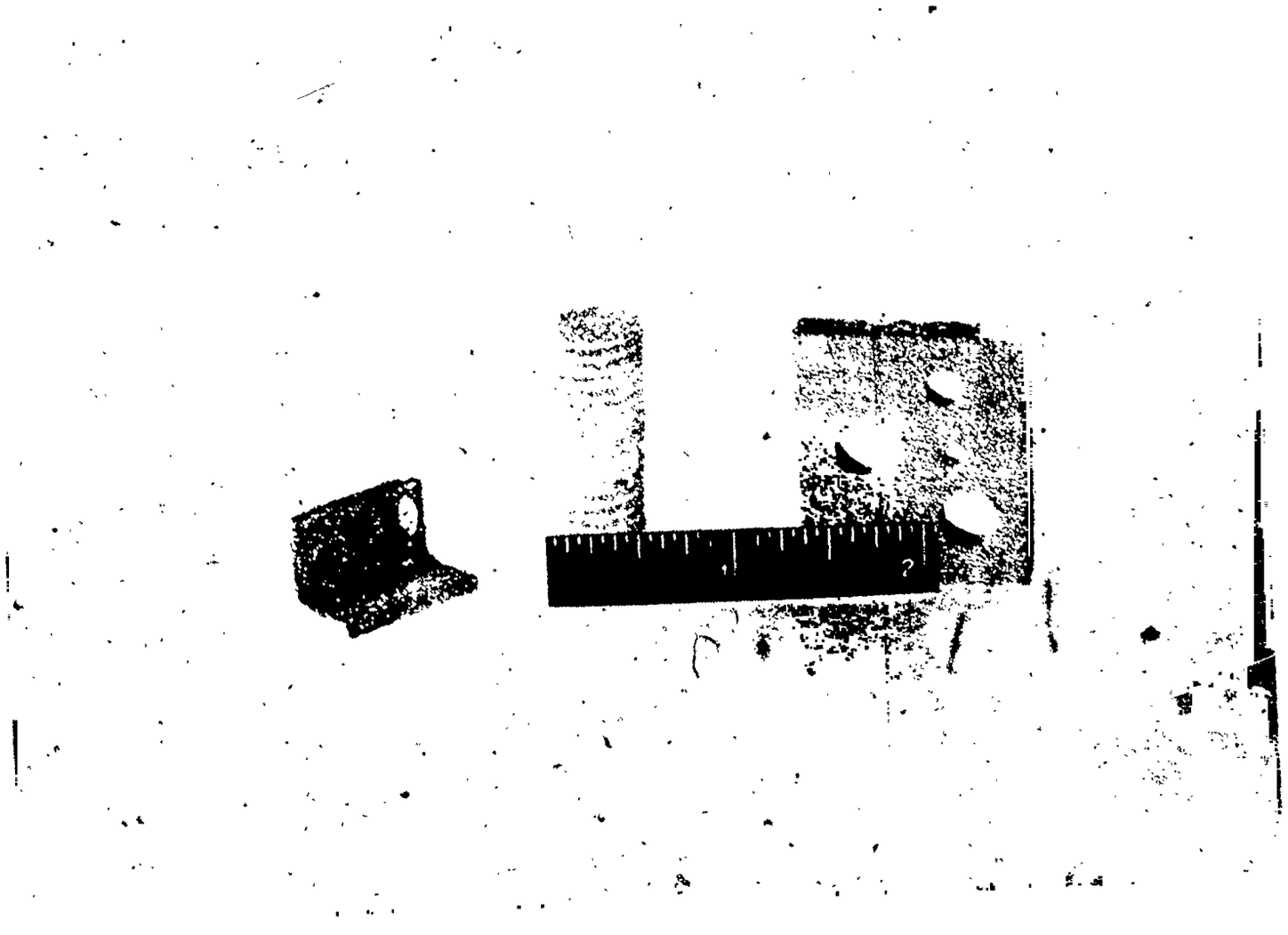

Figure 14. Machined Shapes of Foamed Metals

Heat was then applied slowly until the sample sagged 0.010" under its own weight. This method was abandoned since lateral warpage of the specimens occurred. The test specimens were then loaded lightly using a pressure dial deformation indicator and the maximum useful temperature determined at a sag of 0.010 inch. The results for the foamed nickel and stainless steel are listed in Table 5.

Table 5: Maximum Useful Temperature of Foamed Nickel and 316 Stainless Steel

Foamed Metal	Density, % of Theoretical	Maximum Useful Temperature, °F
Nickel	15	1675
Nickel	18	1675
Nickel	27	2500
Stainless Steel	18	1875
Stainless Steel	27	2000

B. Thermal Expansion

Thermal expansion measurements were made on 1/2 x 1/2 x 2 inch specimens with a sapphire rod dilatometer as illustrated in Figure 15. Thermal expansion was nearly linear between 70 and 1900°F for both foamed metals. In the region between -320 and 70°F the relation between thermal expansion and temperature is nonlinear.

Table C-17 presents the values for thermal expansion of foamed nickel of 18% and 27% density. Figure 16 illustrates these values with thermal expansion values for bar stock [4] included for comparison. It can be seen that the curves for the foamed and solid metals are the same.

Table C-18 contains thermal expansion data on foamed 316 stainless steel of 18% and 27% density. The results are charted and compared to bar stock[4] in Figure 17. As noted from Figure 17, a slight deviation occurs at temperatures above 500°F. Again, it can be seen that the curves for the solid and foamed metals are essentially the same, except for the slight deviation at higher temperatures.

The coefficients of thermal expansion for foamed nickel and foamed stainless steel were calculated and are compared with the solid metals [5] in Table 6. No high temperature values were found in the literature for nickel bar stock. It should be noted that the co-

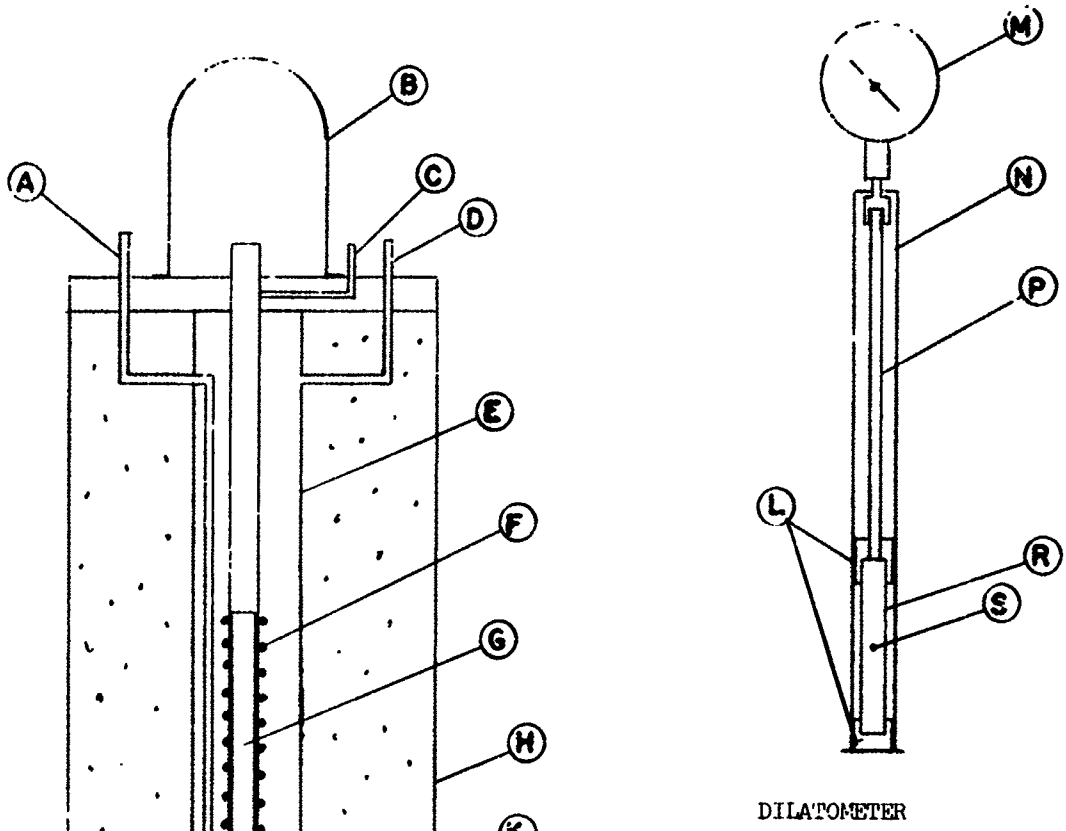

Legend

A - Liquid Nitrogen Inlet
B - Bell Jar
C - Vacuum Port
D - Air Vent
E - Metal Dewar
F - Heater Winding
G - Copper Can
H - Metal Housing
K - Insulation
L - Sample Aligner (Quartz)
M - Dial Indicator
N - Quartz Tube
P - Quartz Rod
R - Specimen
S - Thermocouple

Figure 15. Diagram of Apparatus for Thermal Expansion Measurements

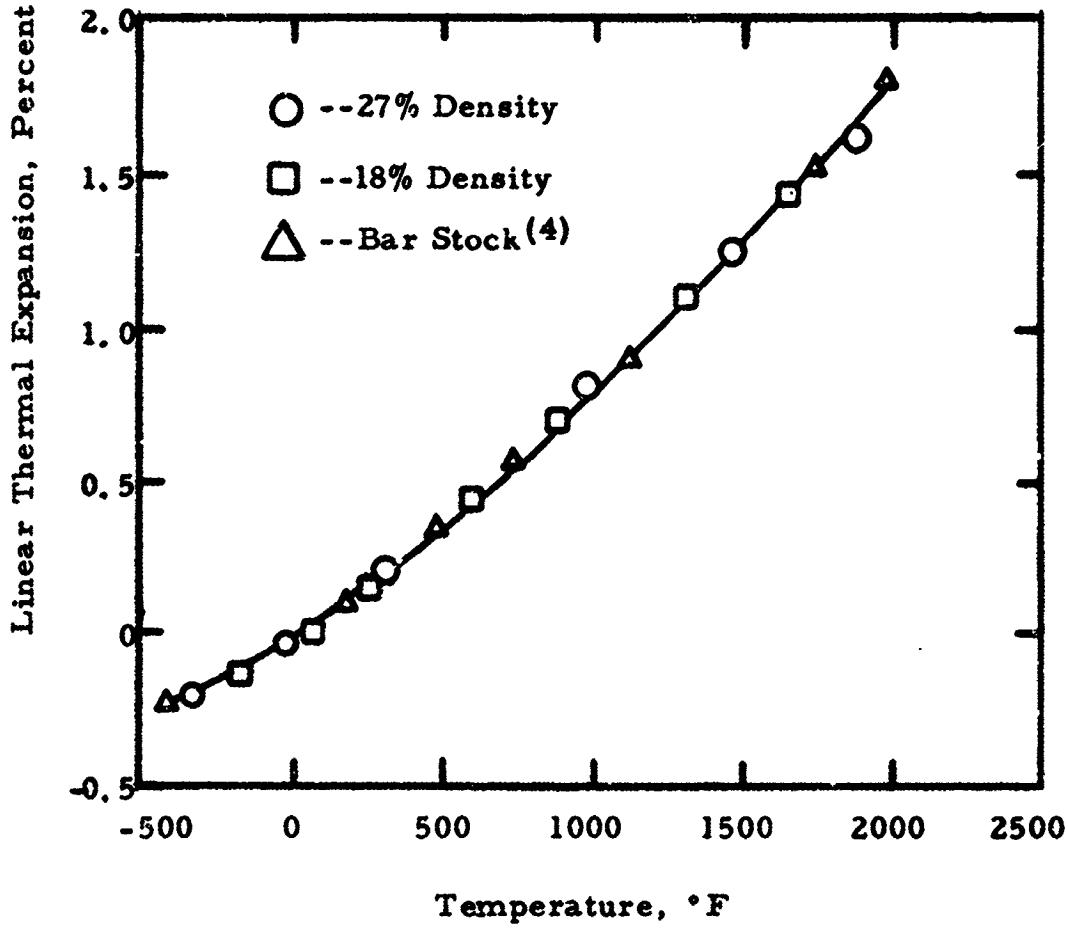

Figure 16: Thermal Expansion vs Temperature for Foamed and Bar Stock Nickel

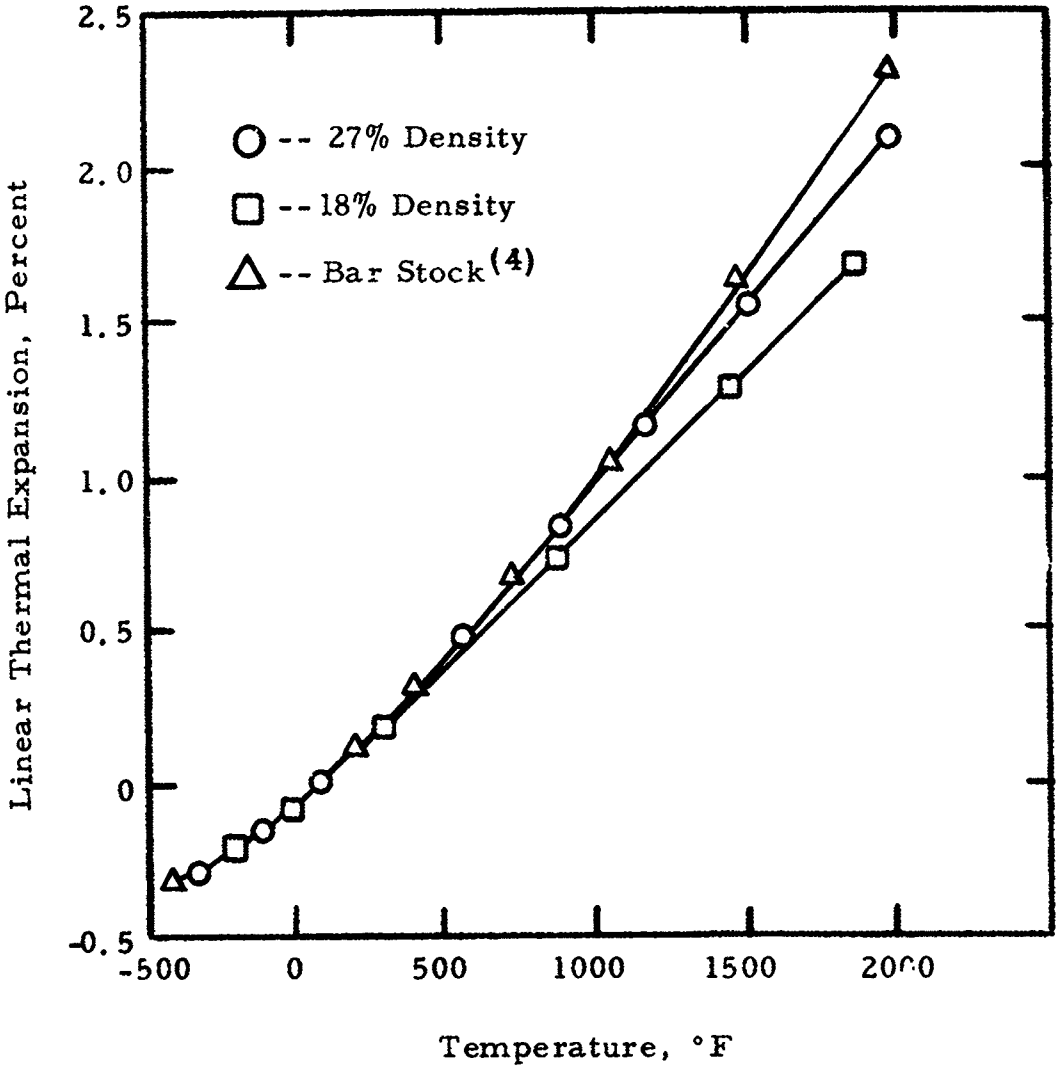

Figure 17. Thermal Expansion vs Temperature for Foamed and Bar Stock 316 Stainless Steel

efficients of expansion of these metals in the solid and foamed states do not differ greatly. The same results may be expected with other foamed metals such as molybdenum and H-11 tool steel.

Table 6: Coefficients of Thermal Expansion for Foamed and Bar Stock Nickel and 316 Stainless Steel

Material	Coefficient of Thermal Expansion
Nickel:	
Bar Stock[5]	7.4×10^{-6}/°F (32-212°F)
27% Density Foam	8.75×10^{-6}/°F (72-1900°F)
18% Density Foam	8.88×10^{-6}/°F (72-1675°F)
316 Stainless Steel:	
Bar Stock[5]	11.1×10^{-6}/°F (32-1500°F)
27% Density Foam	10.45×10^{-6}/°F (72-2000°F)
18% Density Foam	9.1×10^{-6}/°F (72-1875°F)

C. Thermal Conductivity

Thermal conductivities of foamed metals were determined by means of a radial heat flow technique using stacked discs. Fourteen discs of 2 inches in diameter were used; thirteen were 1/2 inch thick and one was one inch thick. Protection of the specimens from the atmosphere was not quite adequate, as indicated by some discoloration of the samples. As illustrated in Figure 18, the thermal conductivity of foamed nickel decreases to a minimum at about 800-900°F and then increases with temperature. A similar minimum conductivity occurs at 700-750°F for solid nickel. This minimum point is related to the magnetic transformation or Curie temperature of nickel. This is actually a temperature range where the material transforms from ferromagnetic to paramagnetic. Theoretically, the intensity of magnetization at a temperature is a function of the degree of atomic order. At higher temperatures, as the disorder increases because of thermal excitation, a sudden and almost complete collapse of atomic order occurs in the structure and correspondingly in the magnetization, thereby changing thermal conductivity. Solutes or alloying elements added to magnetic materials linearly affect the Curie temperature of nickel. In Figure 18, the plotted values of thermal conductivity of solid nickel[4] were multiplied by the fraction of theoretical density of the foamed metals for comparison.

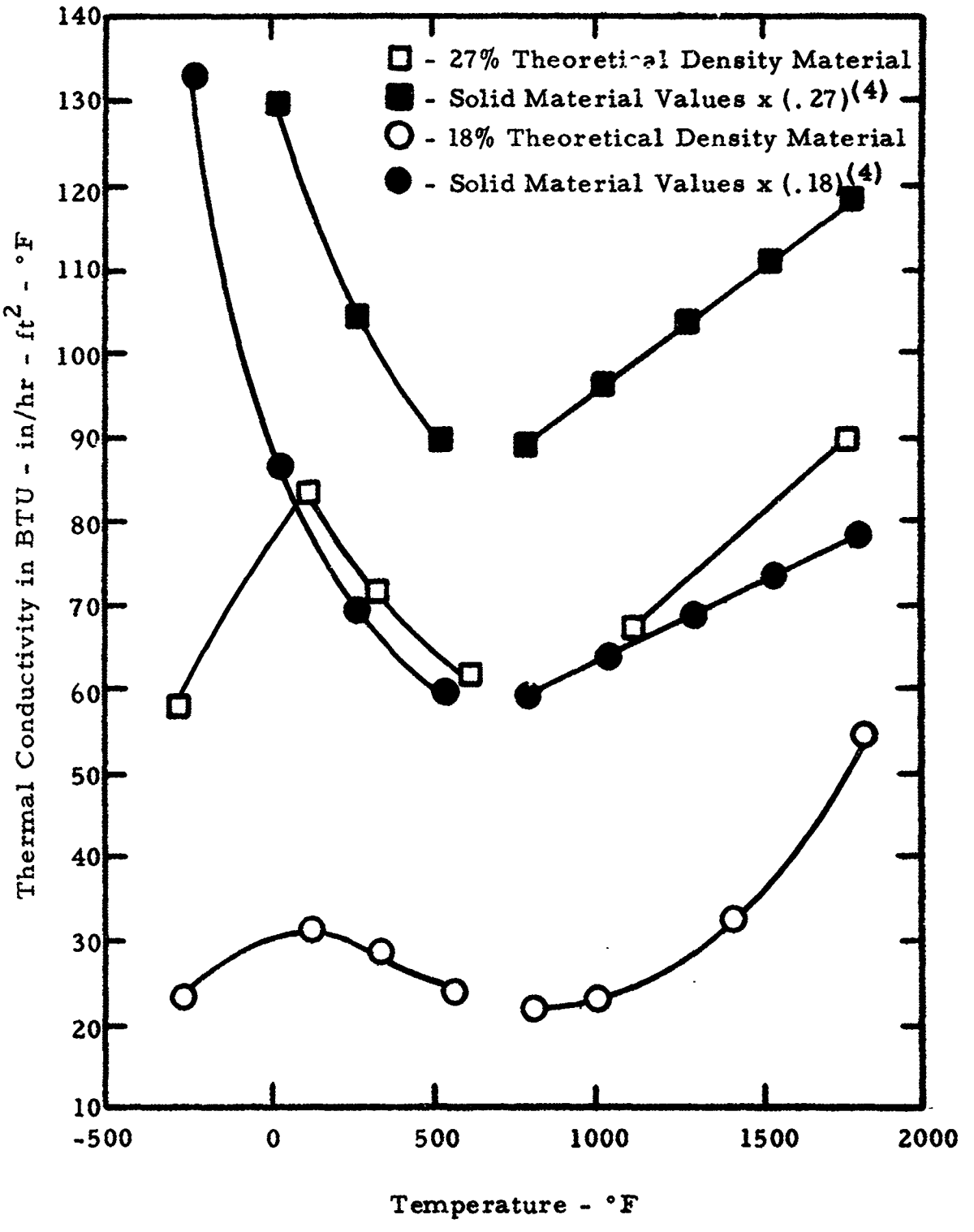

Figure 18. Thermal Conductivity vs Temperature for Foamed Nickel

Table C-19 compares the thermal conductivity of solid nickel[4] and foamed nickel over a range of temperatures. It illustrates the insulating value of the foamed metals.

Table C-20 compares the thermal conductivity values of 18 and 27% density foamed 316 stainless steel and those for the solid metal[4].

As in the case of nickel, the values for thermal conductivity of the fully dense stainless steel have been multiplied by 0.18 and 0.27 respectively, to provide rough comparisons with the values for the foamed metal in Figure 19. The insulating qualities of the foamed products are again evident.

V. MECHANICAL PROPERTY TESTING

A portion of the mechanical property testing was subcontracted to Melpar, Incorporated of Falls Church, Virginia, but the preponderance of testing was conducted at Ipsen Industries. Single test specimens of foamed nickel and stainless steel were tested by Melpar for strength properties at various temperatures. Room temperature testing of foamed molybdenum, H-11 tool steel and 316 stainless steel was conducted at Ipsen Industries.

Post-test specimens are shown in Figure 20, identified as follows:

Item 1. Failed 1/2 inch diameter x 4 inch long tensile specimen of 27% dense stainless steel.

Item 2. Compressive specimen, 1/2 inch square x 1 inch long, of 18% dense stainless steel.

Item 3. Shear strength specimen, 1/2 inch square x 4 inch long, of 27% dense stainless steel.

Item 4. Thermal stability specimen, 1/2 inch square x 5 inch long, of 27% dense nickel.

A. Tensile Tests

Melpar utilized an Instron Universal Testing Machine to measure the tensile strength values of foam metals. Standard threaded end pieces were machined and brazed to foamed metal rods of 1/2 inch diameter, 4 inches long for testing at elevated temperatures. Some specimens failed at the braze, and it was necessary to machine sections at the ends of the rods and fasten collets to them. The specimen usually failed near its midpoint.

Tensile tests were made at Ipsen with a Riehle Universal Testing

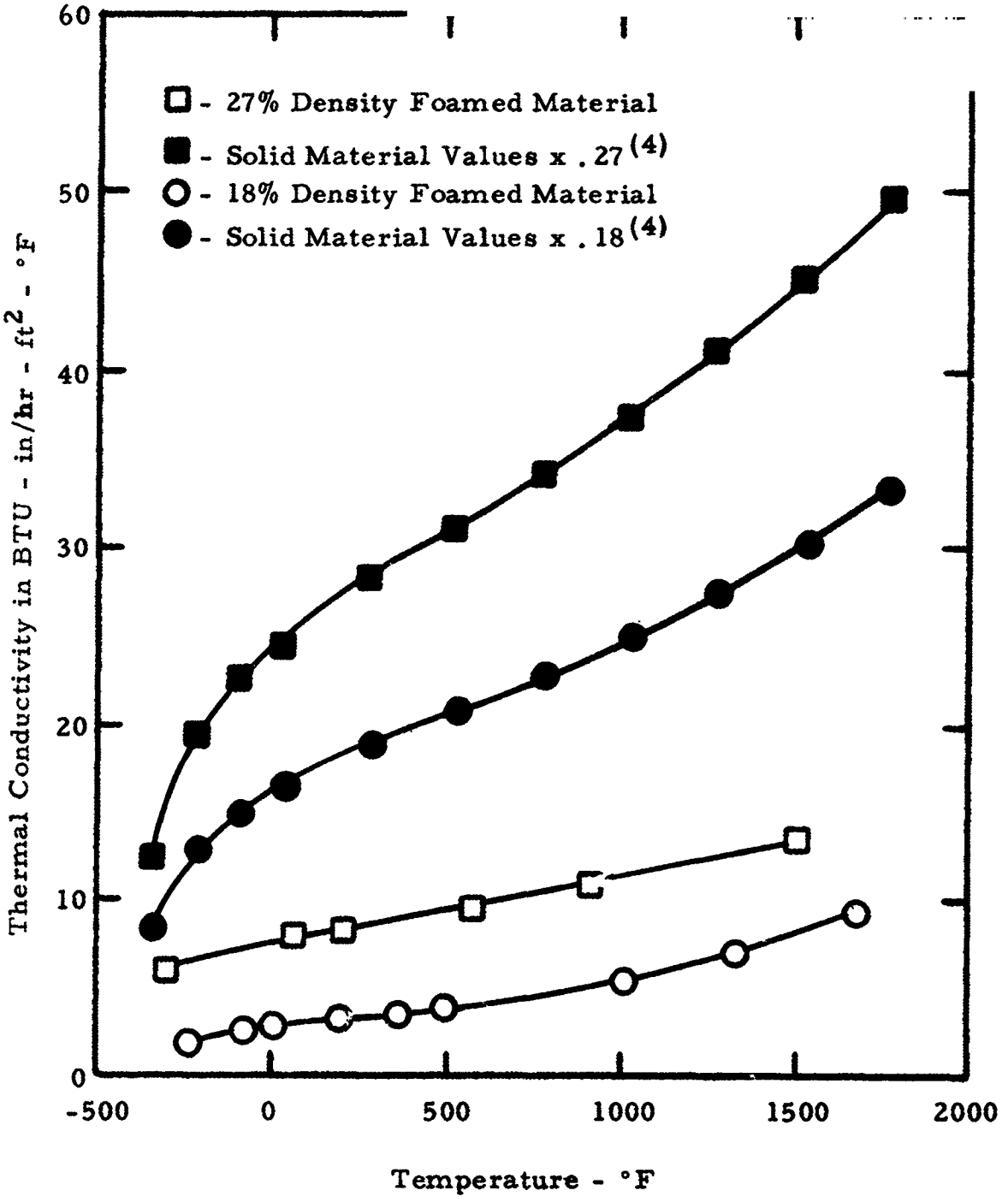

Figure 19. Thermal Conductivity vs Temperature for Foamed 316 Stainless Steel

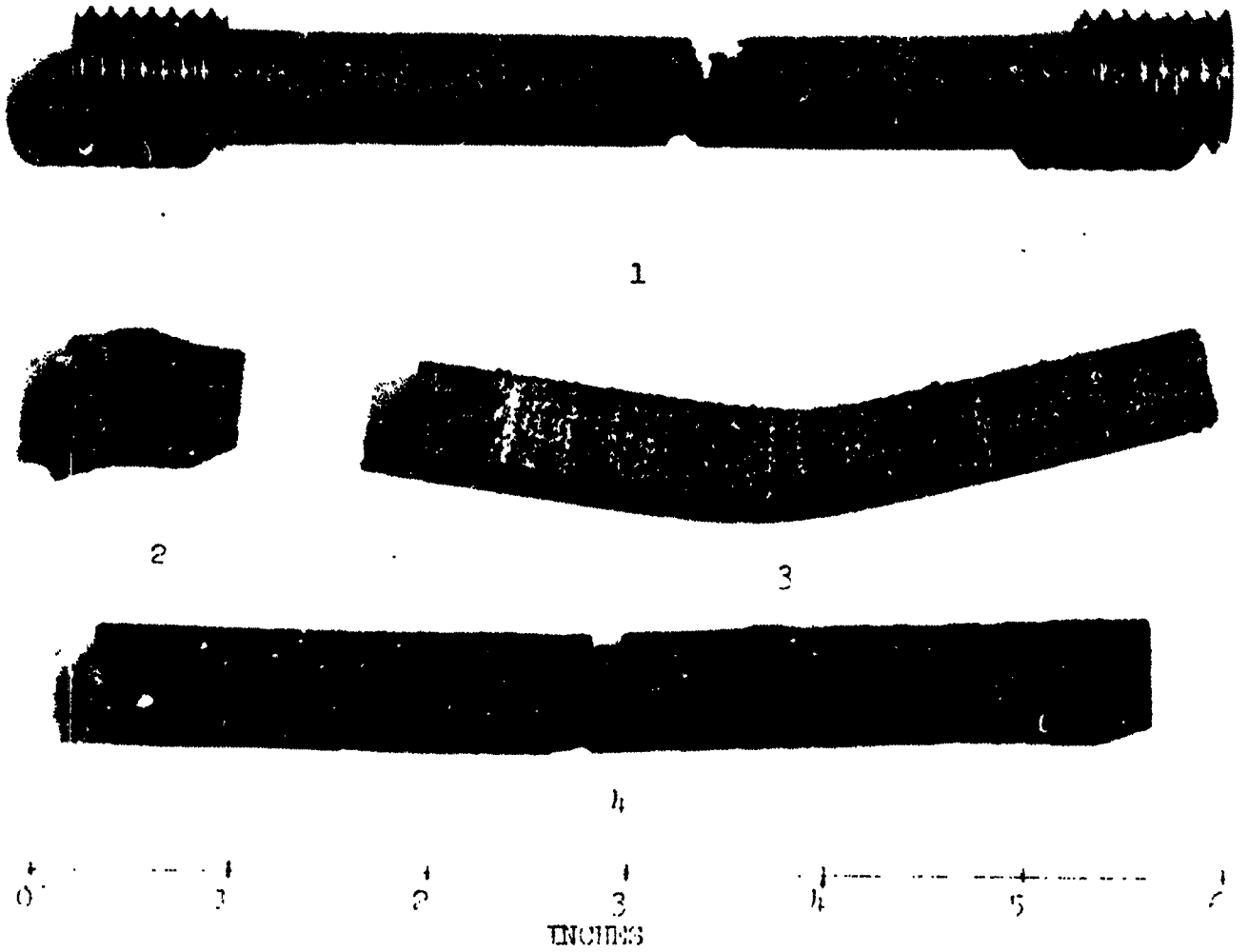

Figure 20. Post-Test Mechanical Property Specimens

Machine at a deformation rate of approximately 0.03 in/min. The standard threaded end pieces were epoxy bonded to foamed metal rods 1/2 inch diameter by 4 inches long for testing at room temperature. In rare cases the epoxy joint failed before the specimen. All tables listing strengths determined by the mechanical property testing are in Appendix C.

1. Foamed Molybdenum Tensile Strength Properties

Although the test results had a broad scatter, the trend was that strength increased as sintered density increased from 12 to 28% of theoretical. The dashed line through the center of the scattered points in Figure 21 represents the average tensile strength obtained from a linear regression analysis of tensile strength to fixed densities. The solid lines represent the approximate deviations from the average strength that can be expected.

All testing was conducted at room temperature where molybdenum is brittle. Because of brittleness ultimate tensile strengths had elongations less than 5 percent. Elevated temperature testing beyond the ductile-brittle transition, would reflect significant increases. Table C-1 in Appendix C lists the ultimate tensile strengths of foamed molybdenum at various densities.

2. Stainless Steel Tensile Strength Properties

The density of the foamed metal appears to have a considerable effect on the relationship between tensile strength and temperature in comparing the materials of 18 and 27% density as listed in Table C-2. Although the tensile strength of the 27% dense material decreased at a much greater rate than that of the 18% material, the relationship in each case followed a smooth curve as shown in Figure 22. The reason for the difference in tensile characteristics of the 18 and 27% density is not apparent.

Although 316 stainless steel is not hardened by heating and quenching, annealing and/or sintering with varying cooling rates may bring about a variation in physical properties. Such variations would be caused by the degree of carbide precipitation with very slow cooling or the induced residual stresses with rapid cooling or quenching.

The tensile strengths of wrought 316 stainless steel[5, 6] are given for comparison.

3. H-11 Tool Steel Tensile Strength Properties

Ambient temperature tensile test results of several samples of

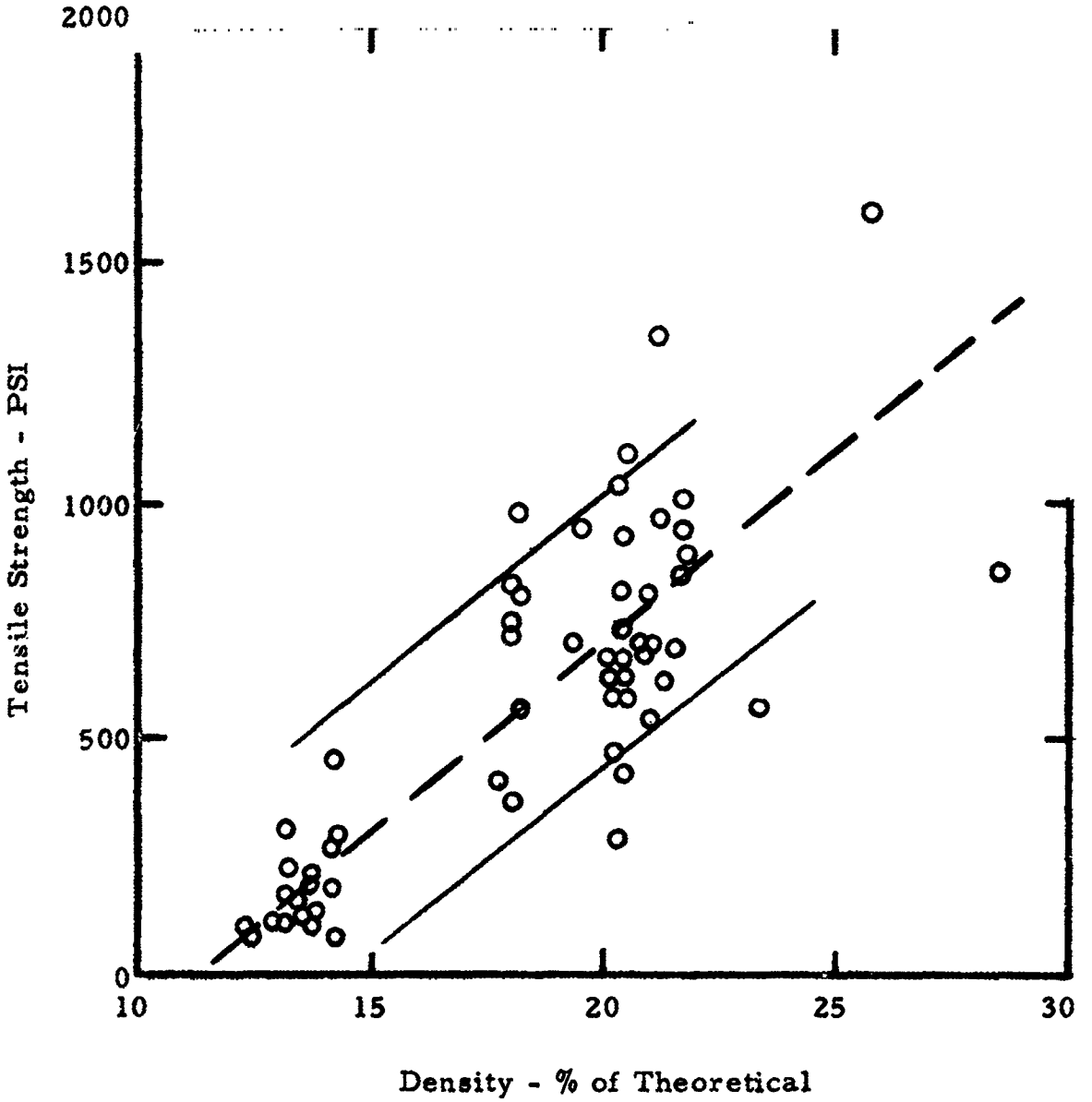

Figure 21. Ultimate Tensile Strength vs Sintered Density of Foamed Molybdenum

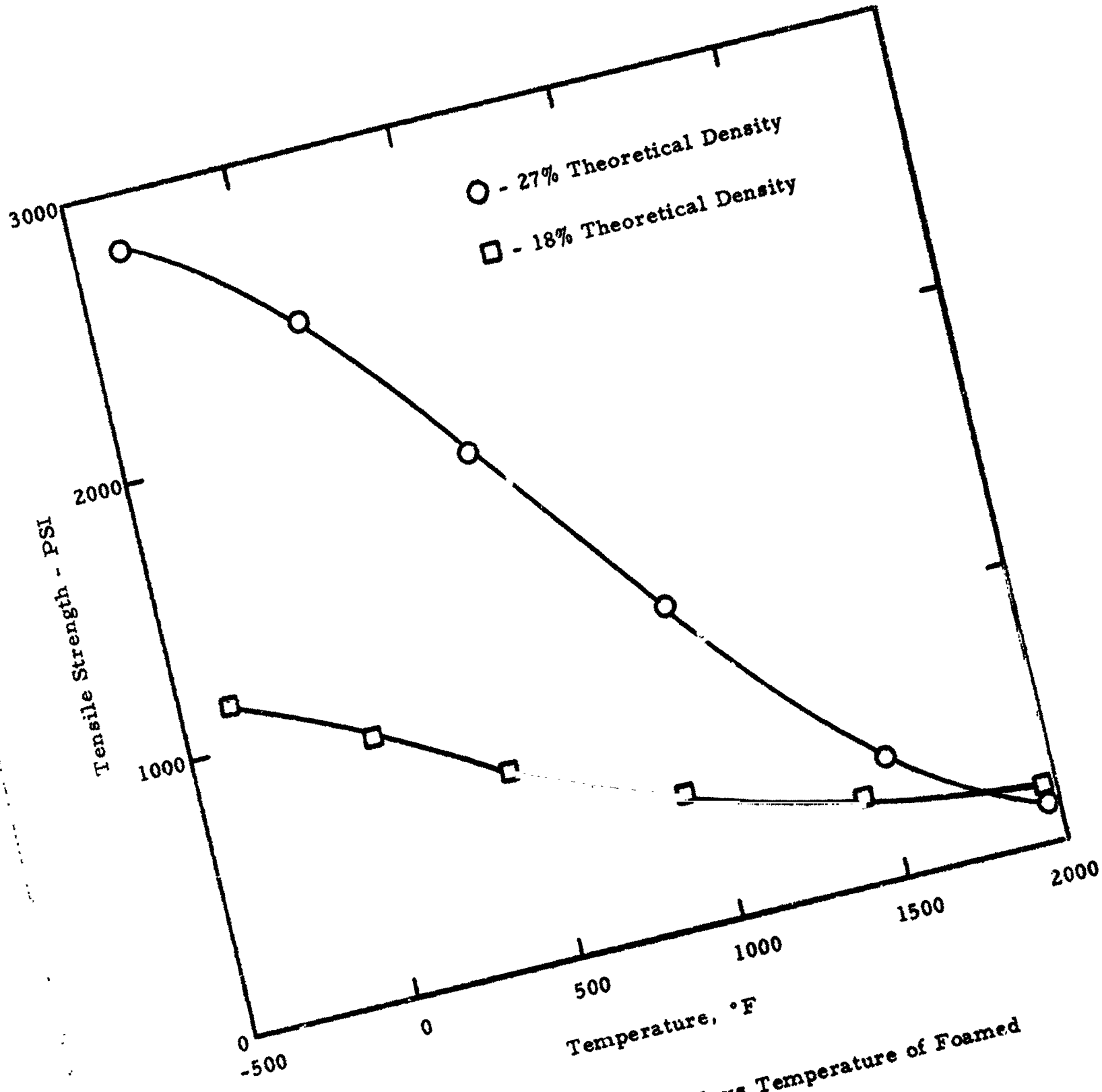

Figure 22. Ultimate Tensile Strength vs Temperature of Foamed 316 Stainless Steel

foamed H-11 tool steel are listed in Table C-3 and illustrated in Figure 23. They also show a general increase of strength with increasing sintered density. There are not enough data points to get a statistical analysis of the data. The dashed line represents an approximate average that could be expected.

4. Nickel Tensile Strength Properties

Two densities of foamed nickel were used to determine the tensile properties. Table C-4 shows the values obtained for samples of 18 and 27% of theoretical density. These are plotted in Figure 24. The decrease in tensile strength with increasing temperature is to be expected. There are very few data points to draw any conclusions from, but it appears that there is a range between 500 and 1250°F where the tensile strength decreases less rapidly with increasing temperature. This may be related to the Curie Temperature or magnetic transformation range of nickel.

B. Compressive Strength

Compressive yield values at various temperatures were determined by Melpar on 1/2 x 1/2 x 1 inch specimens. Compressive yield values at ambient temperatures were determined by Ipsen on 1/2 inch diameter by one inch long specimens. All of the materials, except samples of molybdenum, exhibited ductile properties. Since no ultimate strengths were reached in most cases, the yield point at 0.2% offset and the 2% and 10% total deformation values were taken from the load vs strain curves.

Foamed materials are difficult to evaluate in compression because of the structure of the material. The cushioning effect of the foamed structure results in high stress concentrations at the surface and lower stress concentrations in the core which may partly account for the irregular results.

1. Molybdenum Compressive Strength

This foamed metal was tested at a variety of sintered densities at ambient temperatures. The majority of specimens below approximately 20% density fractured at an ultimate compressive strength while specimens of higher density did not fracture in most cases. These specimens continued to deform beyond 10% at the same or increasing loads until the test was arbitrarily halted. The results are listed in Table C-5 and illustrated in Figures 25, 26 and 27. Again the results were erratic but do show a definite trend within wide limits of increased strength with increased density. The dashed lines on the figures represent the average compressive strength vs

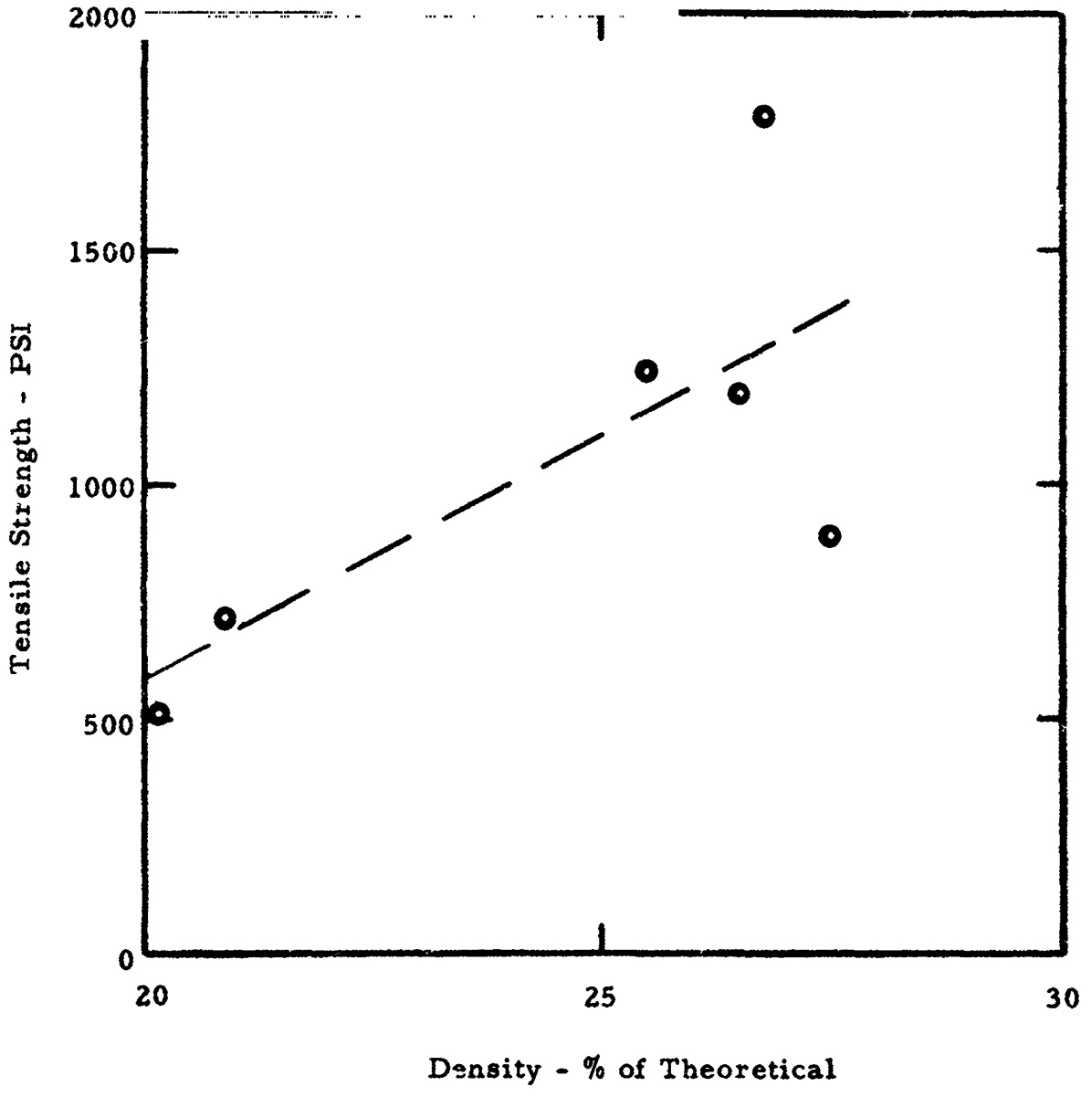

Figure 23. Ultimate Tensile Strength vs Sintered Density of Foamed H-11 Tool Steel

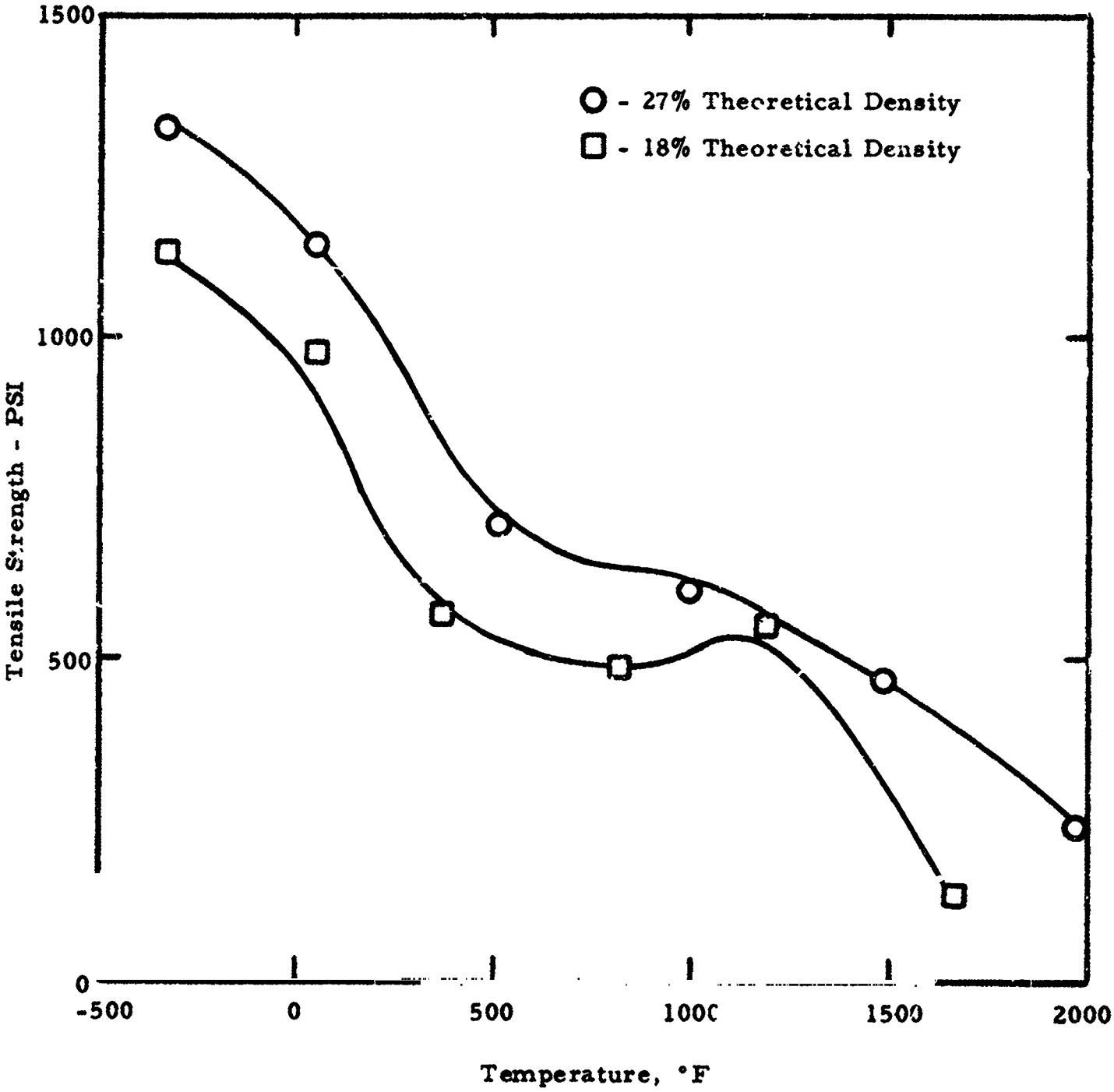

Figure 24. Ultimate Tensile Strength vs Temperature of Foamed Nickel

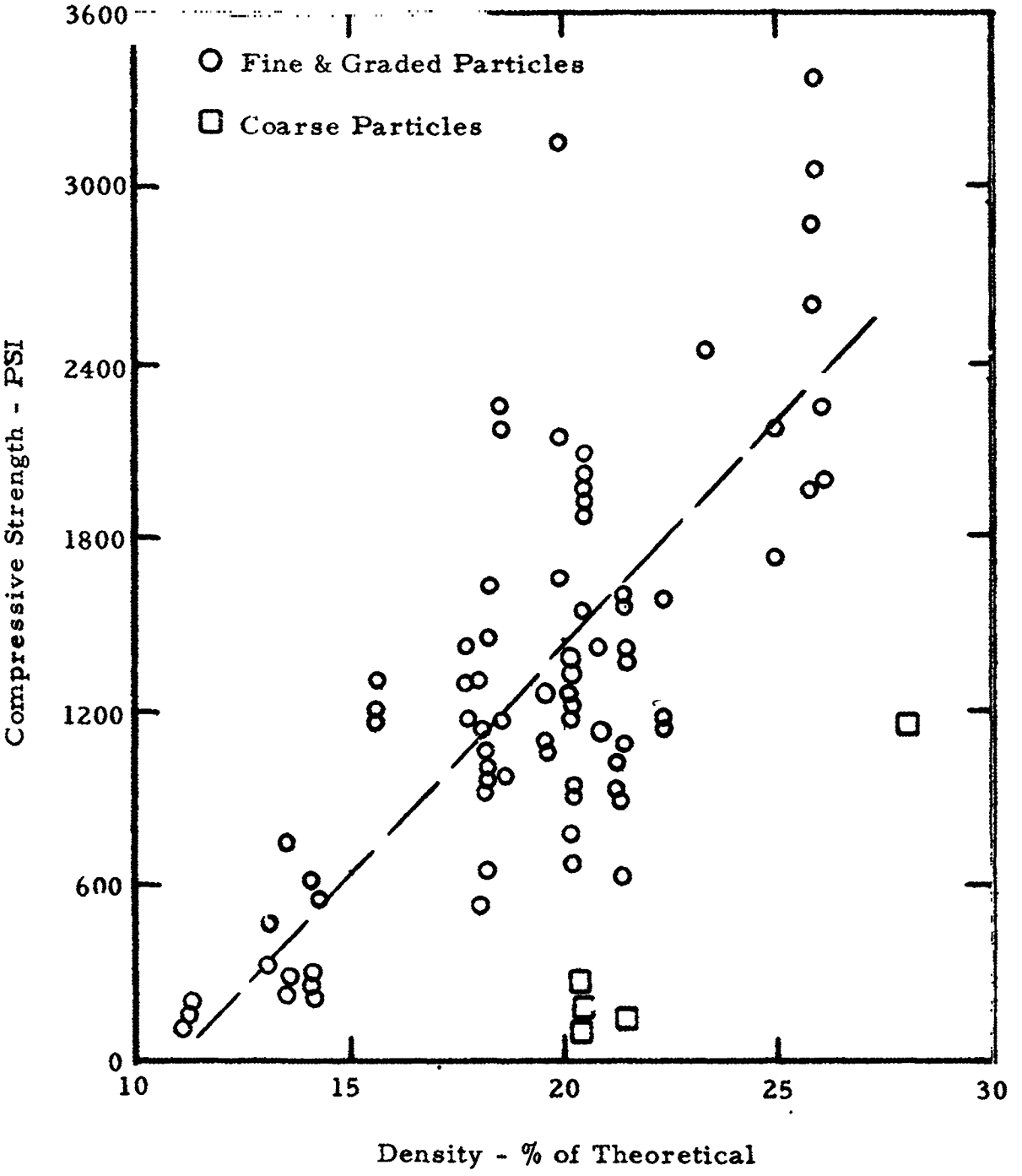

Figure 25. Compressive Yield at 0.2% Offset vs Sintered Density of Foamed Molybdenum

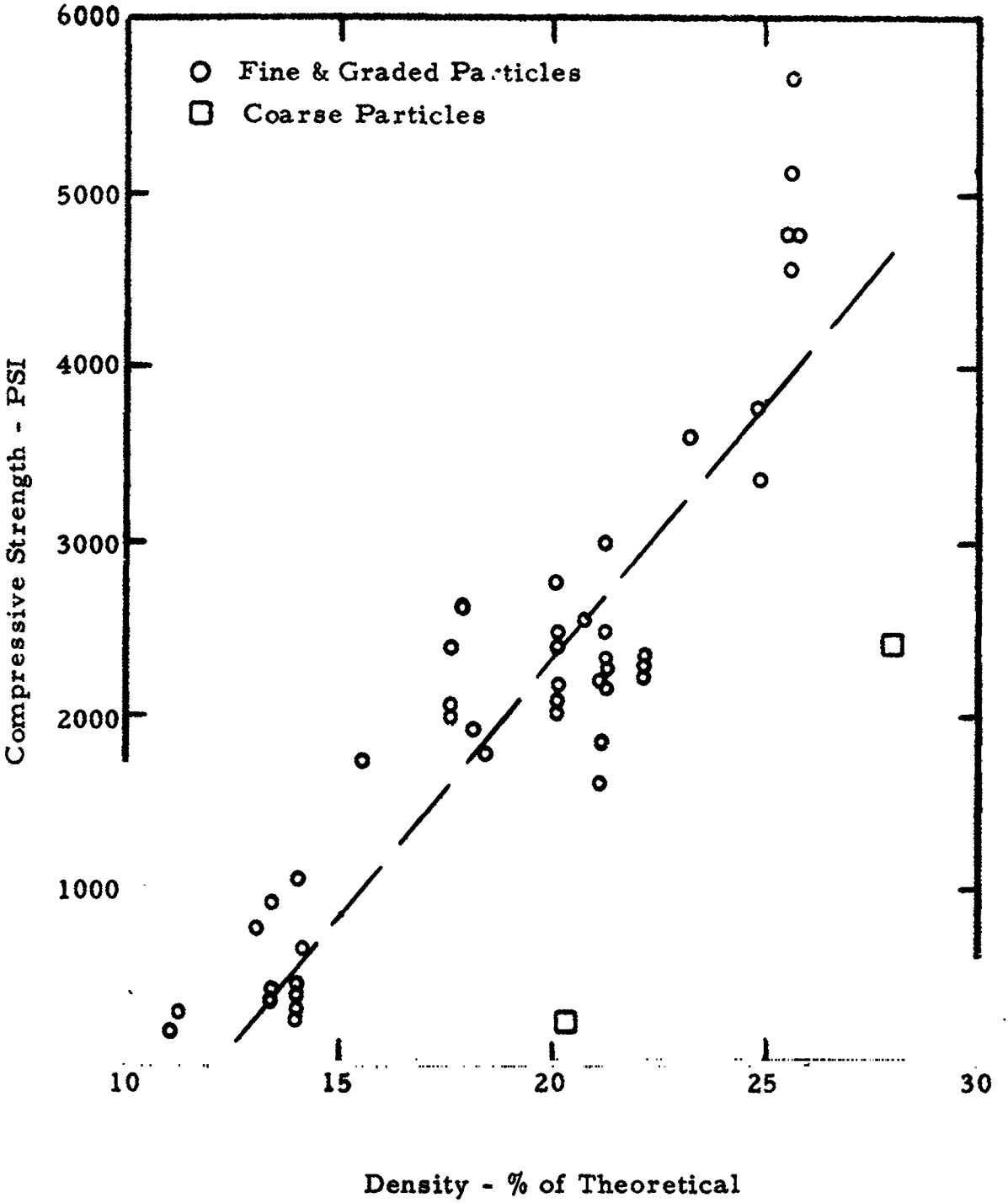

Figure 26. Compressive Strength at 10% Deformation vs Sintered Density of Foamed Molybdenum

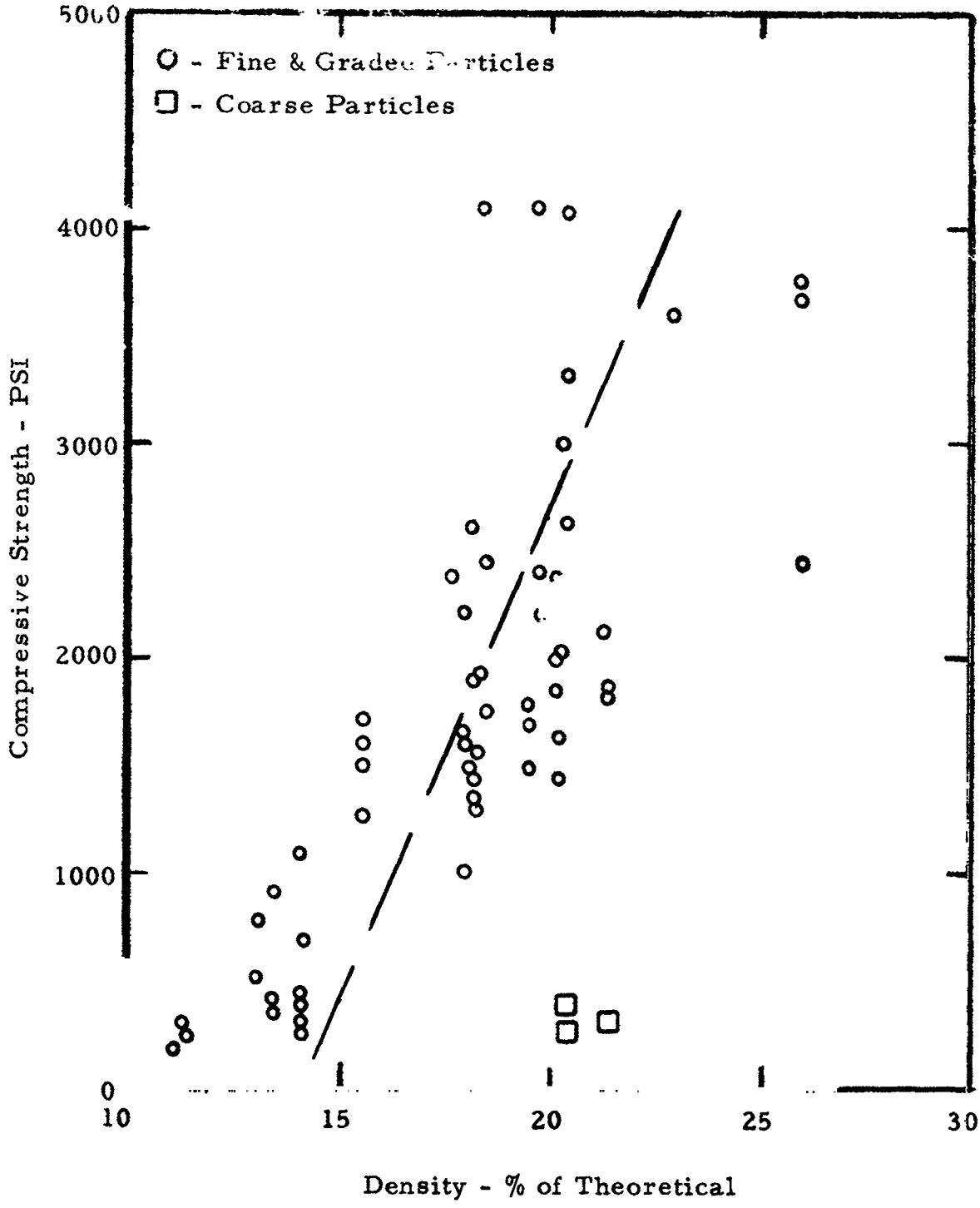

Figure 27. Ultimate Compressive Strength vs Sintered Density of Foamed Molybdenum

density obtained from a linear regression analysis.

2. Stainless Steel Compressive Strength

Values of the compressive strength at ambient temperatures for various sintered densities of this material are listed in Table C-6 and illustrated in Figures 28 and 29. The values are scattered but do show a definite trend for the strength to increase as the sintered density increases. Above approximately 21% density there appears to be a rapid increase of the strength with density.

Test specimens of 18 and 27% density were tested at the various temperatures shown in Table C-7. The highest value of the 0.2% offset compressive yield strengths were recorded at -320°F in each case. The compressive yield decreased markedly to 500°F with the 18% density and to a lesser extent thereafter as illustrated in Figure 30.

3. H-11 Tool Steel Compressive Strength

Specimens of various densities were tested at ambient temperatures. This material was ductile and in no test was an ultimate compressive strength determined. Increasing loads continually deformed the material beyond the reported strengths at 10% deformation. The results are listed in Table C-9 and illustrated in Figures 31 and 32. Again the results are somewhat erratic but show a definite trend within wide limits of increased strength with increased density. The dashed lines on the figures represent the average strength vs density obtained by a linear regression.

4. Nickel Compressive Strength

The specimens were tested at the temperatures listed in Table C-18 for densities of 15, 18 and 27% of theoretical. The results of the 0.2% offset compressive yield are very erratic. For this reason and the small number of results obtained, a plot of the data was not made.

C. Shear and/or Flexural Strength

Shear strength determinations, performed by Melpar, Inc., used a three-point loading technique on specimens of 1/2 x 1/2 x 4 inches. This type of test gives data also referred to as flexural or bending strength or modulus of rupture. The determinations by Ipsen used the same 3-point loading technique over a 2-inch span on specimens 3/8 x 3/8 x 3 inches. The strengths determined were calculated from

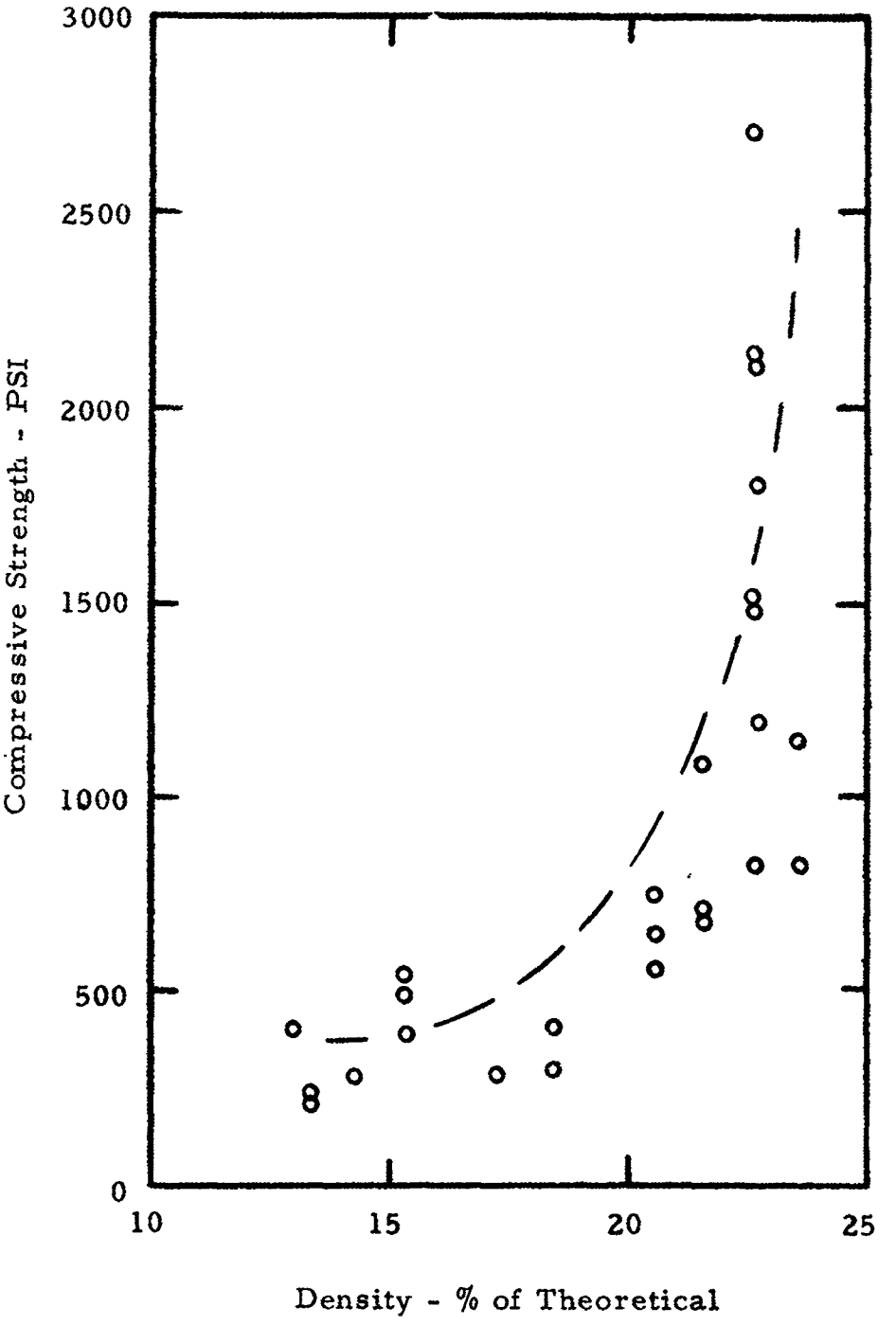

Figure 28. Compressive Yield at 0.2% Offset vs Sintered Density of Foamed Stainless Steel

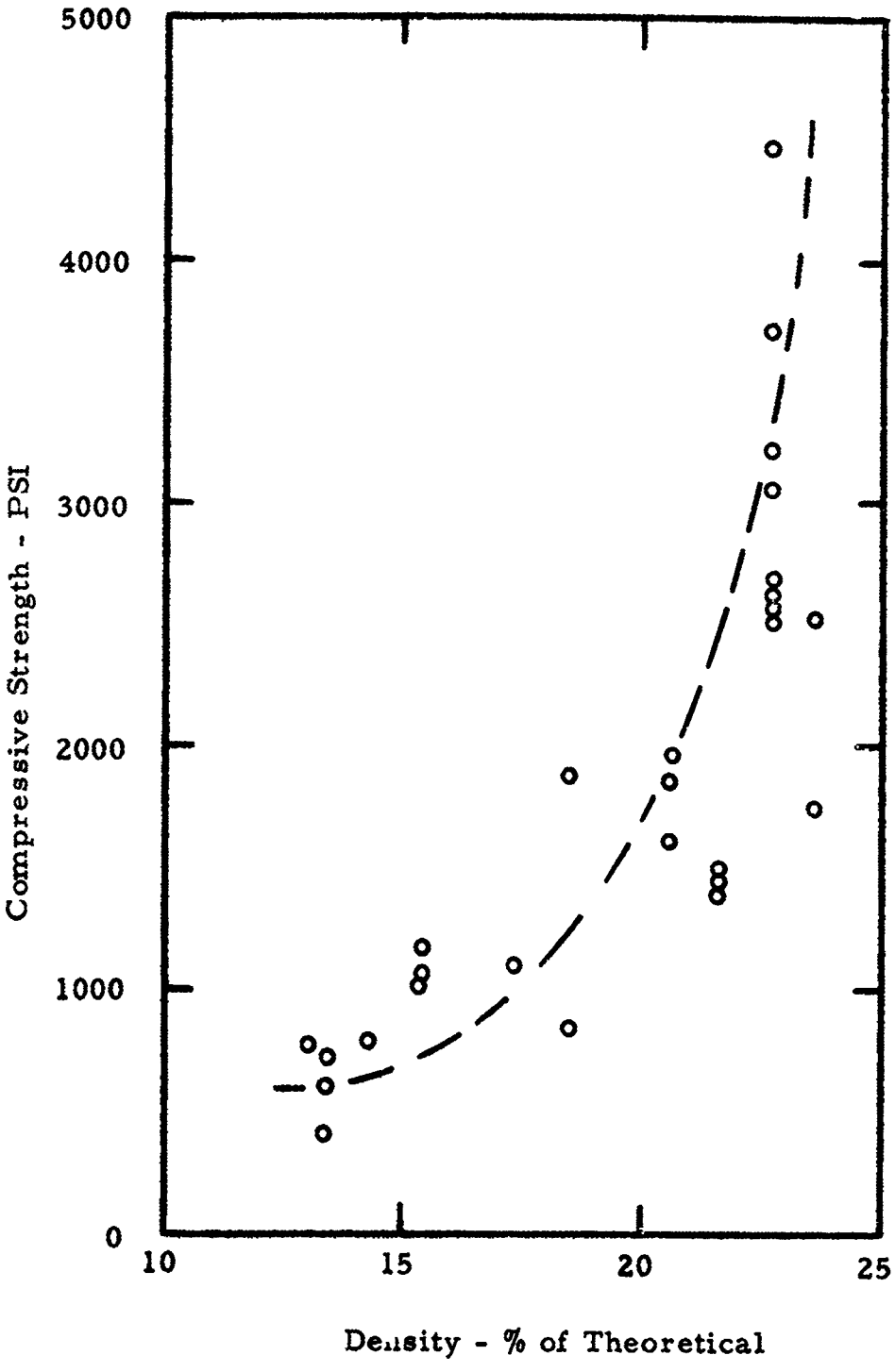

Figure 29. Compressive Strength at 10% Deformation vs Sintered Density of Foamed Stainless Steel

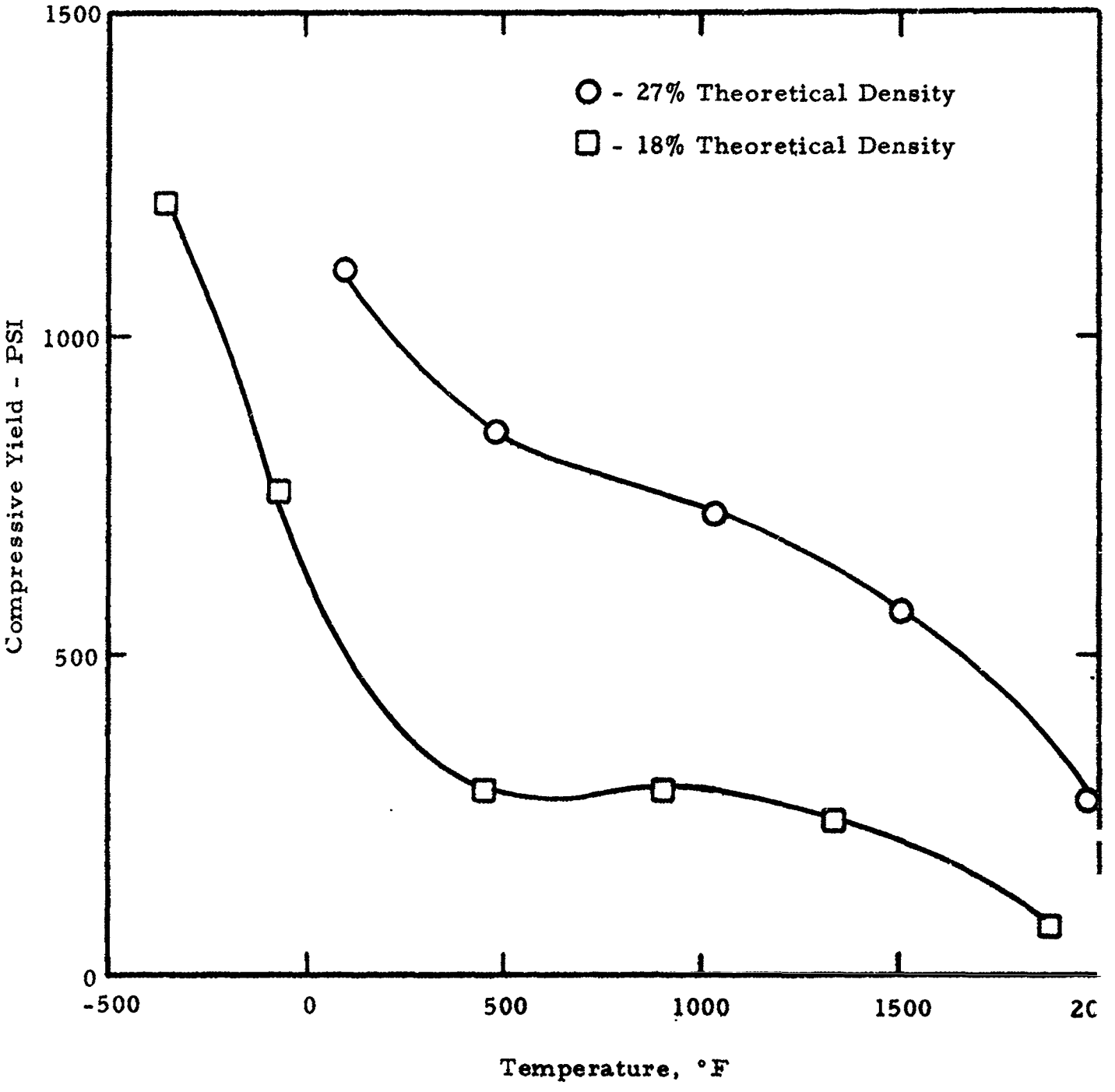

Figure 30. Compressive Yield at 0.2% Offset vs Temperature of Foamed 316 Stainless Steel

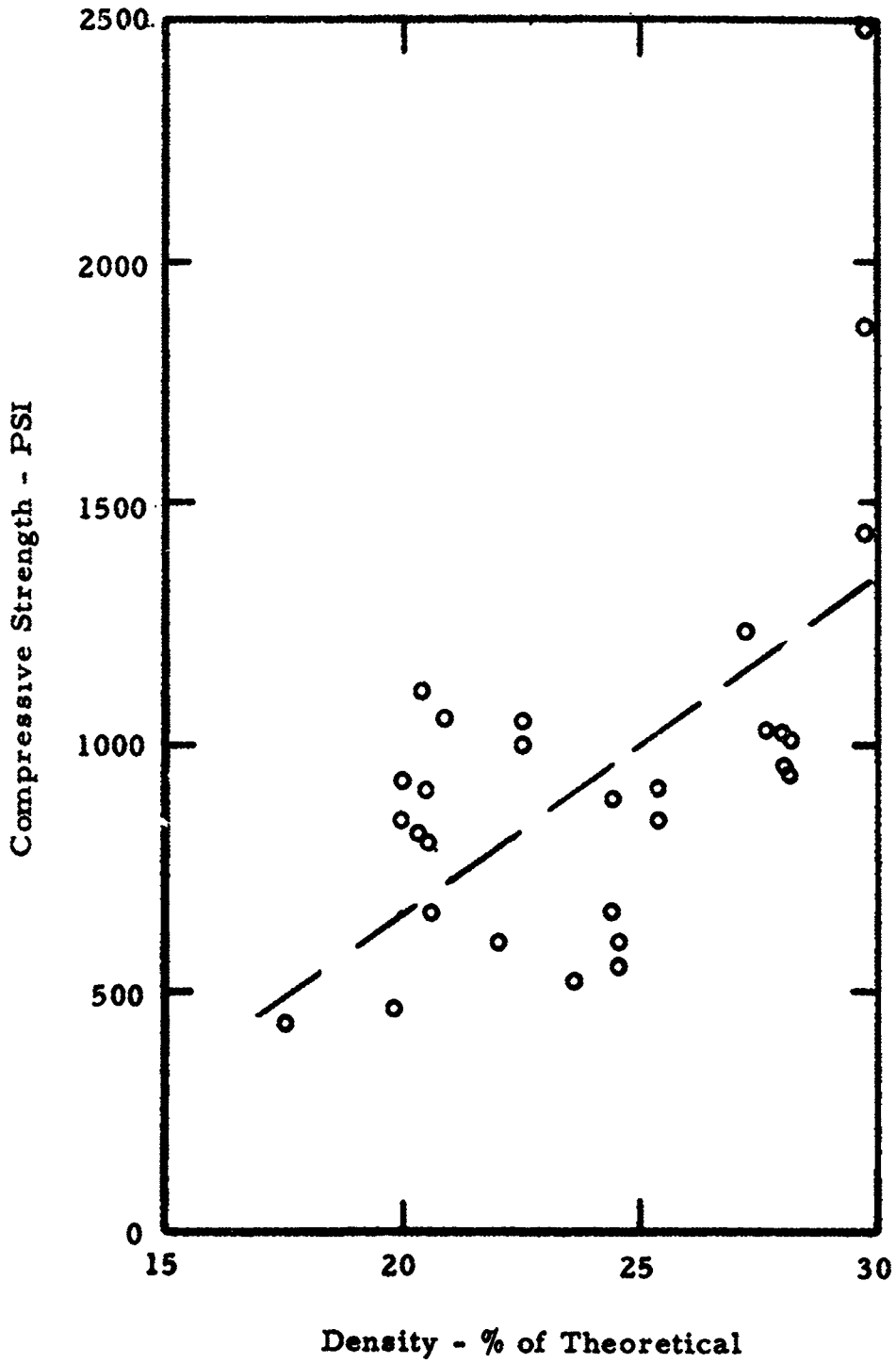

Figure 31. Compressive Yield at 0.2% Offset vs Sintered Density of Foamed H-11 Tool Steel

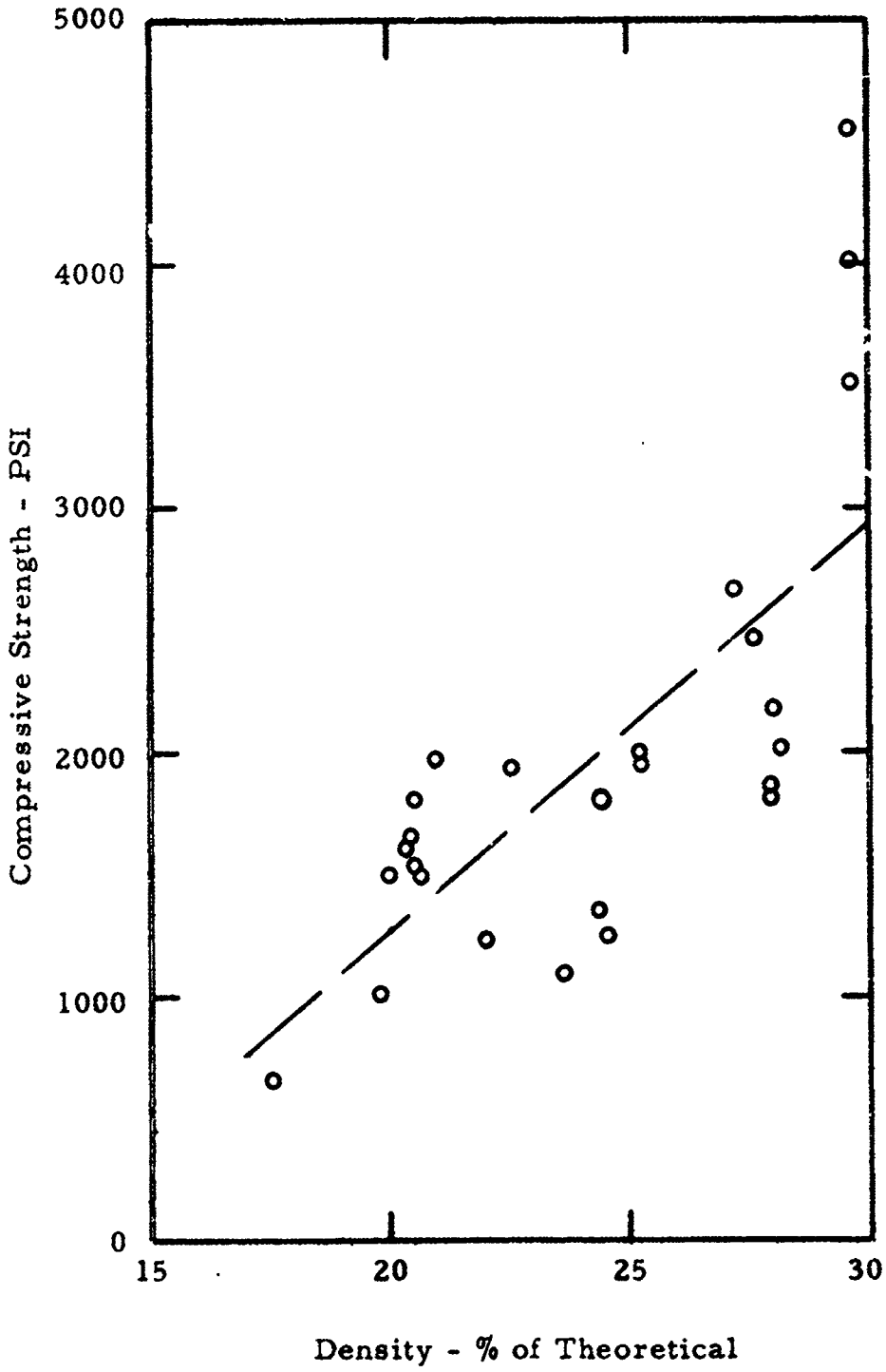

Figure 32. Compressive Strength at 10% Deformation vs Sintered Density of Foamed H-11 Tool Steel

the following equation:

$$\text{Strength (psi)} = \frac{3PL}{2bh^2}$$

P = Load at failure, lbs.
L = Test span, inches
b = Width of specimen, inches
h = Height of specimen, inches

1. Foamed Molybdenum Flexural Strength

This metal was tested at ambient temperature for a variety of sintered densities. The ultimate flexural strengths determined and the sintered densities are listed in Table C-10. Figure 33 illustrates the strength vs density. The large number of specimens tested permitted a statistical average and standard deviation to be calculated for various density ranges. These values are listed in Table C-11 and illustrated in Figure 34. Again the strength increased with sintered density, but there also was an increase of scatter or deviation in the results as the density increased. The strength appears to increase more rapidly with density above sintered densities of 15% of theoretical.

2. Stainless Steel Flexural Strength

Values for the 18 and 27% density stainless steels at various temperatures are listed in Table C-12 and illustrated in Figure 35. The strength of the 27% density material is high (8500psi) at -320°F but shows a sharp decline at ambient and elevated temperatures. The foamed 18% density stainless is low in strength by comparison throughout the entire test temperature interval. Table C-13 and Figure 36 list and illustrate the strength values determined for stainless steel densities tested at ambient temperatures. Again higher strength values are found at higher densities. In Figure 36, the strength increases more rapidly above approximately 18% density. The dashed line in the figure represents the average flexural strength derived from 2 linear regression analyses, one above 17% density and the other below 17%.

Again any annealing with varying cooling rates could change the strength of the foamed stainless steel.

3. Foamed H-11 Tool Steel Flexural Strength

This metal was also tested at ambient temperature for a variety of densities. The results are listed in Table C-14 and

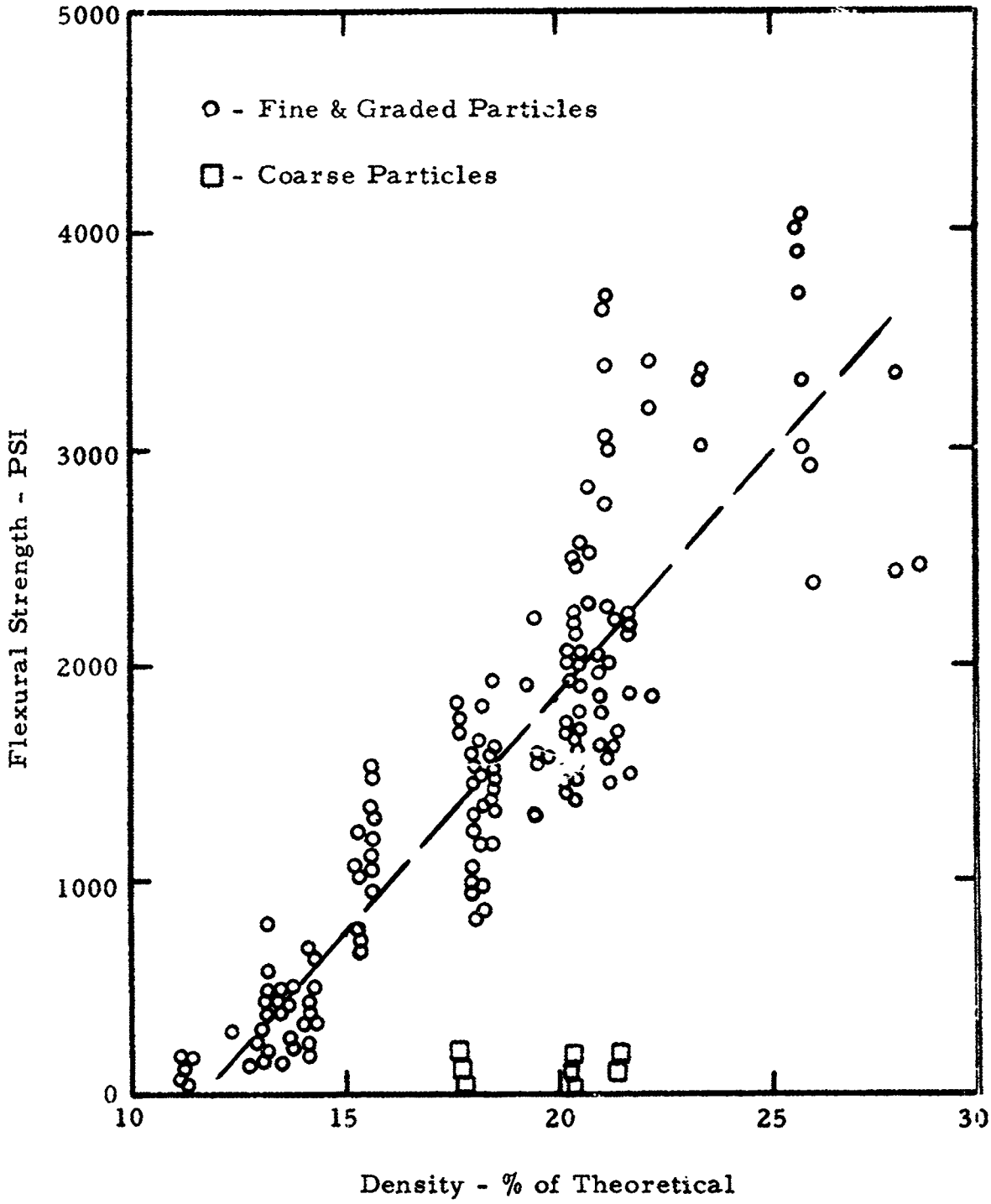

Figure 33. Ultimate Flexural Strength vs Sintered Density of Foamed Molybdenum

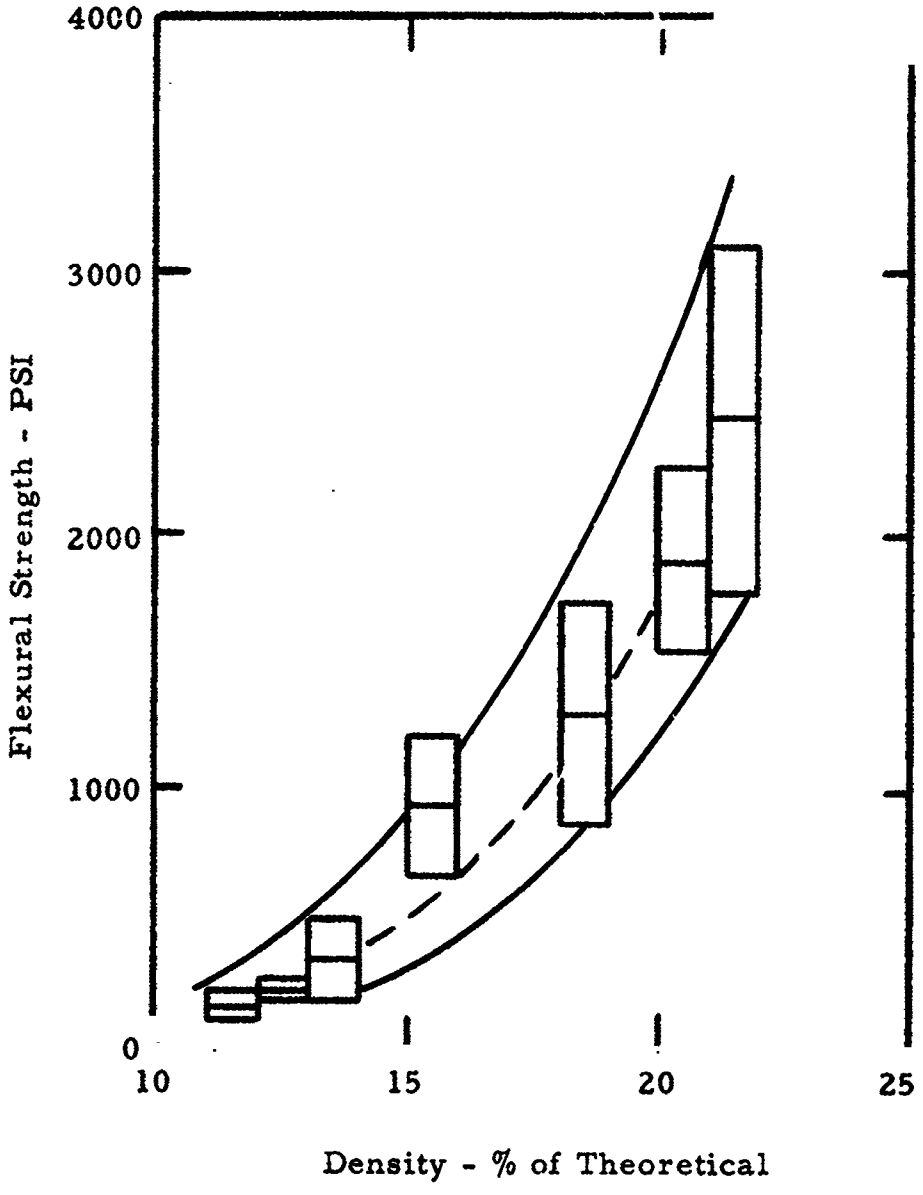

Figure 34. Average and Standard Deviation of Flexural Strength vs Sintered Density at Various Density Ranges of Foamed Molybdenum

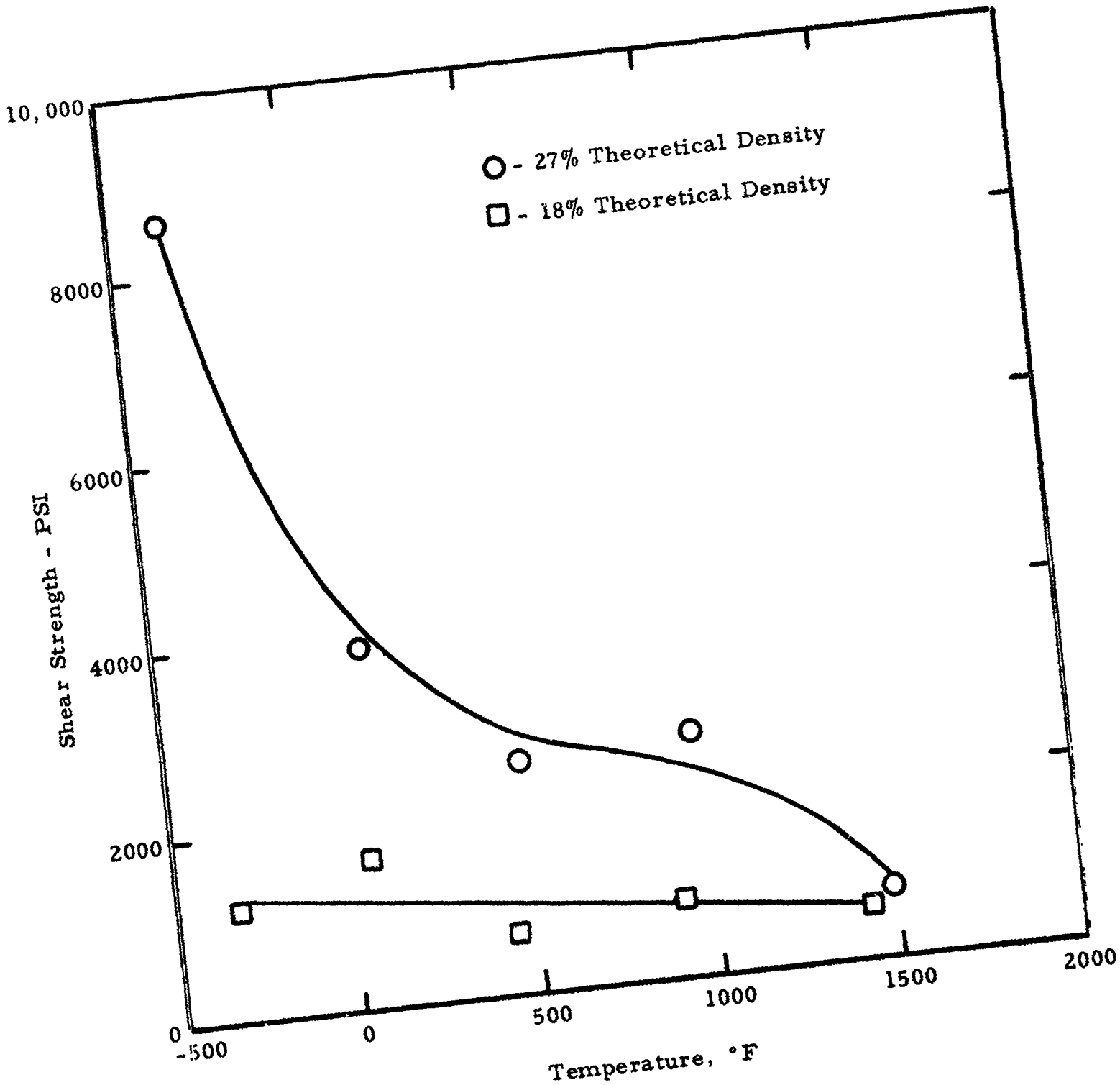

Figure 35. Shear Strength vs Temperature of Foamed 316 Stainless Steel

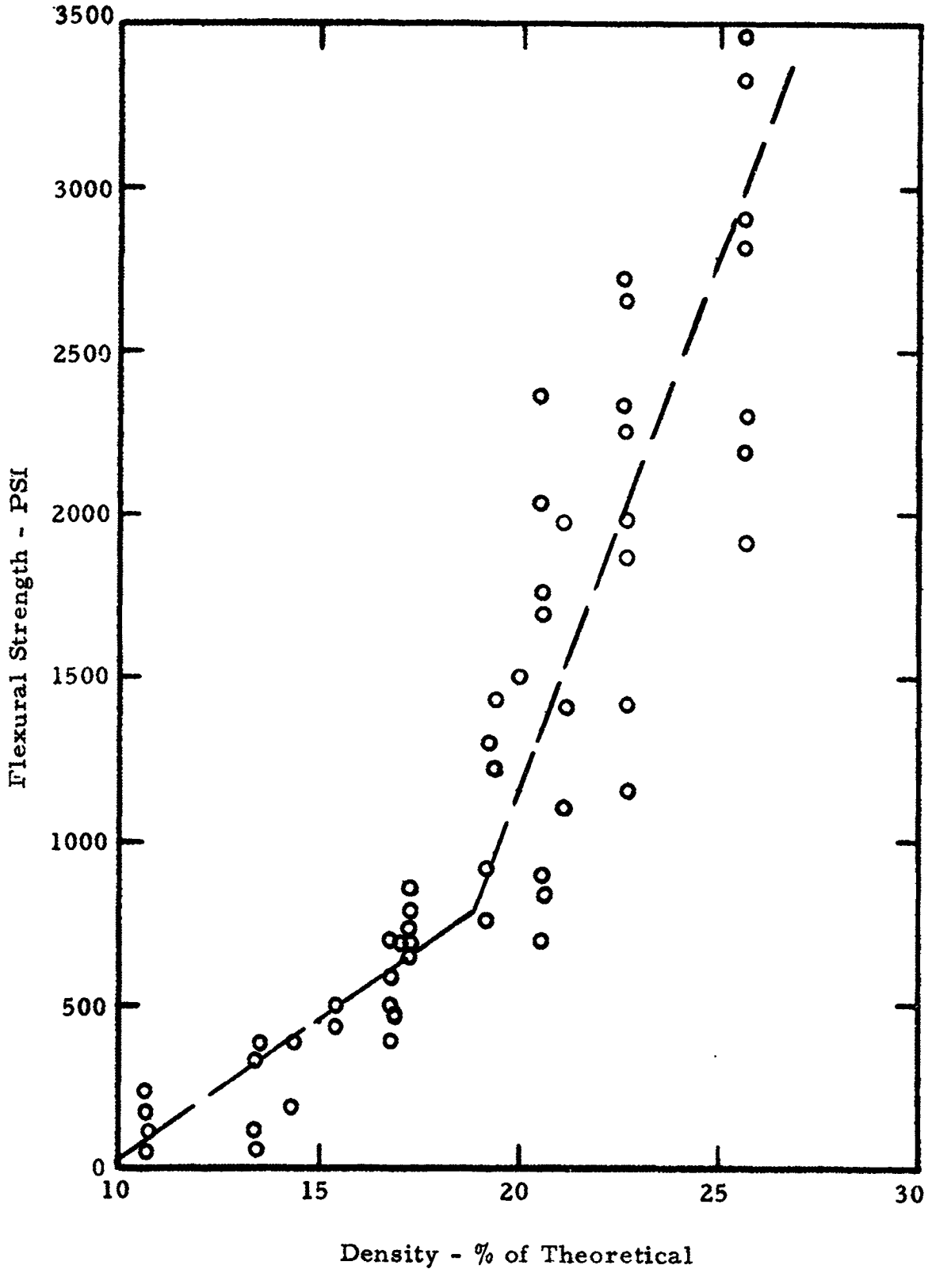

Figure 36. Ultimate Flexural Strength vs Sintered Density of Foamed Stainless Steel

illustrated in Figure 37. Again, the strength increased with density. For any one density the strength appears to vary between ± 1200 psi. The dashed line in the figure represents the average strength from a linear regression analysis.

4. Foamed Nickel Shear Strength

Values at different temperatures for the 15, 18 and 27% density nickel are listed in Table C-15 and presented graphically in Figure 38. The slope of the line for the 27% material is somewhat greater than that of the 18% material, but strengths of higher density foam are increased greatly over that of lower density. The strength value determined at -320°F for the 27% density material is much lower compared to the other values.

D. Vibration Damping

Vibration damping characteristics were measured for foamed 316 stainless steel and foamed nickel. The results were compared to values for the solid metals.

Vibration damping is an inherent material property caused by the internal friction encountered during motion of a body of material. This property is often referred to in terms of a vibration decay rate, or logarithmic decrement, based on energy dissipation per cycle of vibration. Values are determined by amplitude measurements. The amount of damping is usually expressed in terms of percent critical damping (Cc). Critical damping represents the limiting damping value for a particular material above which a body does not vibrate, but gradually creeps back to an equilibrium position or, in other words, is over-damped. It is related to the logarithmic decrement by the equation:

$$\frac{C}{Cc} = \frac{\delta}{2\pi} \times (100)$$ References: 7, 8, 9, 10

C = damping effect of material
Cc = critical damping factor
δ = logarithmic decrement as measured by amplitude variations

Table C-16 lists the vibration damping characteristics for foamed 316 stainless steel, foamed nickel, and the wrought materials.[10] Foamed metal bars of 1/2 x 1/2 x 4 inches were used to determine this property.

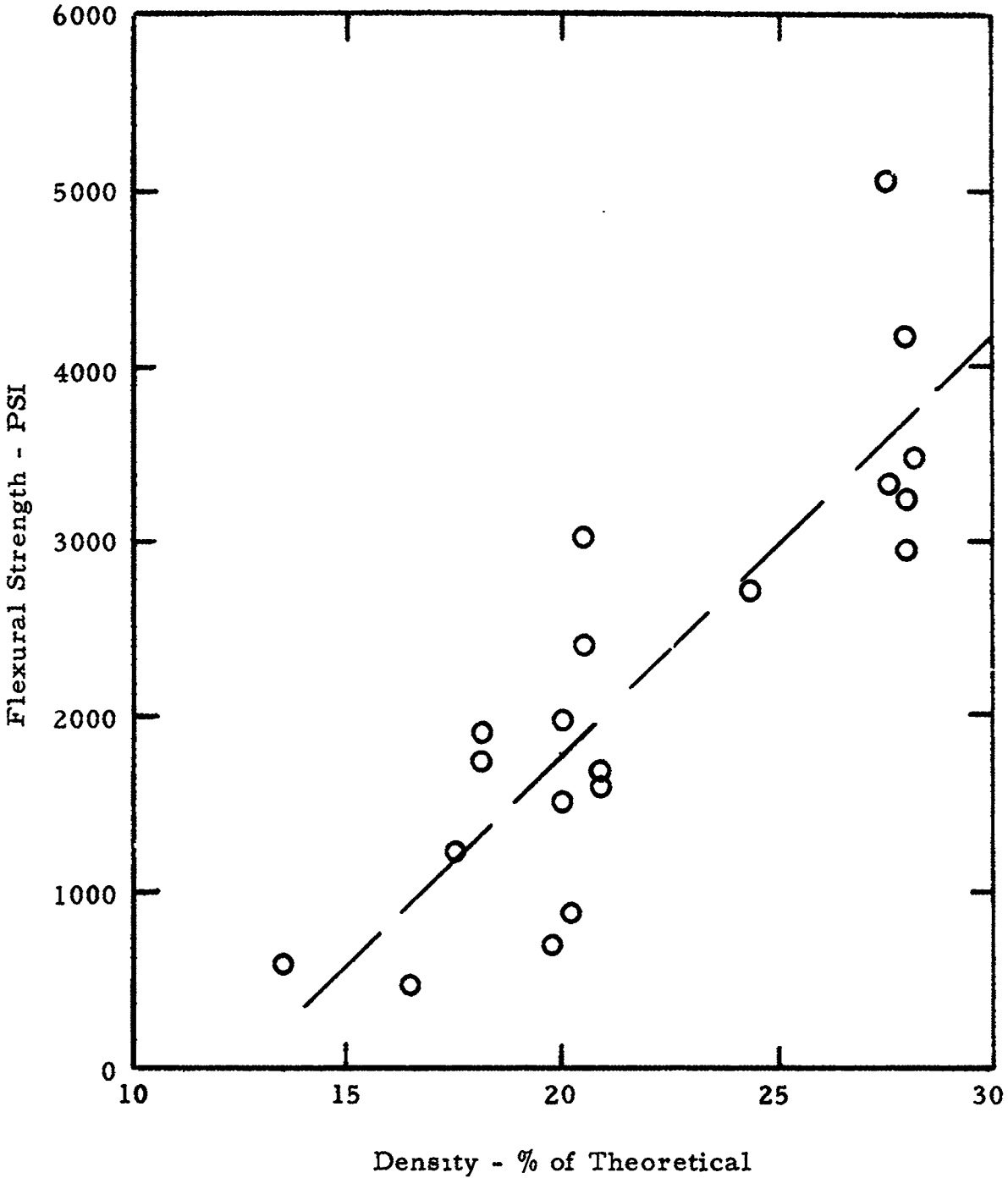

Figure 37. Ultimate Flexural Strength vs Sintered Density of Foamed H-11 Tool Steel

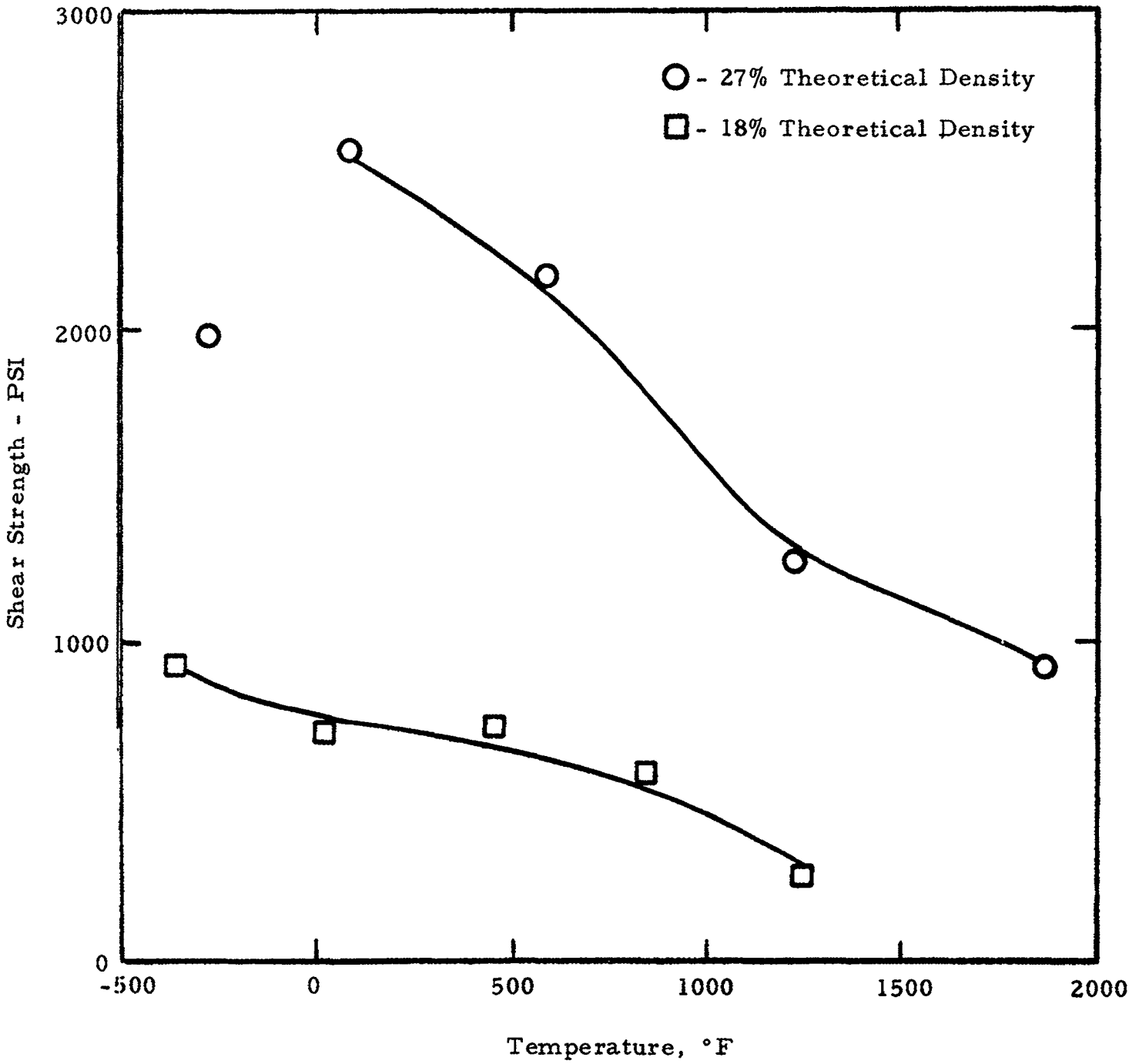

Figure 38. Shear Strength vs Temperature of Foamed Nickel

Electrolytic nickel is far superior to wrought 316 stainless steel in vibration damping capacity. As might be expected, the foamed nickel of 18% theoretical density has a much higher damping capacity than the material of 27% of theoretical density.

Wrought stainless steel has a very low damping capacity, but this property is greatly increased in the foamed state. It is not clear why the vibration damping capacity of the 27% foamed material is higher than that of the 18% material, but possible sources of error have been eliminated.

VI. BRAZING FOAM METALS

Brazing similar and dissimilar metals with selected brazing filler alloys was investigated to determine the potential usefulness of foamed metals as structural sandwich cores. Development of a manufacturing process for sandwich structures was based on the use of commercially available braze filler metals and the evaluation of brazing procedures by investigating the variables of temperature, time, and pre-braze preparation.

The nickel base braze filler metals listed in Table 7 were selected by the following criteria:

1. The material must provide a well-diffused and alloyed, high strength, heat-resistant joint with the foamed metals under study.
2. The brazes must be applicable to standard brazing techniques employing either vacuum or inert gas atmospheres.
3. A variety of ready-mixed pastes, powders, and sheets must be available for selection.

The brazing cycle of time and temperature was first analyzed for the braze filler metals. Recommendations for brazing temperatures supplied by the vendors were essentially followed during the trial runs. Attempts were made to join sheets of the same composition as the foam metal. When time and temperature cycles were established for brazing with several of these filler metals, further testing was conducted by brazing foam metal to sheet metal. Finally, sandwich structures were fabricated using the established cycles.

Prior to brazing, the metal sheet and foam samples were chemically cleaned. Sample preparation consisted of placing some brazing filler metal sheet, powder or paste on a clean piece of sheet metal. The sample to be bonded was then pressed onto the brazing material

TABLE 7: Braze Alloys

Braze Alloy	Composition									Suggested Brazing Temp. Range -°F
	Cr %	B %	Si %	Fe %	C %	Co %	Mn %	W %	Ni %	
AMI 100	19.0	---	10.0	---	---	---	---	---	bal	1975-2200
Nicrobraz 30	19.0	---	10.0	---	0.15*	---	---	---	bal	2125-2175
AMI 104	11.4	0.3	6.8	---	---	---	---	---	bal	2125-2150
AMI 207	5.6	2.8	3.2	---	---	---	---	---	bal	2050-2120
AMI 400	21.0	0.8	8.0	---	4.0	bal	---	4.0	21.0	2150-2200
AMI 750	13.5	3.5	4.5	4.5	0.8	---	---	---	bal	1950-2200
Nicrobraz 125	13.5	3.5	4.5	4.5	0.8	---	---	---	bal	1950-2200
AMI 760	13.5	3.5	4.5	4.5	0.15*	---	---	---	bal	1975-2200
LC Nicrobraz	13.5	3.5	4.5	4.5	0.15*	---	---	---	bal	1975-2200
AMI 770	6.5	3.0	4.5	3.0	0.15*	---	---	---	bal	1850-2150
LM Nicrobraz	6.5	3.0	4.5	3.0	0.15*	---	---	---	bal	1850-2150
AMI 780	---	3.0	4.5	1.5	0.15*	---	---	---	bal	1850-2150
AMI 790	---	1.5	3.5	1.5	0.06	---	---	---	bal	1900-2100
CM 50	---	1.9	3.5	---	---	---	---	---	bal	2200
AMI 300	19.0	---	10.0	---	---	---	10.0	---	bal	2150-2200
Nicrobraz 170	11.5	2.5	3.3	3.8	0.6	---	---	16.0	bal	2100-2200
Nicrobraz 130	---	3.0	4.5	---	0.15*	---	---	---	bal	1850-2150
Nicrobraz 200	7.0	3.2	4.5	3.0	---	---	---	6.0	bal	1850-2150
Copper	Oxygen Free 99.9% Cu									2150

*Maximum Values

and to the sheet metal. The braze samples were then placed on flat ceramic plates in the vacuum furnace. The furnace was evacuated to a preset 100-150 microns at which time the heating cycle was started.

The braze cycles consisted of rapid heating to a temperature of 1800°F. A 15-20 minute hold was then utilized to stabilize the furnace and sample temperatures. The samples were then rapidly heated to the brazing temperature, usually 2050 - 2200°F, and held for 4-10 minutes. The samples were then cooled rapidly by admitting an inert gas until the temperature decreased below 1800°F. In turn, inert gas was fan-circulated for additional quenching. The rapid quenching was recommended for optimum brazed joints with nickel alloys to minimize recrystallization of the molybdenum sheet and excessive reaction and solution of the molybdenum in nickel. The two-step quenching procedure was used to avoid disrupting any liquid braze with high velocity cooling gas.

After brazing, the samples were sectioned and observed visually for flow, bond, and braze characteristics. The samples were also mounted, ground, polished and etched for a microscopic examination. Figures 39 - 41 illustrate the visual and microscopic appearance of several of the brazed joints. Several specimens, also prepared by the above procedure, were tested by tension loading to produce a shear force within the brazed joint.

Brazing foamed metals presented certain difficulties, although good joints were eventually obtained between the foam and sheet metal using the following brazing cycles.

L. C. Nicrobraz	@	2075-2100°F for 4 minutes
Nicrobraz 130	@	2075°F for 4 minutes
Nicrobraz 170	@	2130°F for 4 minutes

During the brazing investigation, it was noted that braze filler metal flowed upward into the pores and voids of the foamed material to the extend of 1/8 - 1/4 inch. This flow depleted the joint of bonding material, and there was insufficient braze to form beads at the points where the cellular walls contacted the sheet. This resulted in much weaker bonds. The problem was easily solved with ductile foam metals, such as nickel and stainless steel, by touching these materials to a grinding wheel and smearing the surface pores closed. This procedure prevented any flow of the brazing alloy and resulted in strong, well-bonded joints because of the increased contact area between the foam and sheet metal. With this procedure, strong and well-bonded brazing joints were made when brazing tensile test specimens of nickel and 316 stainless steel to

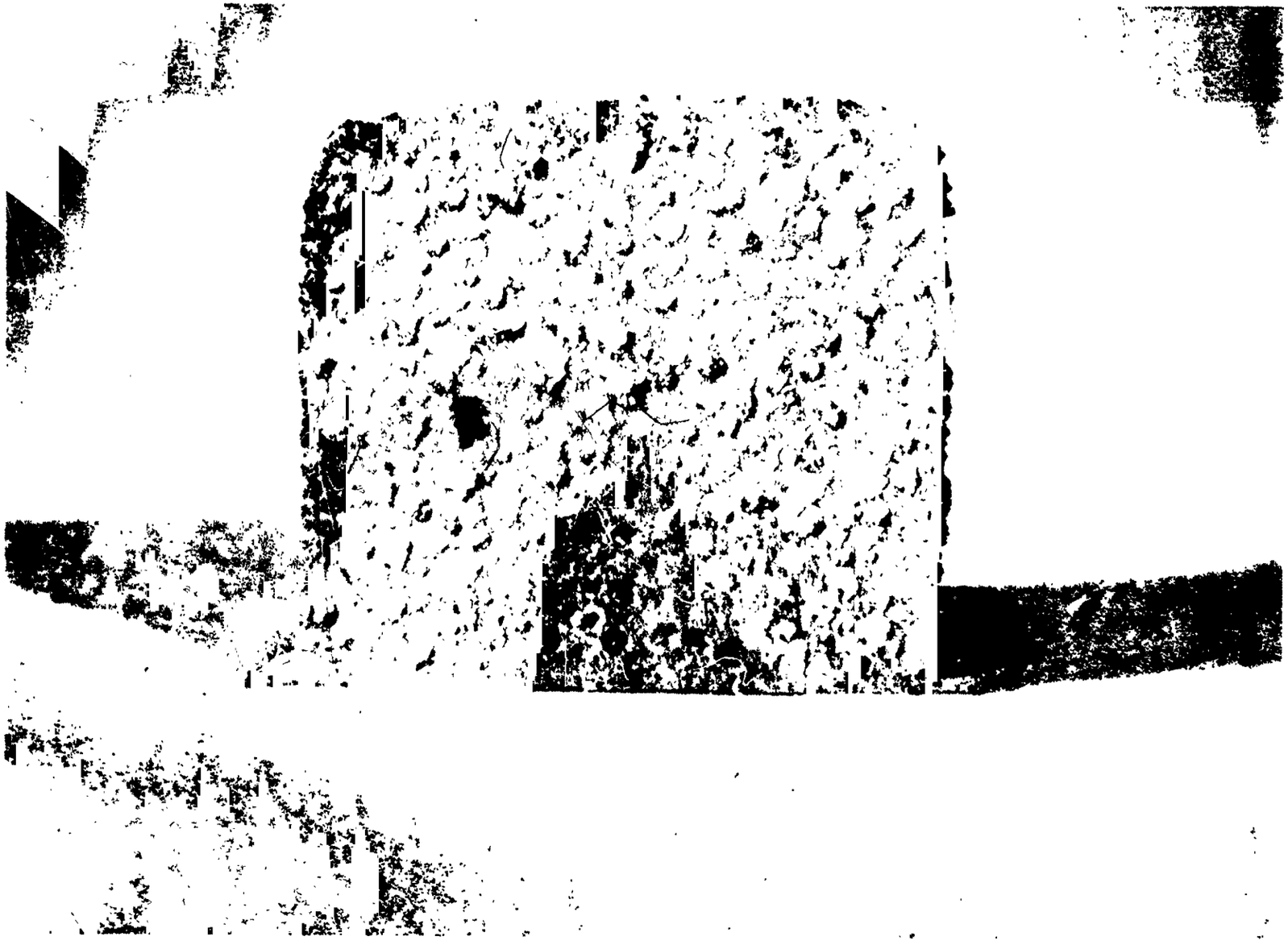

Figure 39. Molybdenum Sheet Brazed to Molybdenum Foam with Nickel Braze Filler Metal

Figure 40. Porous Nickel Foam Brazed with Copper Filler Metal to Molybdenum Sheet, 110X, Etched Sample

Figure 41. Brazing Joint of Nicrobraz 170 Nickel Braze Filler Metal between Molybdenum Foam and Sheet, 100X

standard, threaded, end pieces of stainless and carbon steel. A brazed tensile test specimen of stainless steel is shown in Figure 42.

When brazing foamed molybdenum, the surface pores could not be readily smeared and closed. The room temperature brittleness of molybdenum precludes closing the surface pores by smearing unless the foam molybdenum is heated above its transition temperature during the smearing operation. The problem was solved by forcing molybdenum powder into the pores of the surface to be brazed. The powder reacted with the braze alloys during the brazing cycle and physically and chemically prevented any upward flow. Strong bonds with very few voids were obtained when brazing foamed molybdenum in this manner. Shear test specimens and sandwich structures of molybdenum foam and sheet were fabricated using this procedure. Figures 43 and 44 illustrate the sandwich structures and the appearance of the brazed joints.

Destructive tests were conducted on foam-to-sheet samples brazed with Nicrobraz 170 to determine bond integrity. In one test, the specimens were securely clamped to restrain sheet movement. A bending moment was then applied to the foamed metal at a point furthest from the brazed joint. Brazed joints that appeared strong, voidless, and well-bonded always fractured in the metal foam just above the brazed joint. The foamed metal which remained attached to the sheet appeared uniform and identical to the metal which had broken away. Thus, qualitatively, the bonded joints were found stronger than the foamed parent metal.

Specimens were also loaded in tension to produce a shear force within the brazed joint. These specimens were prepared by taking 2 strips of sheet molybdenum (0.5 x 3.0 x 0.020 inches) and laying them end to end 1/8 inch apart. Nicrobraz 170 filler metal paste was then applied to the ends for exactly 1/2 inch on the strip. A piece of foamed molybdenum (0.75 x 0.50 x 1.25 inches) was pressed into the paste and to both molybdenum strips. After brazing, the joints appeared well-bonded. The free ends of the brazed strips were then clamped in the jaws and between the crossheads of a Riehle Universal testing machine. The specimens were elongated at a constant rate of approximately 0.3 in/min until the specimens failed. Two specimens failed within the brazed joint where the thin cellular walls attached to the strip. After the test an estimated 75% of the braze was still firmly attached to the strip with the remainder attached to the foam in small spots mostly within the pores. The other specimens broke within the foamed molybdenum. The test

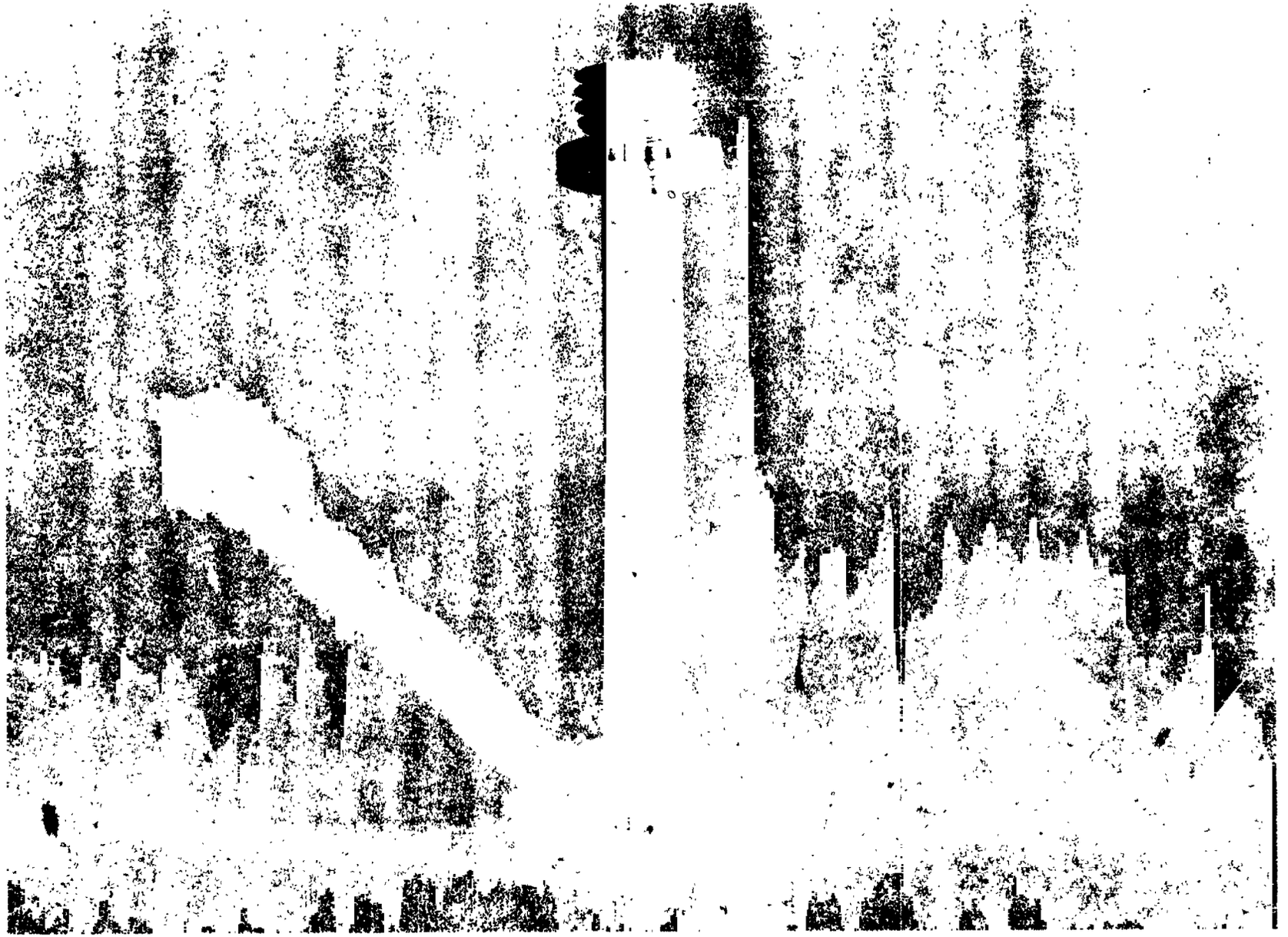

Figure 42. Brazed Tensile Test Specimen of Foamed Nickel and Stainless Steel Endpieces

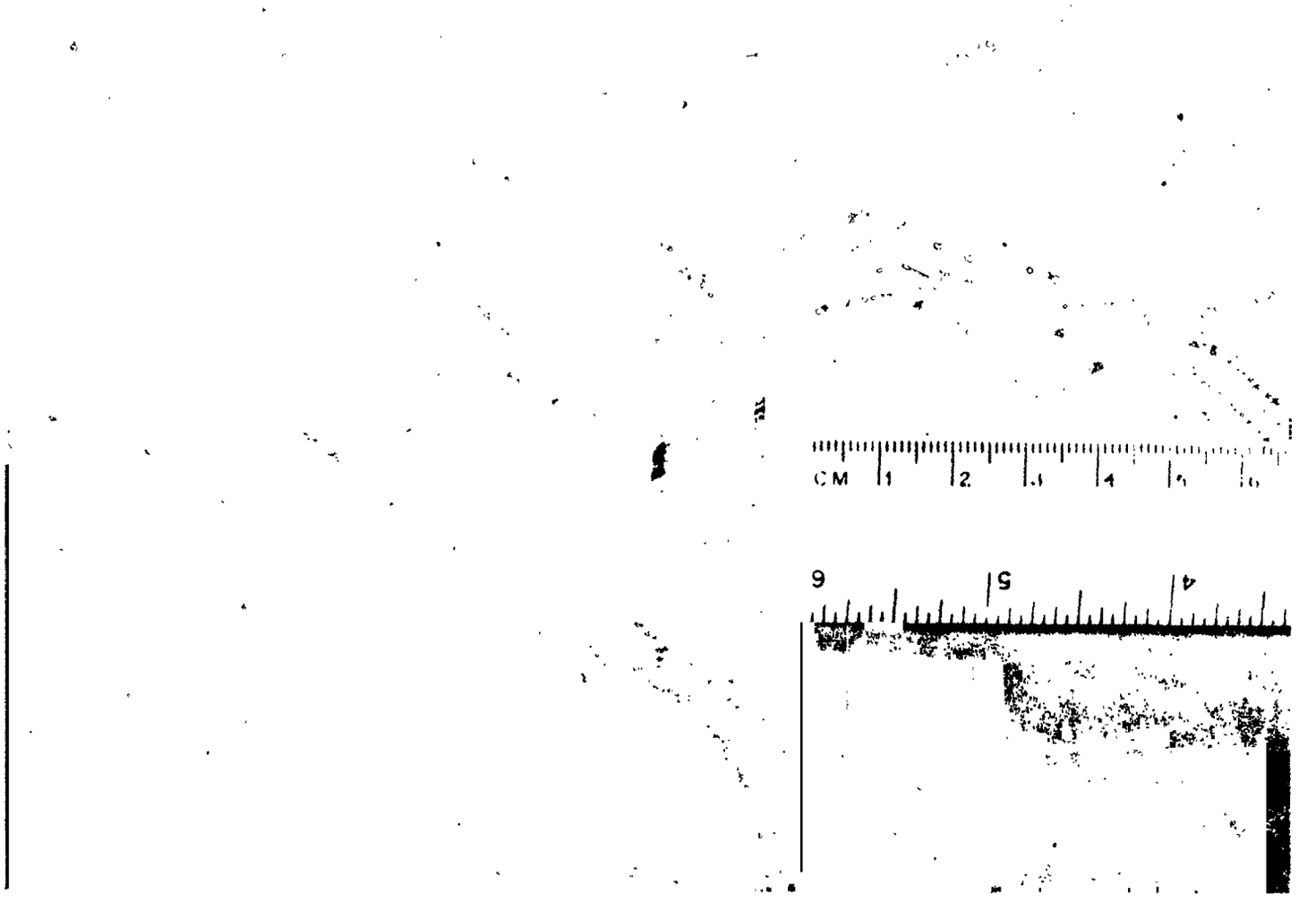

Figure 43. Brazing Joint of Sheet and Foamed Molybdenum Sandwich Structure

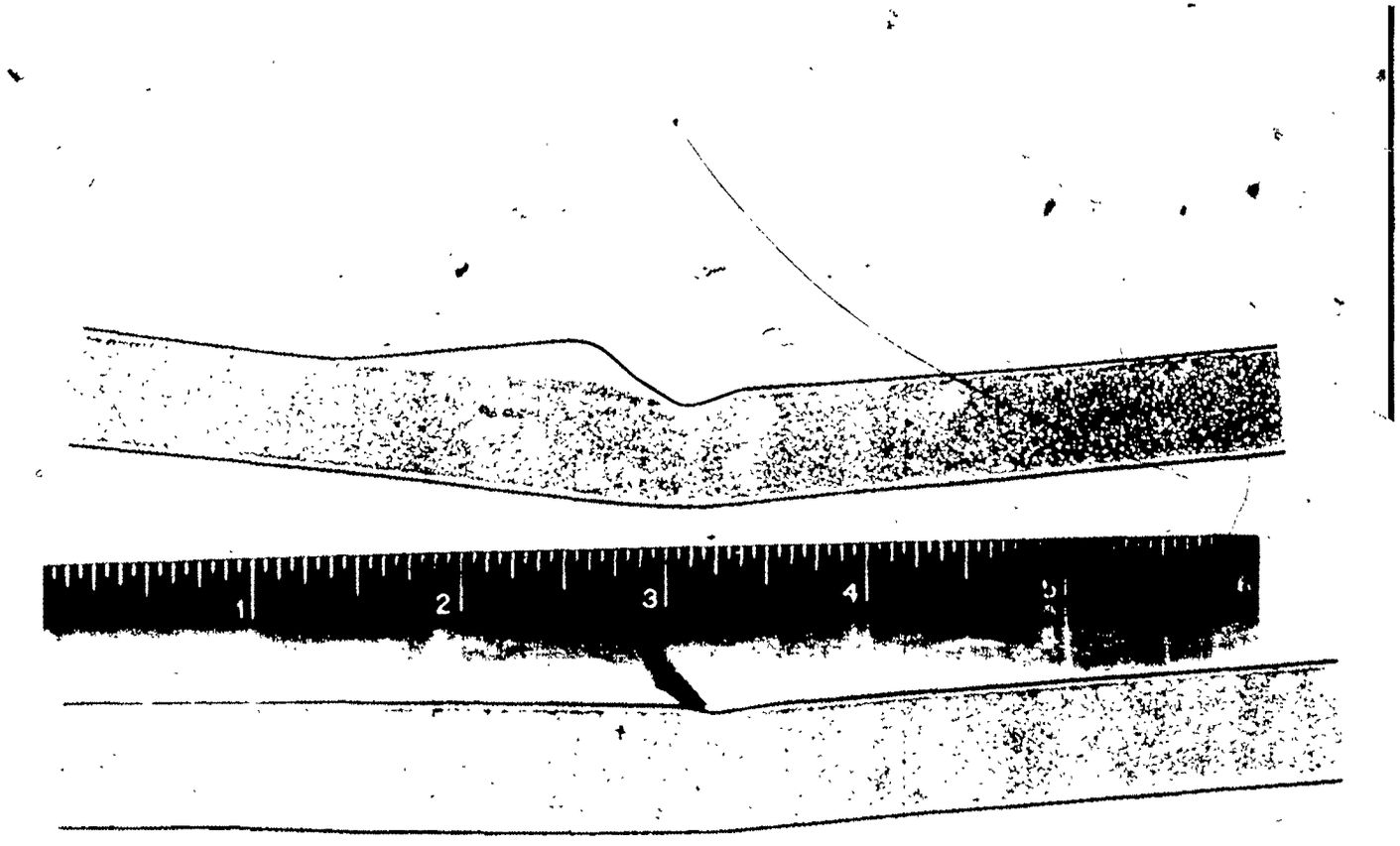

Figure 44. Flexurally Tested Sandwich Structures

results for the specimens were as follows:

Table 8: Results of Shear Testing Brazed Joints

Sample	Brazed Joint Shear Strength psi	Comments
A	580	Failure occurred in Molybdenum foam
B	640	Failure occurred in Brazed Joint
C	780	Failure occurred in Brazed Joint
D	380	Failure occurred in Molybdenum foam

NOTE: All samples brazed with Nicrobraz 170 Braze Filler Metal

Sandwich structures were fabricated by brazing a sheet of molybdenum (1.50 x 6.0 x 0.020 inches) to each side of a piece of foamed molybdenum (1.50 x 6.0 x 0.50 inches). Nicrobraz 170 brazing filler metal was used. These sandwiches were flexurally tested by three-point loading the test specimen at a constant rate of 0.02 in/min until the specimen ruptured or remained at a constant load with increasing deformation. Figure 43 and 44 illustrate the sandwich structures prior to and after testing. The flexural test results for the sandwich structures are listed in Table 9.

Table 9: Sandwich Structure Flexural Test Results

Sample	Core Material % Theo. Density	Ultimate Flexural Strength*	Remarks
#1	19.4	16,900	Sheet & Foam Fractured
#2	18.5	9,900	Continued to Deform at Constant Load
#3	20.1	12,300	Continued to Deform at Constant Load
#4	21.0	17,200	Sheet & Foam Fractured

*Flexural strength calculated for simple beam deflection from stress = $\frac{Mc}{I}$

VII. VARIABLE DENSITY BEAMS

The original study plan specified that aluminum and stainless steel would be used for making foamed metal beams with the lowest density at the core and the highest density at the surface. Since sintered aluminum foam could not be produced, nickel was chosen as a substitute.

The initial procedure was to cast a layer of high density foam in a mold followed by layers of successively lower density. After the foam of minimum density had been cast, successive layers of high density were cast. This procedure proved unsuccessful because of interdiffusion between foam layers of different densities.

A second method consisted of fabricating a low density core and imbedding it in a high density foam. These composites were then dried, presintered, and final sintered as described in Section II. However, fabricating porous variable density beams by this method presented several problems.

The major problem was to equalize the drying and sintering shrinkages of the high and low density foams. There is a definite trend for this shrinkage to decrease with increasing density. This shrinkage differential, and the resultant stresses, caused many composites of this type to develop cracks and sometimes fracture during the processing. This shrinkage is also affected by the metal powder size, the amount of water and cement in the foam, and the sintering time and temperature. However, variable density beams were produced successfully through control of the shrinkage of the low density core prior to imbedding it in the high density foam. In effect, the low density core was preshrunk, such that the subsequent processing shrinkage was approximately equal to that of the high density foam. Other variables were maintained constant as the preshrinkage of the core and the low and high foam "casting" densities were varied, in experimental trials, until satisfactory conditions were established for the successful production of the variable density beams.

Maintaining the position of the low density core in the mold was difficult when high density foam was added. A successful solution consisted of centrally locating and vertically standing the core in a mold. High density foam was then added to the space surrounding the core. A lid inside the mold positions the core by a central cutout through which the core protrudes.

A minor problem was keeping the core parallel to the outer

shell during sintering. When the beams were fixtured horizontally, the composite tended to deflect in the center area. To avoid this, the composite was fixtured perpendicularly and supported on all sides by a bed of zirconia bubble grain.

Variable density nickel beams were prepared successfully when a presintered core of 750 gm/qt foam density was encased with 2125 gm/qt high density foam. The core material was presintered at 2300°F for approximately 3 hours and then positioned (horizontally) in a mold. High density foam was then troweled to the sides of the core for good integration and poured into the mold around the core. The composites were dried, presintered, and sintered at 2500°F in the usual manner for foamed nickel. A resulting variable density nickel beam with a core of approximately 16% density and an outer shell of approximately 22% density is shown in Figure 45.

Stainless steel composites of this type were prepared successfully when "dried cast" cores of 800 gm/qt foam density were encased with 1300 gm/qt high density foam. These composites were dried, presintered, and sintered successfully in the usual manner.

Stainless steel variable density beams were produced successfully when the dried cores were positioned both horizontally and vertically in the molds.

A stainless steel beam approximately 3 inches square by 5 inches long with a core 1-1/2 inch square was prepared in a vertical mold of 4 x 4 x 7 inches. Several stainless steel beams approximately 1 x 1 x 4 inches with a 1/2 inch square core were prepared from 2 x 2 x 6 inch horizontal molds.

The sizes of the variable density beams produced did not meet the generally accepted specimen dimensions for flexural test. For this reason, and the belief that the flexural results would fall somewhere within the individual results for high and low density materials presented elsewhere in this report, no flexural tests were conducted.

In summary, by matching the drying and sintering shrinkages of the low and high density foams, variable density beams with a low density core and high density foam shell can be fabricated. Variable density beams should have strengths intermediate with those determined individually for high and low density foamed metals. Neither the nickel nor the stainless steel variable density samples fabricated were a size sufficiently satisfactory for mechanical property evaluations.

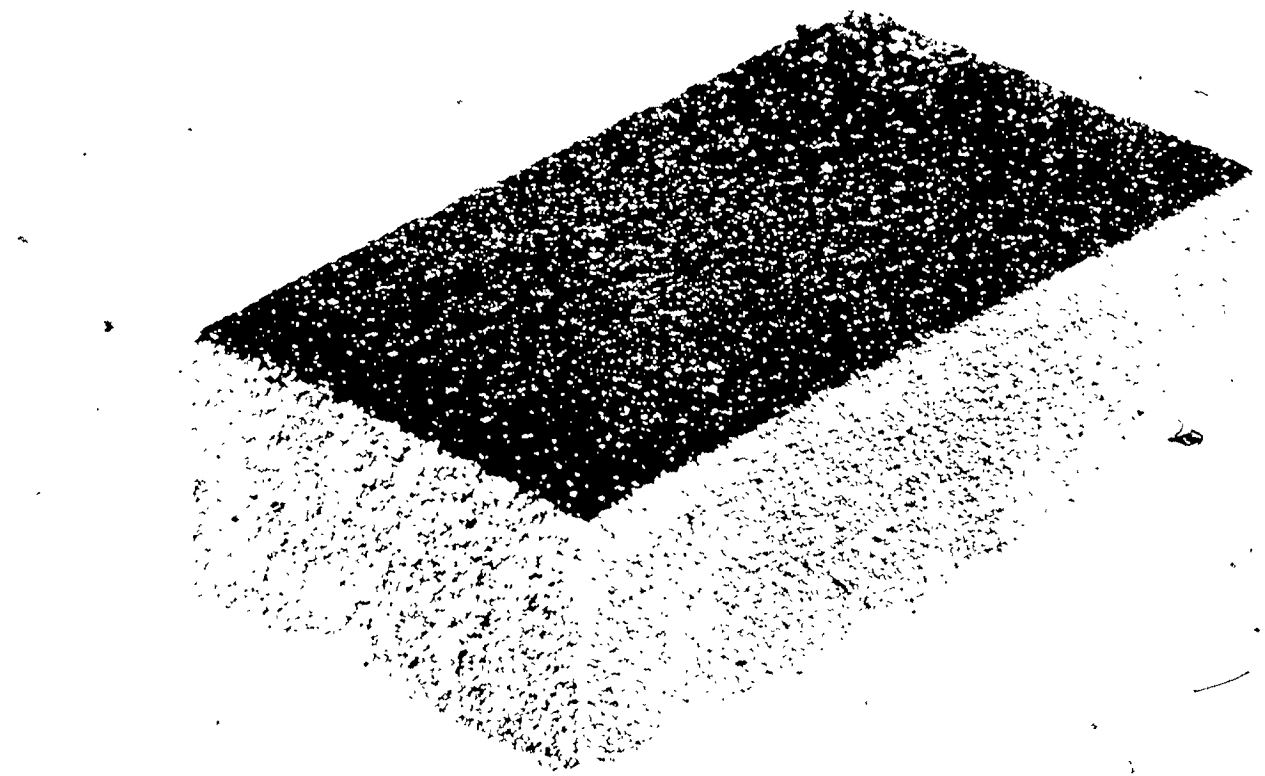

Figure 45. Sintered Variable Density Beam of Nickel, 4X

VIII. SUMMARY AND CONCLUSIONS

Foam metals were produced by suspending metal powders in a liquid containing binders, cements, and foaming agents. This slurry was foamed by entraining air under conditions such that bubbles of gas are distributed throughout the suspension, which is subsequently dried to set the cements and binders. The dried green metal samples were vacuum sintered at specific temperatures and times during which the binders, cements, and foaming agents are volatilized and driven off and the metal particles are bonded.

Production of foam metals having desired densities, pore sizes, and mechanical properties can be achieved by controlling variables in the process. These variables are:

(a) Proportions of powder to liquid in the slurry
(b) Proportions of slurry to foaming agents
(c) Metal grain sizes present
(d) Time, temperature, and degree of vacuum conditions in the presintering and final sintering.

By theoretical calculations and observations, these variables were controlled by experiments which yielded a "best mix" for given densities and pore sizes in the final products made from 4 metals investigated.

The foaming and sintering process produced porous metals of molybdenum, 316 stainless steel, H-11 tool steel and nickel. However, foamed aluminum and titanium, which are highly reactive and easily oxidized, could not be sintered to strong and ductile porous metal. Procedures utilizing additives to aid sintering and other methods were investigated and attempted, but no improvements in strength or ductility were obtained.

The sintered foamed metal had interconnected spheroidal type pores of 5 to 15 thousandths inches nominal size. The range of pore size was between 1 and 40 thousandths inches. The nominal pore size could be varied by the powder particle size distribution, concentration of powder in the cast foam, and sintered density. Densities were obtained ranging from 12 to 30 percent of theoretical and generally were reproducible to plus or minus one percent with the foamed metals.

Composite beams of variable density can be foamed when control of the drying and sintering shrinkages is exercised. The variable density beams have cores of low density foams with large pores and surfaces of high density and fine pores.

Exact control of the drying and sintering shrinkages was thought to be too complicated for casting and sintering the foam metals to final configurations. It was assumed that machining would ultimately be a more feasible method of obtaining various shapes of the foamed metals.

The foamed metals were cut and machined by normal shop techniques. Special tools and fixtures were desirable in some instances, but no particular problems within the limitations of these materials were encountered. Using the technique of closing the surface pores to the flow of braze alloy, the foamed metals were readily brazed to similar or dissimilar wrought metals to obtain a strong sandwich type composite. Other types of composites could be produced via the easy impregnation of the porous metal.

The sintered metal foams have many of the original characteristics of the solid metal. However, the metal is very porous, and its tensile, compressive, and flexural strengths and thermal conductivity have been decreased. For foamed nickel and 316 stainless steel, at temperatures between -320°F and 2000°F, the thermal conductivity was found to have a value below that of the solid wrought material and related directly to density. At ambient temperatures, the foamed metals of molybdenum, H-11 tool steel, nickel and 316 stainless steel had tensile strengths ranging from 50 to 2500 psi and flexural strengths between 50 to 5000 psi over the range of sintered densities tested. These strengths increased with density but were not related directly in proportion to the percents of theoretical density. The strengths were proportionately much lower and this was assumed to be caused by the higher stress concentrations inherent in very porous materials of this nature. Compressive yield strength at 0.2% offset ranged from 100 to 4000 psi for various densities of H-11 tool steel and molybdenum, while this strength ranged from 200 to 2500 psi for 316 stainless steel and nickel. Compressive test specimens deformed linearly to 1.5 to 2% deformation, except for foamed molybdenum of the lowest density and coarsest particle size. These foam materials continued to deform at the same, increased, or decreased loads without fracturing. Thus the ductility or plastic deformation prior to compressive failure was increased. The vibration damping capacity was increased for foamed nickel and 316 stainless steel, and this would be expected with other metals.

The increased ductility could be important in the case of molybdenum or other refractory metals with high brittle to ductile transition temperatures where it is desirable to retain this property independently of the method of working the metal. Foamed metals may have application where lightweight, vibration damping, low thermal conductivity, and increased ductility or plasticity are required while retaining the basic physical properties of the metal.

REFERENCES

1. L. Polonsky, S. Lipson and H. Markus, Lightweight Cellular Metal, Transactions of the American Foundrymen's Society, 69, p. 65-79, (1961)

2. J. Bjorksten, J. C. Eliot, R. J. Roth, Foamed Metal Development for Sandwich Structure Cores, WADC TR 52-51, Part 3, Contract No. AF 33(038)-2134, May 1954

3. Ultra-Lightweight Aluminum Foam, Modern Metals, 13, p. 68, October 1957

4. Goldsmith, Waterman, and Hitschhorn, Handbook of Thermophysical Properties of Solid Materials, Vol. II I-N-3 and II-D-3, The Macmillan Co., New York, (1961)

5. S. Hoyt, ASME Handbook - Metals Properties, McGraw-Hill, Inc. (1954)

6. American Society for Metals, Metals Handbook - Vol. I Properties and Selection of Metals, 8th Ed. (1960)

7. F. Forster, Z. Metalk, 29, 109, (1937)

8. F. Forster and Breitfeld, Z. Metalk, 30, 343, (1938)

9. F. Forster and W. Koster, Engineer, 166, 626, (1938)

10. G. M. Smith and H. D. Berns, Materials Research and Standard, 4, (5), p. 225, May (1964)

11. McGeary, Mechanical Packing of Spheres, Journal of American Ceramic Society, Vol. 44, No. 10, p. 513, (1956)

12. Saxton and Sherby, Viscosity and Mobility of Liquid Metals, Trans. Quar., ASM, p. 82, (1962)

13. G. G. Brown, Unit Operations, John Wiley & Sons, Inc. (1950) New York

ACKNOWLEDGMENTS

The contributions of the following to the program described in this report is hereby acknowledged:

For Fabrication and Testing
J. L. Meier
Sue Anderson
J. Daughtry
G. T. Moreau

For Sintering
I. Bielefeldt
W. Pierick

For Machining and Evaluation
B. C. Ware, Jr.

For Microscopic Examinations
C. K. Bishop

For Preparation of Manuscript
Lois Baker
Carol Fane
Rosemary Washatko
Joan Wenger

For Printing
L. A. Driscoll
E. Layton

APPENDIX A

EXPERIMENTS WITH POWDER METAL FOAMS

A - 1 Metal Powder Inspection

The suppliers, grain sizes, chemical analyses, methods of manufacture, and morphology of powders received and inspected are summarized as follows:

1. Aluminum:

These powders were obtained from the Federal Mogul Division of Federal-Mogul-Bower-Bearings, Inc. The company employs a process where molten metal is atomized in an inert atmosphere to yield specific particle sizes. The grain or particle sizes obtained were -100 and -325 mesh, and the sieve analyses of these are shown in Table C-21. Two alloys were selected and obtained. One was alloy 1100 which is 99% plus Al and designated commercially pure aluminum. The other was alloy 7178 which is 61.2%Al, 6.8% Zn, 27.0% Mg, 2.0% Cu, and 3.0% Cr. Individual particles of both were spheroidal in shape and had indications of oxide films on the particle surfaces.

2. Nickel:

Federal Mogul also supplied -100 and -325 mesh nickel powders produced by the same process as the aluminum powder above. Chemical analysis was 99% plus pure nickel. Particle shape was spheroidal. The sieve analyses are as shown in Table C-21.

Nickel powders were also supplied by Sherritt Gordan Mines, Ltd. They were procured as agglomerated high and low densities and in particle size of -325 mesh. Chemical analysis was 99% plus pure nickel and the particle shape was angular. The sieve analyses were as shown in Table C-21.

3. Stainless Steel:

Federal Mogul supplied 316 stainless steel powder in -100 and -325 mesh sizes with sieve analyses as shown in Table C-21. The method of manufacture was the same as employed for aluminum and nickel powders. The chemical analysis was 17% Cr, 12% Ni, 2.5% Mo, 0.10% C with the balance iron. The particles were mostly spherical

but irregular shapes were noted. There was a wide variation in particle size in the nominally -100 mesh powder.

4. H-11 Tool Steel:

This powder was also obtained from Federal Mogul and had the following chemical analysis: 0.35% C, 0.40% Mn, 1.0% Si, 5.0% Cr, 0.45% V, 1.50% Mo, balance iron. The powder was manufactured in the same manner as aluminum and stainless steel. The particles were mostly spherical and of more uniform size than the 316 stainless. The sieve analysis is shown in Table C-21.

5. Molybdenum:

Molybdenum powder in nominal -325 mesh was obtained from 2 suppliers, Fansteel Metallurgical Corp. and Climax Molybdenum Company. The Fansteel product was designated PM grade and that of Climax designated MMP grade. Both were 99.9% pure molybdenum produced by hydrogen reduction of molybdic oxide. Particle shapes were rounded and spheroidal, elongated and angular, and agglomerated. The sieve analyses were as shown in Table C-21.

6. Titanium:

This powder (99% plus pure) was supplied by Consolidated Astronautics Inc. Both -100 and -325 mesh were used. The particle shapes were angular and flaky and had indications of titanium oxides, both internally and externally. The sieve analyses are in Table C-21.

A - 2 Foaming Metal Powders

The "as-cast" foamed metal structure can be considered as a mass of bubbles with fluid walls, upon which are located particles of metal powder. Factors which influence the bubble size and thus the sintered density, pore size, and strength are as follows:

a. Particle shape and density.
b. Particle size and range of sizes.
c. The metal to foam ratio during foaming.
d. Water content in the foam mixture.
e. Atmosphere, humidity and temperature during drying.
f. Presinter (time, temperature, and atmosphere treatment).
g. Final Sinter (time, temperature, and atmosphere treatment).

Provided metal particles of an equal size are in contact with those

adjacent to it, an optimum packing condition will result on a bubble surface as shown in Figure 46. Though there will be open interstices between equal sized particles, this condition requires a minimum number of particles to cover the bubble surface and would be the lowest energy state of the system. It follows that for a given volume of an ideal foam of one nominal pore size that this condition should be met throughout, and a minimum number of equal sized particles will be needed to cover the total surface area. It can be proved geometrically, that a given volume of bubbles of 0.020 inches nominal size will require half the number of particles as does an equal volume of bubbles of 0.010 inches nominal size. Thus, density varies inversely with bubble size, provided the particles are of the same size and density in all cases. The bubble size can be varied then, to control the density, by controlling the viscosity and/or surface tension of the fluid phase in the walls of the foam structure.

On the basis of this theoretical discussion it may be said that bubble size determines the ultimate density of a sintered foam and that there is little ability to vary ultimate density for a particular bubble size. In fact, variation of density for a given bubble size results when:

a) The metal particles are not in contact with one another on the bubble surfaces.
b) The metal particles are in contact on the surface of the bubbles but are arranged somewhere between a minimum and maximum packing density (see Appendix B).
c) The metal particles are disposed in more than one layer.

When metal particles are not in contact during the drying process (condition "a" above), the bubbles will shrink as the fluid is removed, and the metal particles will draw nearer together until they make contact as shown in Figure 47. The metal to foam ratio thus affects pore size and ultimate density of the sintered product.

In condition "b" above, where particles are in contact but not arranged in the optimum packing density, there will be a tendency during drying for the metal particles to approach this packing condition. This optimum will be affected by the particle sizes, shapes, and size distribution as discussed in Appendix B for a solid bed of particles. An analogous situation should exist in this case. In any case the seeking and approaching of an optimum packing density will reduce the bubble or resulting pore size.

In discussing condition "c" above, it is best to think in terms of a single isolated bubble. If a particle of metal powder is placed on the surface of a bubble, because of surface tension, the product of bubble

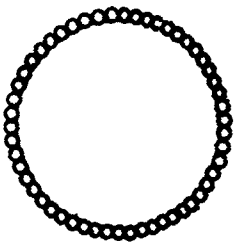

Figure. 46 Optimum arrangement of metal particles around foam bubble. All particles in contact and equilibrium at lowest energy state. Optimum density for bubble diameter.

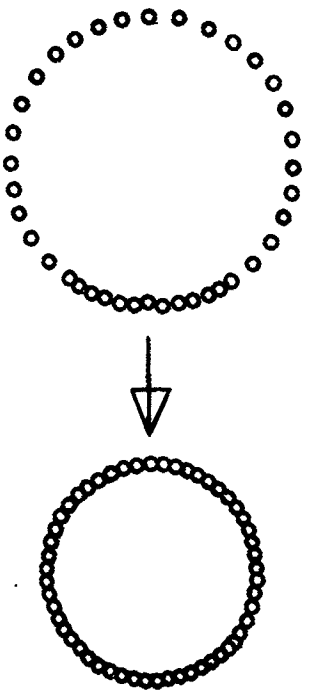

Figure. 47 Insufficient metal particles to cover bubble surface. During drying bubble size decreases until all metal particles are in contact. Thus optimum, lowest energy state is found and density is increased.

diameter and fluid viscosity, and the particle wettability, the metal particle will be accommodated within the wall of the bubble. If the viscosity of the fluid wall is not too high, the metal particle will gravitate to the lowest point in the bubble wall. Additional particles will come to rest upon the particles below them until the bubble wall is filled with a single layer of grains, each in contact with those adjacent to it. This is the optimum state for the system (Figure 46). If additional metal particles are added to the system, we move away from the optimum and increase the load on the bubble wall. A point will be reached where the wall can no longer support the metal weight, or provide a continuous coat of fluid around all the metal particles. Because it can no longer maintain a complete surface film, the bubble will collapse. Large bubbles will break down, and form smaller ones as shown in Figure 48. These, having a greater total surface area, will now be able to support the metal particles at, or near, the optimum condition, provided the ratio of bubble diameter to the quantity of metal particle is at equilibrium. If the system is not at equilibrium, it will tend to readjust until it is.

When a volume of bubbles is examined, it can be seen that their volume does not completely fill the containing space. There are interstices between the bubbles. These interstitial spaces play a part in determining ultimate foamed metal density. By virtue of it's small diameter, the interstitial bubble will possess a greater surface attraction than the larger bubbles of the same viscosity. A small bubble will thus tend to draw into its own system a relatively large amount of metal particles. This will continue until the interstitial spaces are almost packed with metal particles. If there is insufficient metal present to satisfy the demands of the interstitial systems and also coat the surfaces of the main bubbles, the interstitial systems will take preference. This can leave the main bubble structure deficient in metal particles as shown in Figure 49. If the main bubble structure is sufficiently deficient of metal, the bubbles will shrink during drying, and provide a pore diameter of optimum size for the amount of metal particles available.

The above theoretical considerations provided the following guidance:

1. By selecting the bubble size of a foam structure, we can add the optimum amount of powdered metal and thereby control ultimate foamed metal density.
2. Under-loading a foamed structure with metal particles will result in a decrease of bubble size during processing, and therefore, an increase in density.
3. Overloading a foamed structure with metal particles will

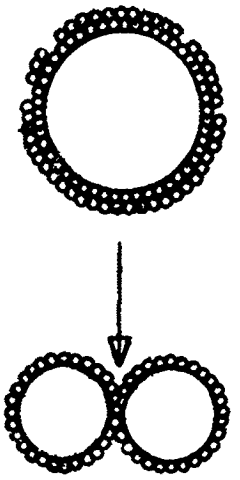

Figure 48. Situation where the bubble is overloaded with metal grain, i. e. more metal than total bubble surface area. System under stress, thus bubbles break down to smaller diameter, increasing total surface area so that grains may be accommodated in the optimum, low energy manner.

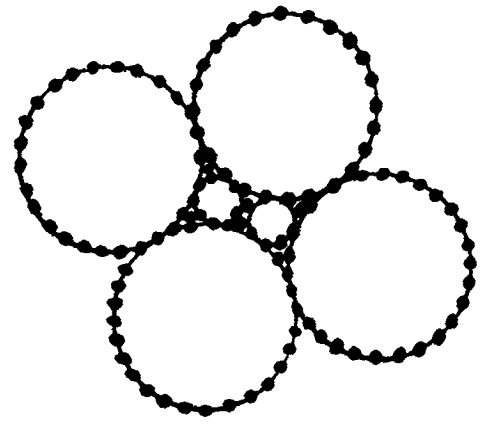

Figure 49. System of mixed bubble diameters: Metal particles drawn to systems of small bubble diameter because of greater surface tension. If insufficient metal powder is present to satisfy demands of interstitial systems and cover total surface area of all bubbles, they will tend to break down. This will create demand for still more metal. System will tend to collapse, taking a smaller total volume with fewer bubbles having less total surface area. Result, high density material, varied pore structure.

break down bubble size and produce greater number of bubbles of smaller diameter which will accommodate the metal particles in the optimum manner.

4. A considerable variation of bubble size within a foamed structure results in the movement of metal particles from large to small bubbles and breakdown of the large bubbles. This results in an increase of ultimate density which is consistent with the smaller bubble size.

5. A high proportion of the metal particles in a foam will be accommodated in the interstitial spaces. The volume of interstitial space decreases as bubble diameter decreases, but the number of interstitial spaces increases.

6. Two batches of foam of equal volume, one with 0.125" diameter bubbles and one with 0.0625" diameter bubbles, to which is added equal amounts of metal powder, will ultimately possess the same density - provided that, in both cases, the metal particles are not present in sufficient quantity to coat the bubble surfaces and be in contact with each other.

While producing foam metal samples and attempting to alter the pore size and density separately, the above theoretical considerations were experimentally proven true. The experimental work to produce foam metals in at least 2 densities and at least 2 pore sizes for each density can be summarized as follows:

1. Foamed molybdenum may be produced having the following ranges of pore size and density:

Percent of Theoretical Density	Nominal Pore Size $\times 10^{-3}$ inches
12 to 15	6 to 10
15 to 20	6 to 12
20 to 25	4 to 8
25 to 30	5 to 16

2. Foamed H-11 tool steel may be produced with the following densities and pore sizes:

Percent of Theoretical Density	Nominal Pore Size $\times 10^{-3}$ inches
13 - 20	8 - 14
20 - 25	9 - 11
25 - 28	8 - 9

3. Foamed 316 stainless steel may be produced with the following densities and pore sizes:

Percent of Theoretical Density	Nominal Pore Size x 10^{-3} inches
10 - 15	8 - 10
15 - 20	7 - 9
20 - 25	3 - 6

4. Rigid control of density for a specific pore size was not possible while the degree of control becomes less for foamed materials with sintered densities below 12% and above 25% of theoretical density.

5. The ultimate sintered density can be controlled within limits by the ratio of metal powder in the foam formulation. The use of metal powders of various particle sizes and distribution also may be used for this purpose. Generally, increased amounts of coarse particles (>325 mesh) result in decreased sintered densities and larger pore sizes for a specific weight of metal powder per unit quantity of foam.

6. There is a general tendency for pore size and pore size range to decrease as the sintered density increases.

7. Increasing water content in a formulation tends toward a slight decrease in pore size and an increase in density. The degree of control in this respect is limited.

8. For samples of all casting densities, a fairly wide range of pore diameters exists within any one sample. The density of that sample will vary internally $\pm 1\%$ of theoretical density from the average density for the bulk of the sample.

The above results confirm a theoretical consideration presented earlier. Apparently metal powders can be foamed and sintered successfully only when the original foam bubble structure is overloaded with metal powders. This would account for the metal powder weight content controlling the ultimate sintered density and the fairly wide range of pore sizes in the individual experimental samples. The slight decrease in average pore size with increasing sintered density and the range of pore sizes results from the greater or lesser degree of break down of original foam bubbles, depending upon the amount of metal powder which must be accommodated. Under-loaded foam structures or very low metal-to-foam ratio samples always broke and crumbled while drying, because of the excessive shrinkage caused by the bubble size decreasing to an optimum value to accommodate the quantity of metal powder.

A - 3 Initial Sintering Procedure

The dried green foam pieces were placed in a mild steel retort which was loaded into a vacuum furnace as shown in Figure 50. The retort had a loose fitting lid and an attached pipe connecting the retort to the outside atmosphere. A valve enabled the pipe to be closed to atmosphere when required. The furnace was sealed and nitrogen admitted thru an irlet to a pressure of about 785 Torr. Heating was started and the exit gas line valve, on the piping from the steel box, was opened permitting the flow of nitrogen to remove the decomposition products from the furnace. Most of the organics are eliminated within approximately one hour when the furnace temperature reaches 500° F.

When the foamed piece reached a temperature of 500° F the nitrogen inlet and exit valves were closed and the furnace pumped down to start the final sintering. The pressure attained was dependent on whether the furnace had been used previously in dewaxing steps. With an uncontaminated furnace the pressures were in the range of 10^{-4} Torr. The vacuum normally attained was 0.5-1.0 Torr due to the vapor pressure of the organic deposit on the furnace walls. This comparatively low vacuum was not considered a disadvantage because it helped to prevent premature volatilization of the remaining binder until the temperature was high enough to allow some metallic sintering to occur.

During the final sintering, the furnace was heated to the sintering temperature under vacuum. Hydrogen was then bled into the furnace for 3 - 5 minutes to a final partial pressure of 5 Torr. After this period, the furnace was pumped down, and the cycle repeated 10 to 20 times. On completion of the cycling, the hydrogen was pumped out and the furnace allowed to cool overnight under vacuum. When more rapid cooling was desired, the furnace was backfilled with argon or helium.

The following tests were made on the sintered products:

a. The foamed pieces were examined for color, completeness of sintering, variations in texture, and for cracking, warping, and other defects.
b. The density was determined by measuring the volume and weight of an accurately cut sample of material. Values were expressed as the percentage of theoretical density of the wrought material.
c. The indentation hardness, in terms of the Brinell Hardness Number (Bhn), was measured. Values ranging from 0.1 to 3.0 were obtained, depending on the density reached by the sintered foam.

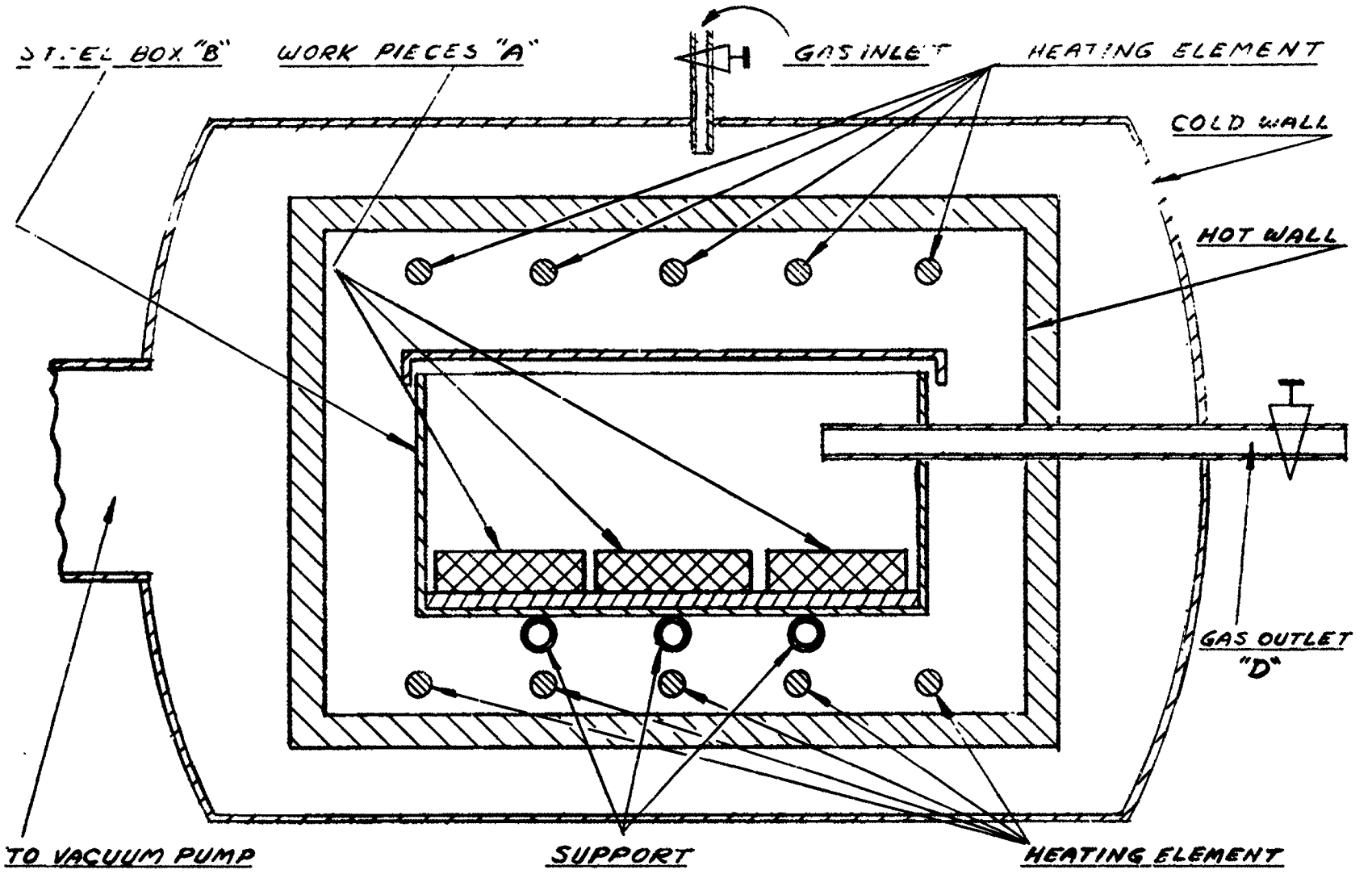

Figure 50. Sketch of Furnace for Sintering Foamed Metals

APPENDIX B

DEVELOPMENT OF TECHNIQUE FOR MOLTEN METAL IMPREGNATION OF PORE FORMING MATERIALS

The heated mold designed and built, described in the text in Figure 13, was to be heated to a temperature above the melting point of aluminum. The molten aluminum was to be poured then and allowed to penetrate the salt bed within the mold. When the salt bed was fully penetrated with the melt, the taper pin was replaced in the bottom of the mold. It was initially removed to prevent a pressure build-up below the salt bed. The mold within the stainless steel tube was then lowered slowly into a bucket of water so as to selectively cool from the bottom upward and prevent any solidification shrinkage voids within the casting. Temperature conditions during this operation were measured by means of a thermocouple positioned within the salt bed. Reference thermocouples were attached at various positions (in relation to the salt bed) on the stainless steel tube exterior so that after the melt was poured a reference cooling rate could be known and evaluated.

B - 1 Literature Search and Theoretical Calculations

A literature search was conducted for necessary data on the packing of spherical particles, the viscosity of molten metals, and also reference information on this type of porous metal production.

McGeary[11] claims that any one size of spheres pack in an orthorhombic arrangement to 62.5% of theoretical density. This was calculated and proved experimentally, provided that the ratio of the container diameter to the sphere diameter exceeds 20. Thus in the initial pours, using one mesh size of salt spheres and subsequent leachings, a porous aluminum of approximately 38% of theoretical density should be obtained provided that, with the 2.50 inch diameter screen container, the sphere diameter is less than 0.125 inch or -6 mesh.

For a binary mixture of spheres, McGeary calculated and proved experimentally that for any given sphere diameters, if the diameter of the coarse sphere exceeded that of the fine sphere diameter by a factor of 20 and if mixed in a proportion of 72% coarse and 28% fines, the maximum obtainable packing density would be approximately 83% of theoretical density. For a quaternary packing it was calculated and proved that a packing density of 95% could be

achieved if a 7 fold difference was maintained between sphere sizes of the individual components. A quaternary packing with a 95% of theoretical density was obtained from spheres with diameter ratios of 1:7:38:316 and a corresponding volume percentage composition of 6:10:23:61. McGeary's data and calculations will be used in later experiments to obtain porous aluminum of any percent of theoretical density between 10 and 40% or whatever value that experimentally proves not to require excessive pressure differentials or time for the metal to flow across the packed bed.

With this data in mind, the viscosity of aluminum as 4.6 centipoises, [12] and principles [13] of the flow of single fluid phases through porous media, some theoretical calculations were made to determine the velocity and time required for the aluminum to flow through the packed bed. The following equations and Figures 219, 220, 221, and 225 from Unit Operations [13] were used in the calculations.

$$Re = \frac{Dp \; Fre \; V \; \rho}{\mu}$$

$$f = \frac{2 \; gc \; Dp \; lwf}{L \; V^2 \; F_f}$$

Where Re = Reynold number (dimensionless)

f = friction factor (dimensionless)

Fre = factor included in Reynold number (dimensionless)

F_f = friction-factor factor (dimensionless)

L = length of packed bed through which fluid flows, inches

Dp = mean surface diameter of particles in packed bed, inches

V = superficial overall velocity of fluid through bed, inches/sec.

ρ = density of fluid, lbs/ft^3

μ = viscosity of fluid, lb/ft-sec.

gc = conversion factor

lw_f = lost work due to friction

The results of the theoretical calculations for a 6 inch high column of melt, gravity feeding a packed bed, six inches high, of several single mesh sizes of spherical particles are as follows:

Mesh Size	Particle Diameter inches	Fluid Velocity in/sec.
- 6 + 8	0.112	1.00
- 8 +10	0.079	.62
-10 +14	0.055	.40
-14 +20	0.039	.22

These calculations were to be checked experimentally and are only an estimation of the time the furnace need be held at 1300°F after the aluminum is poured. When experimental values are obtained, the calculations will be compared and more closely correlated so that with the future castings the pressure differential across the bed and the hold time at the pouring temperature can be predicted.

APPENDIX C

TABLES OF DATA

APPENDIX C

TABLES OF DATA
(Continued)

BLANK PAGE

TABLE C-1: Ultimate Tensile Strength of Foamed Molybdenum at Various Densities

Sintered Density % of Theo.	Individual Test Results of Tensile Strength in psi							
12.3	75	100						
13.0	105							
13.1	105	155	310	230				
13.5	125	100	155	155				
13.6	125							
13.7	180	180	205					
14.1	235	80	185					
14.2	285	290	450					
17.7	400							
18.0	740	700	820	360				
18.2	790	560	960	980				
19.3	690							
19.5	930							
20.2	650	460	280	610	580	650		
20.4	410	580	660	720	800	620	920	1020
20.5	1090							
20.8	670	690						
21.0	690	530	790					
21.2	610	1330	1340	950				
21.4	680							
21.7	990	830	880	920				
23.3	550							
25.8	1590							
28.5	840							

TABLE C-2: Ultimate Tensile Strength of Wrought and Foamed 316 Stainless Steel at Various Temperatures

Wrought 316 Stainless Steel (Annealed)		Foamed 316 Stainless Steel			
100% Density		18% Density		27% Density	
Temp. °F	Tensile Strength psi	Temp. °F	Tensile Strength psi	Temp. °F	Tensile Strength psi
----	------	-320	1100	-320	2850
70	85,000	70	970	70	2450
1000	73,000	469	700	500	1880
1100	70,000	938	465	1000	1100
1200	67,000	1450	320	1500	380
1300	65,000	1875	285	2000	265
1400	51,000				
1500	40,000				

TABLE C-3: Ultimate Tensile Strength of Foamed H-11 Tool Steel at Various Densities

Sintered Density % Theoretical	Ultimate Tensile Strength psi
20.1	500
20.9	710
25.5	1240
26.8	1780
26.5	1190
27.5	890

TABLE C-4: Ultimate Tensile Strength of Foamed Nickel at Various Temperatures

18% Density Nickel		27% Density Nickel	
Temperature °F	Tensile Strength psi	Temperature °F	Tensile Strength psi
-320	1160	-320	1340
70	990	70	1200
418	620	500	700
836	560	1000	640
1255	580	1500	475
1675	145	2000	225

Tensile strength of electrolytic nickel at ambient temperature = 46,000 psi.[2]

TABLE C-5: Compressive Strength of Foamed Molybdenum at Various Densities

Sintered Density % of Theo.	Compressive Strength		
	@ 0.2% Offset Yield psi	@ 10% Deformation psi	Ultimate psi
11.1	100	165	175
11.3	150	---	230
11.3	185	285	300
13.1	315	---	590
13.1	455	770	780
13.5	730	905	905
13.5	210	350	350
13.5	295	395	415
14.1	250	320	320
14.1	260	435	445
14.1	220	405	405
14.1	115	270	270
14.1	610	1050	1090
14.2	545	650	670
15.6	1180	---	1500
15.6	1070	---	1270
15.6	1170	---	1610
15.6	1300	1730	1730
17.7	1390	2380	2390
17.7	1290	2040	---
17.7	1160	1980	---
18.0	1040	---	1660
18.0	1130	---	1900
18.0	1300	---	2220
18.0	900	2350	---
18.0	520	---	1610
18.2	1625	---	2620
18.2	1005	---	1485
18.2	650	---	1325
18.2	935	---	1345
18.2	1160	---	1575
18.2	1425	---	1505
18.2	1450	1900	1900
18.5	1175	1760	1760
18.5	965	---	1930
18.5	2160	---	4100
18.5	2240	---	2440
19.5	1255	---	1500

* Samples with coarse particles

TABLE C-5: Continued

Sintered Density % of Theo.	Compressive Strength		
	@ 0.2% Offset Yield psi	@ 10% Deformation psi	Ultimate psi
19.5	1180	----	1695
19.5	1140	----	1795
19.8	3150	----	4100+
19.8	2130	----	2400
19.8	1650	----	2210
20.2	1170	2750	----
20.2	930	2450	----
20.2	920	2040	----
20.2	1330	2160	----
20.2	1220	2000	2000
20.2	1160	----	1630
20.2	1200	----	1630
20.2	760	----	1840
20.2	1160	2380	2380
20.2	665	----	1440
20.4*	115	245	245
20.4*	165	----	305
20.4*	265	----	375
20.4	1940	----	3030
20.4	1540	----	2630
20.4	1880	----	2050
20.4	1960	----	2990
20.5	2000	----	4080
20.5	2080	----	3720
20.8	1120	2540	----
20.8	1420	2540	----
21.2	920	1600	----
21.2	1025	1830	----
21.3	1600	2240	----
21.3	----	2070	----
21.3	1360	2980	----
21.3	620	2220	----
21.3	1580	2490	----
21.3	880	2180	----
21.3	1080	2120	2130
21.4*	135	----	305
21.4	1400	----	1850
22.2	1170	2210	----
22.2	----	2260	----
22.2	1580	2250	----

* Samples with coarse particles.

TABLE C-5: Continu 1

Sintered Density % of Theo.	Compressive Strength		
	@ 0.2% Offset Yield psi	@ 10% Deformation psi	Ultimate psi
22.2	1130	2200	----
23.3	2440	3600	3600
24.9	1715	3350	----
24.9	2170	3750	----
25.7	4150	7300	----
25.7	2870	4750	----
25.7	2600	5100	----
25.7	1950	4550	----
25.8	3370	5650	----
25.8	3060	4750	----
26.0	1995	----	2450
26.0	2245	----	3670
26.0	1995	----	2450
26.0	2245	----	3760
28.0	1150	2400	----
30.3	3225	5900	----
30.3	3225	4550	----

* Samples with coarse particles.

TABLE C-6: Compressive Strength of Foamed Stainless Steel at Various Densities

Sintered Density % of Theo.	Compressive Strength		
	@0.2% Offset Yield psi	@ 2% Deformation psi	@ 10% Deformation psi
13.1	407	470	770
13.4	240	325	410
13.4	225	425	733
13.4	225	417	620
14.3	280	400	800
15.4	396	702	1190
15.4	546	672	1066
15.4	480	625	1020
17.3	280	645	1120
18.5	410	880	1900
18.5	300	465	855
20.6	650	[illegible]	1980
20.6	565	[illegible]	1627
20.6	750	1030	1870
21.6	1070	1000	1445
21.6	700	1130	1500
21.6	675	1270	1400
22.7	820	1350	2620
22.7	1180	1700	2700
22.7	1480	1810	2520
22.7	2100	2450	3720
22.7	1500	2385	3075
22.7	1800	2610	3220
22.7	2120	2240	2575
22.7	2700	2975	4470
23.6	820	1110	1760
23.6	1140	1470	2540

TABLE C-7: Compressive Yield of Foamed 316 Stainless Steel at Various Temperatures

18% Density		27% Density	
Temp. °F	Compressive Yield, psi	Temp. °F	Compressive Yield, psi
-320	1190	-320	3150
70	770	70	1100
469	308	500	855
938	305	1000	730
1405	234	1500	689
1875	59	2000	260

TABLE C-8: Compressive Yield of Foamed Nickel at Various Temperatures

15% Density		18% Density		27% Density	
Temp. °F	Compressive Yield, psi	Temp. °F	Compressive Yield, psi	Temp. °F	Compressive Yield, psi
-320	210	-320	410	-320	1170
70	243	70	305	70	1100
418	254	418	296	625	900
836	115	838	304	1250	1350
1255	186	1255	332	1875	1396
1675	223	1675	220	2500	204

TABLE C-9: Compressive Strength of Foamed H-11 Tool Steel at Various Densities

Sintered Density % of Theo.	Compressive Strength		
	@ 0.2% Offset Yield psi	@ 2% Deformation psi	@ 10% Deformation psi
17.5	430	470	870
19.8	460	560	1020
20.0	935	1100	1720
20.0	850	1040	1500
20.4	810	960	1620
20.4	1110	1040	1640
20.5	805	920	1540
20.5	910	1120	1800
20.6	660	760	1500
20.9	1060	1280	1970
22.0	590	700	1240
22.5	1050	1240	1940
22.5	1000	1240	1940
23.6	520	600	1100
24.4	660	760	1360
24.4	895	970	1800
24.5	605	700	1260
24.5	550	630	1260
25.3	850	1120	2060
25.3	910	1000	1750
27.2	1240	1640	2680
27.6	1030	1400	2470
27.6	1030	1250	2470
28.0	1020	1250	2180
28.0	945	1100	1850
28.0	925	1100	1800
28.2	1010	1250	2030
29.7	1860	2830	4530
29.7	2480	2100	4200
29.7	1440	2100	3520

TABLE C-10: Flexural Strength of Foamed Molybdenum at Various Densities

Sintered Density % of Theo.	Individual Test Results of Flexural Strength - psi									
11.1	125	125	180	120	30	115	100			
11.3	170									
11.6	235	235								
12.3	295									
12.7	125									
12.9	240									
13.0	305	175	135							
13.1	185	465	175	460	375	775	565			
13.3	410									
13.5	460	415	375	150	415	480				
13.6	410									
13.7	495	175	175	265	230	205				
14.1	650	375	180	325	355	180	355	235	200	410
14.2	350	290	630	490						
15.3	735	980	705	650	650	1000	1000	1200	735	980
15.3	1030									
15.6	1030	920	1290	1160	1270	1470				
15.6	1090	1480								
17.7*	175	85	30	30						
17.7	1720	1800	1660							
18.0	1030	920	1510	1560	1200	1410	790	1280	950	
18.2	1630	1470	1780	1150	1780	1300	1470	830	940	
18.2	890	1770	1160	1530	1470	1510	1720	1660		
18.5	1450	1150	1410	1470	1330	1150	1210	1510	1590	1480
18.5	1350	1300	1390	1900						
19.3	1880									
19.5	1560	1530	2190	1280						
19.8	1540									
20.2	1700	1980	1650	1380	1480	1410	1990	1980		
20.4*	175	85	30	30						
20.4	1650	2080	1650	2110	2450	2200	1970	2020	1840	2150
20.4	1950	2430	2150	1890	1420					
20.5	1510	1330	1560	1560	1650	1880	2130	1690	1560	1960
20.5	2020	1750	2520							
20.8	2250	2780	2480	1770	2780					
21.0	1750	1820	1930	2000	1710	1590				
21.2	2230	2230	1970	3600	3350	3660	1410	1590	3000	2710
21.2	2960	1540								

* Samples with Coarse Particles

TABLE C-10: Continued

Sintered Density % of Theo.	Individual Test Results of Flexural Strength - psi					
21.4*	115	170	170			
21.4	2170	1660				
21.7	1470	1840	2080	2140	2130	2200
22.2	1820	3140	3370			
23.3	2970	3280	3310			
25.7	3860	3970				
25.8	4030	2960	3270	3670		
26.0	2340	2840				
28.0	2390	3300				
28.5	2410					

* Samples with Coarse Particles

TABLE C-11: Statistical Average and Standard Deviation of the Flexural Strength of Foamed Molybdenum at Various Density Ranges

Sintered Density % of Theo. Range	Number of Samples	Flexural Strength		
		Average psi	Standard Deviation psi	Range psi
11 - 12	10	145	±60	85 - 205
12 - 13	6	230	±40	190 - 270
13 - 14	37	430	±160	180 - 500
15 - 16	17	935	±270	665 - 1205
18 - 19	37	1310	±445	865 - 1755
20 - 21	45	1910	±355	1555 - 2265
21 - 22	21	2445	±670	1775 - 3125

TABLE C-12: Shear Strength of Foamed 316 Stainless Steel at Various Temperatures

18% Density		27% Density	
Temp. °F	Shear Strength psi	Temp. °F	Shear Strength psi
-320	1047	-320	8555
70	1370	70	3821
469	602	500	2256
938	670	1000	2353
1405	449	1500	931
1875	*	2000	*

* Samples at maximum temperature yielded at less than 50 psi.

TABLE C-13: Flexural Strength of Foamed Stainless Steel at Various Densities

Sintered Density % of Theo.	Individual Test Results of Ultimate Flexural Strength - psi						
10.6	55	170	235				
10.7	55	165	55	110			
13.4	60	120	330				
13.7	385						
14.3	180	180					
15.4	500	430					
16.8	690	390	480	470	580		
17.3	650	730	670	810	710	640	
19.2	910	760					
19.3	1300						
19.4	1220	1430					
20.0	1500						
20.6	840	2360	1700	1670	700	1760	1650
20.6	890	2030					
21.1	1405	1100	1970	1100			
22.7	1980	1860	1420	1150	2250	2720	2330
24.3	2650						
25.7	2190	2300	2900	1910	3520	3460	3560
25.7	3540	3320	2810				

TABLE C-14: Flexural Strength of Foamed H-11 Tool Steel at Various Densities

Sintered Density % of Theo.	Individual Test Results of Flexural Strength - psi		
13.5	580		
16.5	480		
17.5	1250	1180	
18.1	1730	1900	1760
19.8	710		
20.0	1520	1790	
20.2	890		
20.5	3020	2400	
20.9	1670	1580	1570
24.4	2730		
27.6	5060	3340	
28.0	3250	4190	2960
28.2	3490		

TABLE C-15: Shear Strength of Foamed Nickel at Various Temperatures

15% Density		18% Density		27% Density	
Temp. °F	Shear Strength psi	Temp. °F	Shear Strength psi	Temp. °F	Shear Strength psi
-320	127	-320	922	-320	1985
70	70	70	719	70	2542
418	164	418	722	625	2180
---	---	836	540	1250	1278
---	---	1255	276	1875	966
---	---	1675	*	2500	*

* Samples at maximum temperature yielded at less than 50 psi.

TABLE C-16: Vibration Damping Characteristics of Nickel and 316 Stainless Steel

Material	C_c %	Logarithmic Decrement x 10^{-4}
Electrolytic Nickel (theoretical density)	0.201	126.3
27% Density Foamed Nickel	0.211	132.5
18% Density Foamed Nickel	0.340	213.4
Stainless Steel (wrought)	0.014	5.4
27% Density Foamed Stainless Steel	0.192	120.4
18% Density Foamed Stainless Steel	0.101	63.6

TABLE C-17: Thermal Expansion of Foamed Nickel

18% Density Foamed Nickel		27% Density Foamed Nickel	
Temp. °F	Thermal Expansion in/in x 10^{-4}	Temp. °F	Thermal Expansion in/in x 10^{-4}
-320	-21.80	-320	-22.25
-168	-15.17	-180	-16.04
-112	-12.43	-168	-15.42
-101	-11.31	-160	-14.99
- 4	- 4.90	+ 5.2	- 4.66
+ 72	0.00	24.8	- 3.30
91	1.37	71.6	0.00
288	15.87	324	+18.59
601	42.23	1000	79.64
903	69.12	1500	123.47
1328	109.00	1900	160.66
1674	142.15		

TABLE C-18: Thermal Expansion of Foamed 316 Stainless Steel

18% Density 316 Stainless Steel		27% Density 316 Stainless Steel	
Temp. °F	Thermal Expansion in/in 10^{-4}	Temp. °F	Thermal Expansion in/in 10^{-4}
-304	-27.31	-320	-29.50
-204	-20.49	-288	-27.30
-188	-19.64	-178	-20.41
-124	-15.00	-117	-15.78
- 22	- 7.97	+ 5	- 5.65
- 20	- 7.82	9	- 5.60
- 15	- 7.37	72	0.00
+ 64	- 0.51	320	22.96
72	0.00	557	46.25
296	18.57	900	82.57
588	47.41	1175	115.86
890	73.19	1526	154.28
988	100.90	2003	207.74
1477	127.09		
1876	167.15		

TABLE C-19: Thermal Conductivities of Solid and Foamed Nickel

Electrolytic Nickel 100% Density		Foamed Nickel 27% Density		Foamed Nickel 18% Density	
Temp. °F	Thermal Conductivity $\frac{\text{BTU-in}}{\text{ft}^2\text{-hr-}^\circ\text{F}}$	Temp. °F	Thermal Conductivity $\frac{\text{BTU-in}}{\text{ft}^2\text{-hr-}^\circ\text{F}}$	Temp. °F	Thermal Conductivity $\frac{\text{BTU-in}}{\text{ft}^2\text{-hr-}^\circ\text{F}}$
-320	937	-269	57.7	-251	23.0
-210	739	118	83.0	133	30.5
40	480	313	70.8	358	28.1
540	330	619	61.2	568	23.3
1040	354	1191	66.5	819	21.4
1540	408	1776	89.6	1008	22.6
2040	462	2359	127.4	1418	31.7
				1812	54.0

TABLE C-20: Thermal Conductivities of Solid and Foamed 316 Stainless Steel

316 Stainless Steel 100% Density		Foamed Stainless Steel 27% Density		Foamed Stainless Steel 18% Density	
Temp. °F	Thermal Conductivity BTU-in / ft²-hr-°F	Temp. °F	Thermal Conductivity BTU-in / ft²-hr-°F	Temp. °F	Thermal Conductivity BTU-in / ft²-hr-°F
-335	45.6	-301	6.1	-238	1.7
-210	70.8	77	7.8	- 62	2.4
40	90.0	212	8.1	-0.4	2.5
540	114.7	581	9.5	194	3.1
1040	137.5	932	10.7	365	3.5
1540	166.2	1513	13.2	496	3.8
2040	199.2			1022	5.4
				1346	6.9
				1688	9.3

TABLE C-21: Sieve Analyses of Metal Powders used in Foamed and Sintered Materials

Material	Sieve Analysis						Tap Density gm/cc
	on 100	on 150	on 200	on 270	on 325	thru 325	
Aluminum							
1100 Alloy							
Nominal-100 Mesh	22.3	18.3	15.0	25.2	14.1	3.3	1.57
Nominal-325 Mesh	0.0	0.05	0.05	0.05	0.05	99.8	1.56
7178 Alloy							
Nominal-100 Mesh	0.9	5.2	11.5	10.8	16.8	54.8	1.71
Nominal-325 Mesh	0.0	0.0	0.0	0.0	0.0	100.0	1.69
Nickel							
Federal Mogul							
Nominal-100 Mesh	0.01	7.5	9.6	6.8	13.0	61.6	6.54
Nominal-325 Mesh	0.0	0.0	0.0	0.1	3.4	96.5	6.28
Sherritt-Gordan							
Low Density	0.0	0.0	0.2	---	0.6	99.2	1.44
High Density	0.0	0.0	0.0	0.0	0.9	99.1	4.45
Stainless Steel							
Nominal-100 Mesh	0.0	5.6	20.1	16.0	14.6	43.6	5.47
Nominal-325 Mesh	0.0	0.0	0.0	0.1	0.2	99.7	5.23
H-11 Tool Steel	0.0	---	45.3	---	25.6	29.1	5.12
Molybdenum							
Fansteel Powder	0.0	0.0	0.0	0.4	2.0	97.6	3.65
Climax Powder	0.0	0.0	0.0	0.0	0.2	99.8	2.70
Titanium							
Nominal-100 Mesh	0.0	24.8	27.7	16.0	18.1	12.6	1.65
Nominal-325 Mesh	0.0	0.0	0.0	0.0	0.1	99.9	1.47

TABLE C-22: Materials for Packed Bed in Pouring Molten Aluminum

Material	Grade	Manufacturing Company	Results of Cursory Examination
KBr	Coarse -8+20	Morton	Larger particles are solid spheres or ellipsoidal shaped particles. Smaller particles are solid cubes with rounded corners.
KBr	Fine -20 mesh	Morton	Small solid cubical particles with round corners.
NaBr	Fine -20 mesh	Morton	Small solid cubical particles with round corners.
NaBr	Coarse -8+20 mesh	Morton	Small solid cubical particles with round corners.
KCl		AP&C	Small solid cubical particles with rounded corners.
KCl		Trona	Small solid cubical particles with rounded corners.
KCl	Coarse -8+20 mesh	USB&C	Solid cubical particles with rounded corners.
KCl	-20+28 mesh	IM&CC	Small hollow spheres with an off center void which breaks thru the transparent skin in most spheres.
KCl	-28+35 mesh	IM&CC	Small hollow spheres with an off center void which breaks thru the transparent skin in most spheres.

TABLE C-22: Continued

Material	Grade	Manufacturing Company	Results of Cursory Examination
KCl	-14+20 mesh	IM&CC	Small hollow spheres with an off center void which breaks thru the transparent skin in most spheres.
KCl	-8+14 mesh	IM&CC	Hollow spheres with an off-center void which breaks thru the transparent skin in most spheres.
Lime	Kiln fines	NGC	Solid irregularly shaped granular particles of many sizes.

AP&C - American Potash & Chemical Company

IM&CC - International Minerals & Chemical Company

USB&C - U. S. Borax & Chemical Company

NGC - National Gypsum Company

Morton - Morton Chemical Company